Biological Cybernetics

Volume 26 Number 3 1977

Indexed in Current Contents

Springer-Verlag Berlin Heidelberg New York

Biol. Cybernetics ISSN 0340-1200 BICYAF 26 (3) 125-186 (1977) 17. V. 1977

Instructions to Authors

1. General

Manuscripts should be typewritten, double-spaced throughout, with wide margins. Papers should be as short and concise as possible. Generally 3 double-spaced manuscript pages correspond to about 1 printed page.

In general manuscripts should not exceed 25 manuscript pages including figures and tables.

To accelerate publication only **one set of proofs** is sent to authors. This shows the final layout of the paper as it will appear in the journal. It is therefore essential that manuscripts are submitted in their *final form,* ready for the printer, and that the approximate desired *positions of figures and tables are marked* on the margins. Proofreading should be *limited to the correction of typographical errors.* Any other changes involve time-consuming and expensive work, *and the costs will be charged to the author(s).* If absolutely necessary and space permits, additions may be made at the end of the paper in a "Note added in proof".

Each manuscript should include a separate sheet of "Instructions for the compositor" explaining markings and special types used.

2. Text

Abstract. All papers must have an **English abstract** and, if written in German or in French, an **English translation of the title** in addition.

Headings. Subheadings (Introduction, Materials and Methods, etc.) should be placed on separate lines. Nouns, adjectives, etc., should be capitalized.

Subheadings should be classified according to the following system:

1. = first subheading
1.1. = second subheading
1.1.1. = third subheading
1.1.1.1. = fourth subheading.

Italics should be used for emphasis in text. Underline to indicate *italics.*

Small print. Materials and methods, and sections of lesser importance should be marked for small type. Because of higher composition costs, small type is no less expensive than regular type but serves to improve the organization of the text. Footnotes and tables are always printed in small type.

Footnotes to the text should be numbered consecutively. They should be placed at the foot of each page (not at the end of the article).

3. Formulae

Equations should be typewritten whenever possible, showing special typefaces (alphabets) by underlining in color (see *Marking*). As there is no difference in size, extra special attention should be given to the placing of indices and exponents so that they are recognizable as such. Formulae should preferably be written in the "linear" form (see *Notations*). Equations should be numbered sequentially with arabic numerals in parentheses on the right-hand side of the page. In the text they are cited simply by the arabic numeral in parentheses, e.g., (7); the form Equation (7) or Equations (7) and (8) should be used only at the beginning of a sentence.

Marking. Letters in formulae are normally printed in italics, figures in ordinary typeface.
It will help the printer if in doubtful cases the position of indices and exponents is marked thus:

$$b \overset{\wedge}{,}\ a \overset{\vee}{,}$$

Underlining for special type should be done according to the following code:

single underlining = Small letter
double underlining = Capital letter

yellow = Upright: abbreviations e.g. Re, im, grad, div, lim, NGC, and all elements

brown = Boldface:

A, B, C, D, E, F, G, H, I, J, K, L, M, N, O, P, Q, R, S, T, U, V, W, X, Y, Z

a, b, c, d, e, f, g, h, i, j, k, l, m, n, o, p, q, r, s, t, u, v, w, x, y, z

red = Greek Lettering:

$\Gamma, \Delta, \Theta, \Lambda, \Xi, \Pi, \Sigma, \Phi, \Psi, \Omega$
$\alpha, \beta, \gamma, \delta, \varepsilon, \zeta, \eta, \theta, \vartheta, \iota, \varkappa, \lambda, \mu, \nu, \xi, o, \pi, \varrho, \sigma, \tau, \upsilon, \varphi, \phi, \chi, \psi, \omega$

green = Script:

$\mathcal{A}, \mathcal{B}, \mathcal{C}, \mathcal{D}, \mathcal{E}, \mathcal{F}, \mathcal{G}, \mathcal{H}, \mathcal{I}, \mathcal{J}, \mathcal{K}, \mathcal{L}, \mathcal{M}, \mathcal{N}, \mathcal{O}, \mathcal{P}, \mathcal{Q}, \mathcal{R}, \mathcal{S}, \mathcal{T}, \mathcal{U}, \mathcal{V}, \mathcal{W}, \mathcal{X}, \mathcal{Y}, \mathcal{Z}$
$a, b, c, d, e, f, g, h, i, j, k, l, m, n, o, p, q, r, s, t, u, v, w, x, y, z$

violet:
the single letters I and capital O (to distinguish them from the numerals 1 and zero)

The following are frequently confused:

$\cup$, **u**, **U**; $o, O, 0$; $x, X, \varkappa$; v, υ, ν; $\phi, \varphi, \Phi, \varnothing, \mathcal{O}$; $l, \mathrm{l}, \varepsilon, \in$

also the handwritten Roman letters:

c, C; k, K; o, O; p, P; s, S; u, U; v, V; w, W; x, X; z, Z; e, l.

Please take care to distinguish them in some way.

Notations

preferred form	instead of
$7/8, (a+b)/c$	$\frac{7}{8}\frac{a+b}{c}$
$\exp(-(x^2+y^2)/a^2)$	$e^{-\frac{x^2+y^2}{a^2}}$
$\frac{\cos(1/x)}{(a+b/x)^{1/2}}$	$\frac{\cos\frac{1}{x}}{\sqrt{a+\frac{b}{x}}}$
$f: A \to B$	$A \xrightarrow{f} B$
sub lim, inf lim	$\underline{\lim}, \lim$
inj lim, proj lim	$\varinjlim \varprojlim$

4. References

Literature citations in the text should be preferably by author(s) and year. Where there are more than two authors, only the first should be named, followed by "et al.".

The list of **References** should include only publications cited in the text. The references should be cited in alphabetical order under the first author's name, listing all authors (*surnames followed by initials throughout;* do *not* use "and") and the complete title (in English and French titles do *not* capitalize nouns, adjectives, etc.), according to the following rules and examples:

a) *Articles from journals and other serial publications:* author(s), title, series (abbreviated), volume followed by a comma, *inclusive* pages, year (in parentheses).

Example:
O'Leary, D. P., Segundo, J. P., Vidal, J. J.: Perturbation effects on stability of gravity receptors. Biol. Cybernetics **17**, 99—108 (1975)

b) *Articles from non-serial collective publications* (symposia volumes, encyclopedias, etc.); author(s), title followed by "In:", title of the volume and/or part (Vol., pt.) if appropriate, inclusive pages of article (pp.), name(s) of editor(s) followed by "ed(s).", publisher (place: name), year.

Example:
Hartline, H. K., Ratliff, F.: Inhibitory interactions in the retina of *Limulus.* In: Handbook of sensory physiology. Vol. VII/2, pp. 381—447. Fourtes, M. G. F., ed. Berlin-Heidelberg-New York: Springer 1972

c) *Books:* author(s), title, edition (edn.) if appropriate, publisher as under b), year.

Example:
Ledbetter, M. C., Porter, K. R.: Introduction to the fine structure of plant cells. Berlin-Heidelberg-New York: Springer 1970

5. Tables

Tables should be prepared consulting a recent issue of the journal and should be numbered consecutively with Arabic numerals. Footnotes in tables should be indicated by lower-case suffix letters, beginning with [a] in each table.

6. Illustrations

Illustrations should be limited to materials essential for the text, and line drawings should be used wherever possible. Double documentation of the same point in figures *and* tables is not acceptable.
Requests for color illustrations cannot be approved unless the author(s) agree to bear the costs.
Figures, tables and *diagrams* should be submitted on separate sheets and not incorporated into the text.
The figures should not extend beyond the column width (8.1 cm) or page width (16.8 cm). Print area: 16.8 cm × 22 cm. Several figures should be grouped into a plate on one page. For *line drawings,* sharp glossy prints in the desired final size are preferred. The inscriptions should be clearly legible. Letters 2 mm high are recommended. For *half-tone illustrations,* well-contrasted photographic prints, trimmed at right angles and in the desired printing size are essential. Inscriptions should be about 3 mm high. Parts of figures should be indicated by lower-case boldface letters (a, b, c). All figures must have legends, which should be submitted on a separate sheet. Illustrations taken from other publications should be accompanied by full information as to their source.

7. Offprints

Fifty (50) offprints of each paper will be supplied free of charge. Additional copies may be ordered at cost price when the proofs are returned.
Manuscripts must be accompanied by the full address of the author. Should the author change his address before the manuscript appears in print, he should in his own interest notify the publisher immediately.

Biological Cybernetics

Communication and Control in Organisms and Automata

Nachrichtenübertragung, Nachrichtenverarbeitung, Steuerung und Regelung in Organismen und in Automaten

Springer-Verlag Berlin Heidelberg New York

Biological Cybernetics

Communication and control in organisms and automata.
Continuation of „Kybernetik" (Volume 1—16)

Biological Cybernetics appears about every month.

Subscription Information
Volumes 25—28 (4 issues each) will appear in 1977. Information about obtaining back volumes available upon request.

All Countries (Except North America). Subscription rate: DM 592,— plus postage and handling. Orders can either be placed with your bookdealer or sent directly to: Springer-Verlag, Heidelberger Platz 3, D-1000 Berlin 33.

North America. Subscription rate: $ 254.00 including postage and handling. Subscriptions are entered with prepayment only. Orders should be sent to your bookdealer or subscription agency or directly to: Springer-Verlag New York Inc. 175 Fifth Avenue, New York, N. Y. 10010.

Manuscripts should be addressed to:
Prof. Dr. W. Reichardt
Max-Planck-Institut für biologische Kybernetik
Spemannstraße 38
D-7400 Tübingen, FRG

It is a fundamental condition that submitted manuscripts have not been and will not be, simultaneously submitted elsewhere.

Correspondence concerning advertisements should be sent to the Advertisement Department of the publishing firm in Berlin: Kurfürstendamm 237, D-1000 Berlin 15, Tel. (0 30) 8 82 10 31, Telex 01-85 411.

Springer-Verlag

Heidelberger Platz 3	Postfach 105 280
D-1000 Berlin 33	D-6900 Heidelberg 1
Tel. (0 30) 82 20 01	Tel. (0 62 21) 4 87-1
Telex 01-83 319	Telex 04-61 690

Springer-Verlag New York Inc.
175 Fifth Avenue
New York, N. Y. 10010
Tel. 2 12 (6 73-26 60)
Telex 00-23 22 235

The concepts of transmission of information, processing of information and automatic control engineering originated within technology and physics. Today, however, these concepts have also proved useful in the biological sciences where analogous processes of communication and control are encountered. Despite the differences between nonliving and living systems, many of the logical procedures, the experimental and theoretical approaches and the mathematical techniques applicable to the physical sciences also find natural applications in the realm of the life sciences. In particular, by adopting this approach to sensory and neurophysiological problems new insight has been gained into the principles by means of which organisms handle and utilize information. Conversely, physicists and engineers have shown increasing interest in natural mechanisms of communication and control, including genetic communication and the control of reproduction.

The aim of "Biological Cybernetics" is to promote the exchange of experimental and theoretical information in the following fields: Quantitative analysis of behaviour, in both vertebrates and invertebrates; quantitative micro- and macro-physiological studies of information-processing in receptors, neural systems and effectors; mathematical models of communication and control processes in organisms, including reproductive mechanisms; biologically relevant aspects of information theory, network theory, theory of automata, theory of control systems.

Contents of the next issue

Biol. Cybernetics 26, 125—129 (1977)

Biological Cybernetics

Quantitative Description of End Plate Current and its Reconstruction

H. Yagi and T. Hashimoto
Faculty of Engineering, Toyama University, Takaoka, Japan

K. Sugimoto
Faculty of Education, Toyama University, Toyama, Japan

Abstract. An attempt was made to quantify the postsynaptic current based on the experimental data of the voltage clamp method. The conductance change in postsynaptic membrane was derived from the postsynaptic conductance of voltage clamped postsynaptic membrane, then it's temporal characteristics and dependence on the clamped voltage have been quantified. The temporal characteristics was found to be explained by the introduction of two schematic operators, active and inactive. This idea was applied to a simple electrical circuit model of the postsynaptic cells. Besides the change in postsynaptic potentials of normal synapse in excitable state was culculated as its application.

Introduction

The voltage clamp of postsynaptic membrane had been executed by N. Takeuchi and A. Takeuchi (1959) and Oomura and Tomita (1961). The dependence of the conductance characteristics on the voltage was confirmed by Magleby and Stevens, (1972). Magleby and others have quantified the characteristics partially based on their data availed. In their model, they assumed that the conductance was controlled by the reaction and the resolution of the transmitter which has an effect on the postsynaptic membrane. They explained that the contactable quantity of the transmitter to receptive site controlled the membrane conductance depending on the clamped voltage.

In this paper, based on the physiological data of Magleby and others, it was found feasible to express the conductance change by a set of simple mathematical expression with good accuracy. This work is based on such an idea as that of Hodgkin and Huxley (1952); the conductance of the postsynaptic membrane is controlled not only by an active operator which opens the ion channels but also by an inactive one which closes the channels.

The authors calculated the temporal characteristic of conductance from the current variance divided by clamped voltage, utilizing a series of the data for postsynaptic current under voltage clamp by Magleby and others.

Mathematical Description of Voltage Clamped Postsynaptic Current

The result of its detailed analysis showed that it was reasonable to assume that the time variance of conductance change under voltage clamped should be determinable by two variables, each of which could be expressed by first order differential equations. Each variable should be called active operator, m, and inactive operator, h, respectively. The former acts to increase the membrane conductance and vice versa for inactive one. There are some assumptions here;

$$g = \bar{g} m^3 h, \tag{1}$$

$$\frac{dm}{dt} = \alpha_m (1-m) - \beta_m \cdot m, \tag{2}$$

$$\frac{dh}{dt} = \alpha_h (1-h) - \beta_h \cdot h. \tag{3}$$

Here, $\bar{g}$ is a constant having the dimensions of $(\mho)$, and αm, βm, αh, and βh are functions of the clamped voltage v, but not those of time. These equations are derived directly from the data of actual membrane, but these operators would have a physical significance assuming that the conductance of the postsynaptic membrane should be proportional to the number of the transmitter receptive sites of it's outer side. The receptive sites should be occupied by three active substances and left vacant by the occupation of an inactive one at the same time. Therefore m represents the probability of occu-

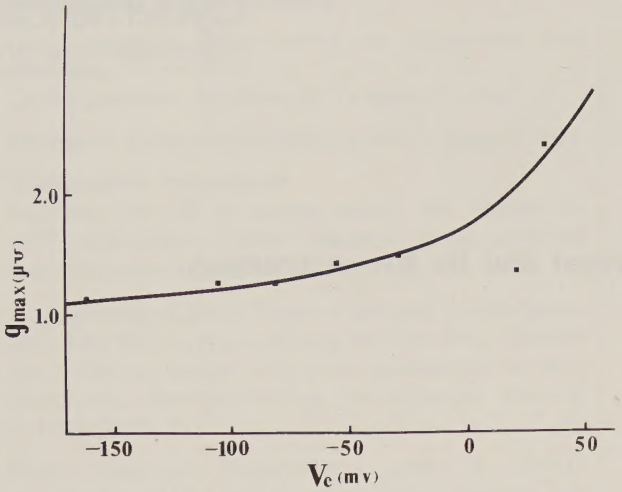

Fig. 1. Relation between maximal conductance and clamp voltage *Vc*. Here, maximal conductance g_{max} correspondes to h_∞. Solid line is curve calculated by theoretical formula. ■ is experimental data

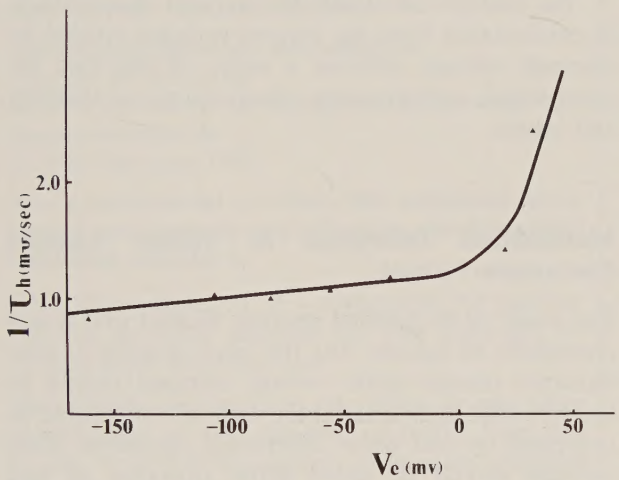

Fig. 2. Relation between time constant τ_h and clamp voltage *Vc*. τ_h is obtained by computing (11). ▲ is experimental data

pation of receptive site of postsynaptic membrane by active substance, and $1-m$ represents that of non-occupation.

αm, βm, and αh, βh represent the rate constant of transmission velocity of reciprocal directions respectively. Both m and h are variables between 1 and 0 as probabilistic coefficient. Under such initial conditions as $m=m_0$ and $h=h_0$ at $t=0$, the solutions of the Equations (2) and (3) would be solubled as follows

$$m=m_\infty-(m_\infty-m_0)\exp(-t/\tau_m), \tag{4}$$

$$h=h_\infty-(h_\infty-h_0)\exp(-t/\tau_h). \tag{5}$$

Here,

$$m_\infty=\frac{\alpha_m}{\alpha_m+\beta_m}, \quad \tau_m=\frac{1}{\alpha_m+\beta_m}, \tag{6}$$

$$h_\infty=\frac{\alpha_h}{\alpha_h+\beta_h}, \quad \tau_h=\frac{1}{\alpha_h+\beta_h}, \tag{7}$$

and

$$m_0=\frac{\alpha_{m_0}}{\alpha_{m_0}+\beta_{m_0}}, \quad h_0=\frac{\alpha_{h_0}}{\alpha_{h_0}+\beta_{h_0}},$$

where α_{m_0}, β_{m_0}, and α_{h_0}, β_{h_0} are initial values prior to the change in membrane potential.

Now from (6) there should be such relations as follows between m_∞, τ_m, α_m, and β_m

$$m_\infty=\alpha_m\cdot\tau_m, \tag{8}$$

$$\beta_m=(1-m_\infty)\cdot\tau_m, \tag{9}$$

and still more, between h_∞, τ_h, α_h, and β_h

$$h_\infty=\alpha_h\cdot\tau_h, \tag{10}$$

$$\beta_h=(1-h_\infty)\cdot\tau_h. \tag{11}$$

Before the change in membrane potential, the conductance of postsynaptic membrane is very small compared with it's maximum value. So, m_0 would be negligible when the depolarizing potential is smaller than 30_{mV}, and it is also true for h_∞, because the inactivity is accomplished. Then the donductance would be given by the product of m^3 in (4) and h in (5);

$$g=g'[1-\exp(-t/\tau_m)]^3\cdot\exp(-t/\tau_h). \tag{12}$$

Here, $g'=\bar{g}\cdot m_\infty^3\cdot h_0$, representing the conductance when h is equal to h_0 and m_∞ would be given by

$$m_\infty=\frac{\sqrt[3]{g'}}{\bar{g}'\cdot h_0}. \tag{13}$$

Formularization of the Rate Constants, α_h and β_h

Conductance was calculated by the method above mentioned from the physiological data of Magleby and others in order to express α_h and β_h as the functions of the membrane potential. The maximum value of the rate constants of velocity at the decay process was derived from these values of conductance of postsynaptic membrane as availed above, and described as a function of the clamped voltage. In this way, the maximum value of the conductance is also calculable, and Figure 1 is given. These calculated values correspond to $1/\tau_h$ which is shown in Figure 2, and h_∞ which is shown in Figure 1 respectively.

α_h and β_h would be derived from h_∞ and $1/\tau_h$ which are already known as the functions of clamped voltage by using (10) and (11), and Figure 3 is given. That is

$\alpha_h=1.25$, $\beta_h=0.25$ for $V=0\,(\mathrm{mV})$

$\alpha_h=0.75$, $\beta_h=3.20$ for $V=-10\,(\mathrm{mV})$

$\alpha_h=0.25$, $\beta_h=3.50$ for $V=-30\,(\mathrm{mV})$.

α_h and β_h fitting to the experimental values are represented by the following equations by the method of the least squares

$$\alpha_h = \frac{0.6\left(\frac{-V-15}{10}\right)}{\exp\left(\frac{-V-15}{10}\right)-1}, \tag{14}$$

$$\beta_h = \frac{3.5}{\exp\left(\frac{V+5}{2}\right)+1}. \tag{15}$$

Here, α_h and β_h are represented by $(\mathrm{m\,s})^{-1}$ and V by mV respectively. The solid line in Figure 3 are plotted from (14) and (15).

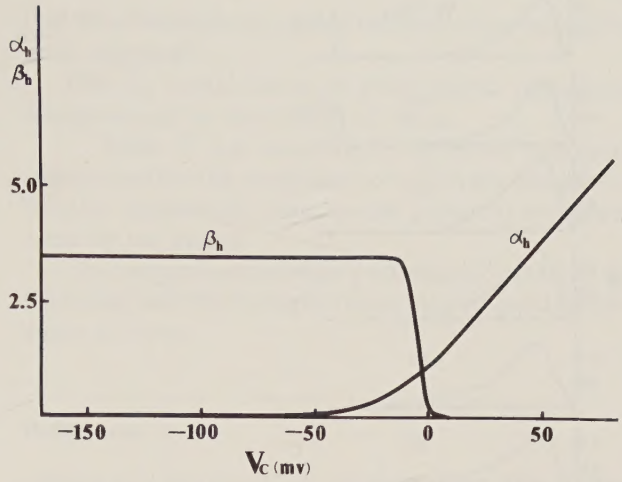

Fig. 3. Relation between α_h and β_h and clamp voltage Vc. α_h and β_h are calculated according to (14) and (15) respectively

Formularization of the Rate Constants of Velocity, α_m and β_m

In order to express α_m and β_m as the functions of clamped voltage, the maximum values of the rate constant of velocity at the rising phase, which were calculated from the conductance characteristic of postsynaptic membrane and were matched to $1/\tau_m$ and m_∞, were derived from (13), and Figure 4 was obtained by representing $1/\tau_m$ values above obtained as the function of clamped voltage.

α_m and β_m were determined by applying (8) and (9) to these values. Figure 5 shows the relations between α_m and β_m, and the clamped voltage. The relations between α_m and β_m, and the clamped voltage are similar to those between α_h and β_h, and the clamped voltage. Examining the practical numerical values, the former is of the order of fifth of the latter, that is

$\alpha_m = 0.18,\ \beta_m = 0.40$ at $V = 0\,\mathrm{mV}$

$\alpha_m = 0.50,\ \beta_m = 0.25$ at $V = -10\,\mathrm{mV}$

$\alpha_m = 0.70,\ \beta_m = 0.09$ at $V = -30\,\mathrm{mV}$.

α_m and β_m fitting to the experimental values are represented by the following equations,

$$\alpha_m = \frac{0.7}{\exp(v+5/5)+1}, \tag{16}$$

$$\beta_m = \frac{0.2(-v-15/10)}{\exp(-v-15/10)-1}. \tag{17}$$

Here, α_m and β_m are represented by $(\mathrm{m\,s})^{-1}$ and V by mV respectively. The solid lines shown in Figure 5 are plotted by (16) and (17).

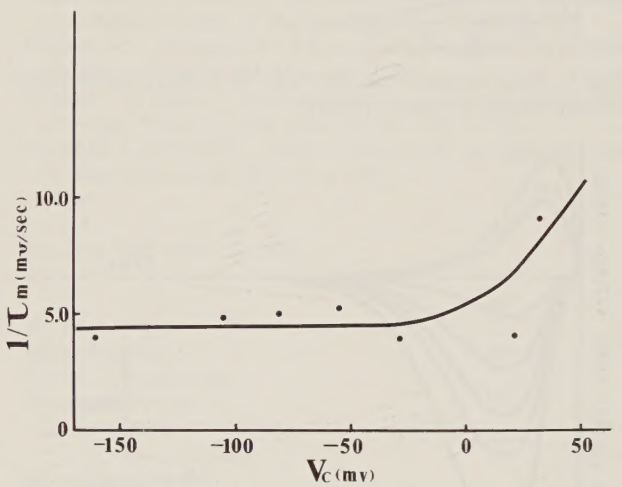

Fig. 4. Relation between time constant τ_m and clamp voltage Vc. ● is experimental data

Voltage Clamped Postsynaptic Current

The approximation of the conductance change in the postsynaptic membrane is found to be feasible by assuming the existence of two operators.

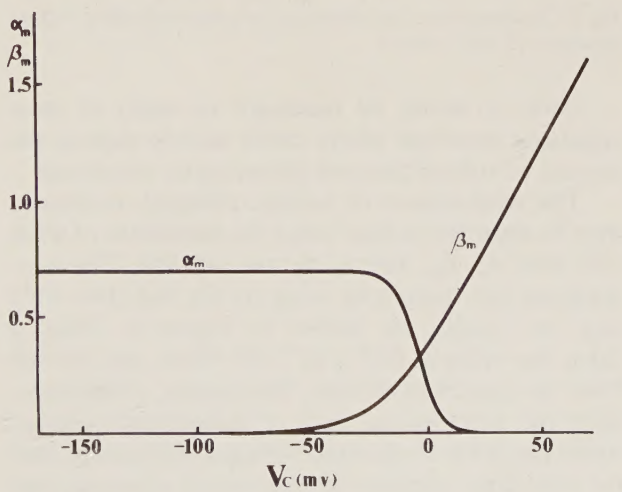

Fig. 5. Relation between α_m and β_m and clamp voltage Vc. Solid line shows α_m and β_m calculated according to (16) and (17) respectively

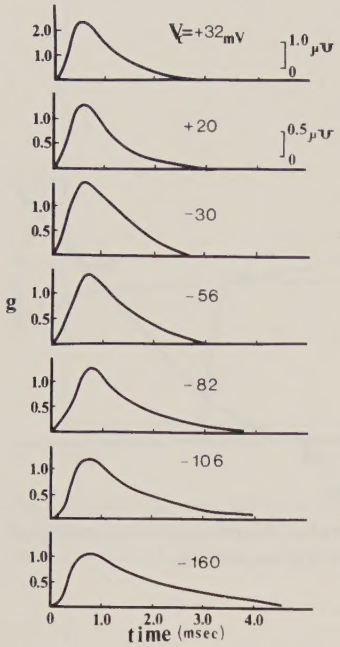

Fig. 6. Time dependent characteristics of conductance in clamp voltage between +32 and −160 mV

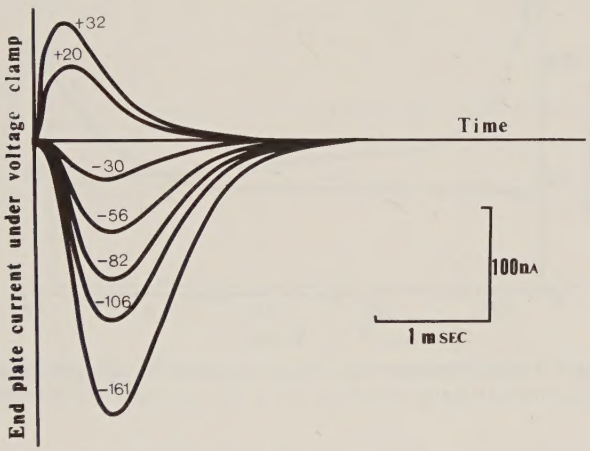

Fig. 7. Characteristics of calculated end plate current in clamp voltage between +32 and −161 mV

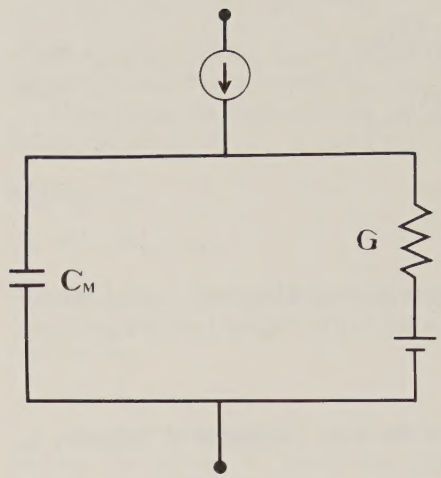

Fig. 8. Equivalent circuit of postsynaptic membrance at end plate

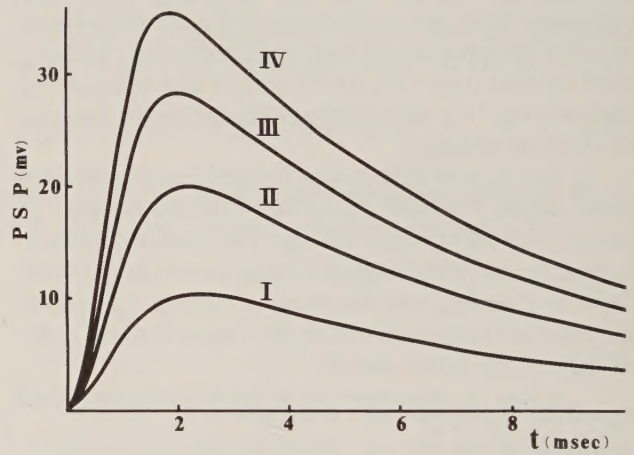

Fig. 9. Calculated postsynaptic potential at end plate

Now, it would be necessary to verify if these equations described above could exactly express the current of voltage clamped postsynaptic membrane.

The conductance of voltage clamped membrane may be regarded as that under the conditions of $dv/dt = 0$, here α_m, β_m, and α_h, β_h are constant. The conductance was derived by using (1)–(3), and (14)—(17), and the results are shown in Figure 6. Here, $\bar{g}$ takes the value of 0.37×10^{-6} (℧) which was derived from the experimental data. The symbol of (●) represents the experimental data of conductance change which are given at the fixed voltages respectively, and the solid lines represent the theoretical values derived from such equations as described in this paper. The membrane current is derived from the product of value by (1) and V, the clamped voltage;

$$I = g \cdot V$$
$$= \bar{g} m^3 h V. \tag{18}$$

Figures 6 and 7 show the conductance, and postsynaptic current characteristics were calculated respectively for the comparison on various clamped voltages derived from the above equations with experimental data of Magleby and others. There are good approximations, but there is some slight difference that the theoretical characteristics have earlier peak of current when the voltage is hyperpolarized. It seems to be caused by the large value of rising velocity of active operator and that of decay velocity of inactive operator.

Postsynaptic Potential

The electrical action of postsynaptic membrane may be represented by such an equivalent circuit as shown in Figure 8. For simplicity the equilibrium potential of the transmitter control channels is taken as zero taking only the displacement of the conductance into consideration. Postsynaptic current is the sum of the current for charging up the membrane capacitance and that flowing through the membrane conductance parallelled with the membrane capacitance. The current flowing through the membrane conductance depends upon the voltage and the conductance of the membrane. Therefore, the total current is the sum of the current determined by the product of the conductance and the potential and that charging the membrane capacitance. Representing the former as Ig and the latter as Ic, the total current I can be represented by the following equations;

$$I = Ig + Ic + i$$

$$= \bar{g} m^3 h V + c \frac{dv}{dt} + i \,. \tag{19}$$

Here, i represents the effect of transmitter caused when the transmitter attaches to the receptive site of external surface of the postsynaptic membrane. Figure 9 shows the solution of (19) by applying (1)–(3) and (12) and (13). There is a good coincidence with the result of the experimental data of postsynaptic potential for frog sartorius muscle.

Conclusion

From the physiological data in postsynaptic potentials, its mathematical model was constructed by use of both operators such as active and inactive. It was assumed that the controllability of ions channel was governed by these operators.

That is, conductance of postsynaptic membrane was governed by the change of them.

When it was assumed in electronic computer simulation that the postsynaptic membrane was stimulated by transmitter, postsynaptic potential was generated by the model.

The comparison between postsynaptic potential by the model and the biological data showed good coincidence in them.

References

Hodgkin, A.L., Huxley, A.F.: A quantitative description of membrane currents and its application to conduction and excitation in nerve. J. Physiol. **117**, 500—544 (1952)

Magleby, K.L., Stevens, C.F.: The effect of voltage on the time course of end-plate currents. J. Physiol. **223**, 151—171 (1972)

Magleby, K.L., Stevens, C.F.: A quantitative description of end-plate currents. J. Physiol. **223**, 173—197 (1972)

Oomura, Y., Tomita, T.: Some observations concerning the end-plate potential. Tohoku J. Exp. Med. **73**, 398—415 (1961)

Takeuchi, A., Takeuchi, N.: Active phase of frog's end plate potential. J. Neurophysiol. **22**, 395—411 (1959)

Received: September 10, 1976

Dr. Hiroshi Yagi
Teruo Hashimoto
Faculty of Engineering
Toyama University
Takaoka, Japan

Keiro Sugimoto
Faculty of Education
Toyama University
Toyama, Japan

Biol. Cybernetics 26, 131—139 (1977)

Biological Cybernetics

Multidimensional Analysis of Sleep Electrophysiological Signals*

D. Burger, P. Catani, and J. West

Laboratoire de Neurophysiologie Clinique et de Psychophysiologie Expérimentale (Groupe INSERM U. 144), Hôpital Henri Rousselle, Paris, France, and Istituto di Psicologia, Bologna, Italy

Abstract. A night sleep polygraphic recording was coded by 20 s epochs, taking into account the recognizible features, summarized into 24 variables. In a 24 dimension space, the values of these variables are the coordinates of a point representative of each 20 s epoch. The coordinates of these points are given by a 24 column data table to which a factor analysis is applied in order to provide a bidimensional representation of the electrophysiological phenomena's evolution in time. Such a representation of the possible combinations of variables illustrates the structure of sleep without any biased ideas about this structure. The results obtained make it possible to consider the classical division of sleep into cycles and stages. Sleep seems to evolve continuously in time between a certain number of typical combinations, which supports the concept of cycle, but never following the same evolution between these combinations, which questions the reality of stages and their similarity from one cycle to the other.

The method described seems to reflect more accurately than the classical hypnogram the phenomena of continuous modulation of nervous activity during sleep, and to open interesting possibilities for an analytical automatic treatment of sleep electrophysiological signals.

Introduction

The visual scoring of a polygraphic sleep record requires the analysis, by the human brain, of a large number of electrophysiological signals which are both simultaneous and diverse in nature, comprising the electroencephalogram (EEG), electrooculogram (EOG), electromyogram (EMG), and respiratory rhythm (R).

This usually results in the breaking-down of sleep into "stages", that is to say, categories supposed to be homogeneous as regards the combinations of variables which constitute them, and as regards the psychophysiological states which these combinations define. This breaking-down leads, on the one hand, to the representation of sleep in the form of a hypnogram, on the other hand to quantifications in percentages of total sleep time occupied by the different stages.

The heuristic value of such a procedure is quite obvious, since it permits, in a relatively economic manner, a high degree of data reduction to be attained. But it is equally evident that the decision to classify such or such an electrophysiological configuration in a given stage is, whatever the classification accepted (Loomis et al., 1937; Dement and Kleitman, 1957), whatever the text book taken as reference (Rechtschaffen and Kales, 1968) or whatever the experience of the electrophysiologist, tainted with subjectivity or even arbitrariness.

It can schematically be said that human subjectivity intervenes at two levels:

a) During the reading of the record, in the evaluation of the signals (frequency, relative amplitude, waveform, topography, rhythmic organisation, etc.). Automatic programmes for signal analysis and pattern recognition will in the future eliminate this possible source of error.

b) During the treatment of this varied information, in overrating certain signals and minimizing others to validate the diagnosis of a particular stage.

The aim of the present work is to attempt to remove the human subjectivity in the treatment of the information [level b)], by applying a programme of multidimensional data analysis, a domain where the computer works more systematically than the human

* Supported by Grant CRAM Paris No. 1871973 and by International Contract between Consiglio Nazionale delle Ricerche and C.N.R.S.

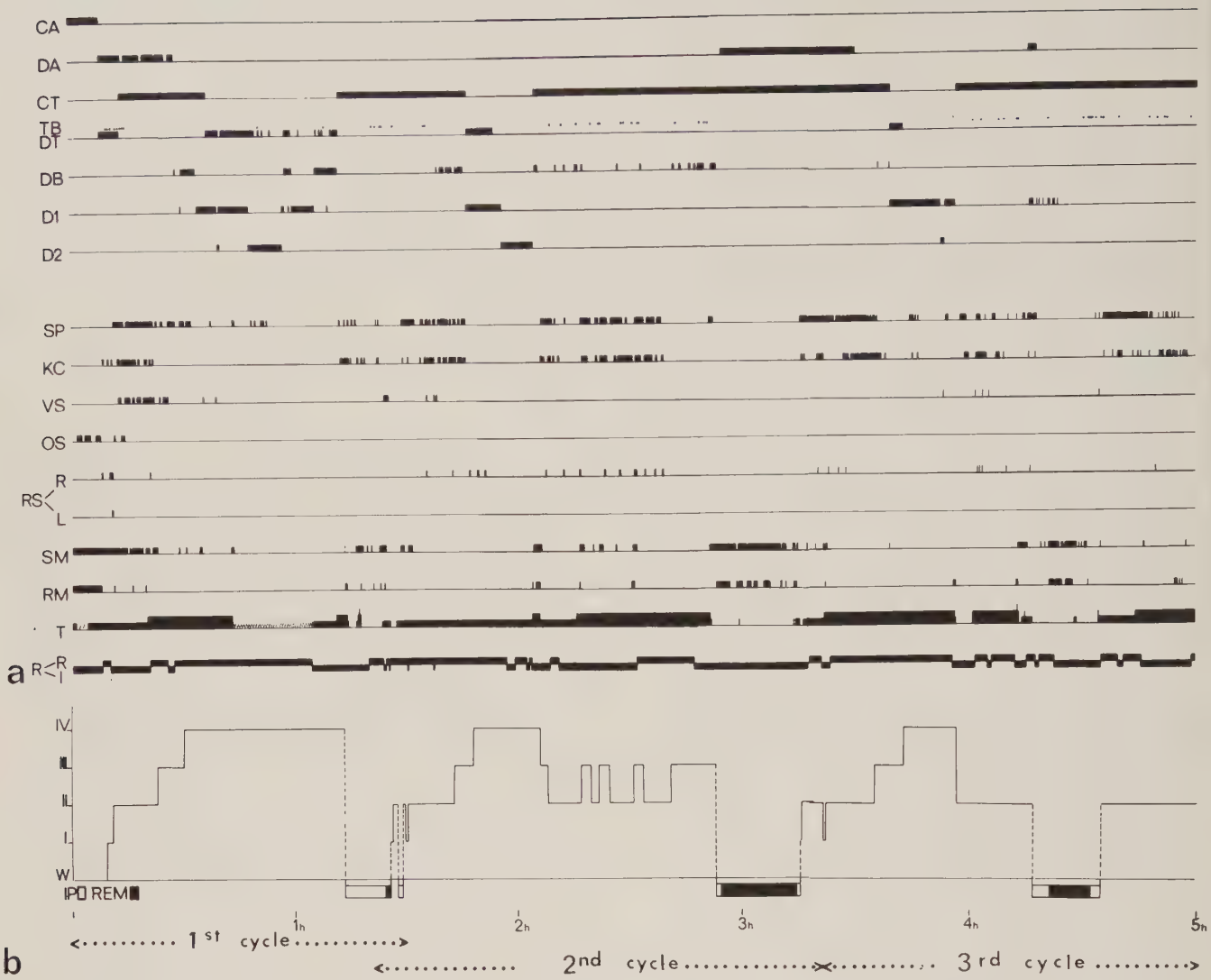

Fig. 1a and b. Two modes of graphic representation of the visually analysed data. **a** Distribution of the variables in time: For the firsts 16 variables (from top to bottom), value 1 is represented by a vertical line covering the 20 s epochs where it occurs, or by a point (variable TB). For variable T, complete atonia (T_0) is represented by the horizontal baseline; very feeble activity (T_1) by hatchings; feeble, average and maximum activity (T_2, T_3, T_4) by vertical lines of increasing height. For variable R, regular and irregular respiratory rate (RR, IR) are represented by vertical lines situated respectively above and below the baseline. One can note that the cyclic organization of sleep is mainly observable by the evolution in time of those EEG variables which define the continuous background activity (CA to D_2). **b** Hypnogram: Abscissa: time in hours, ordinate: stages of sleep as defined by classical criteria, W = waking; I, II, III, IV = Stages I to IV of NREM sleep, IP = Intermediate phases represented by white squares, REM = REM sleep, represented by solid blocks. Under the abscissa are marked the temporal limits of the three analyses performed (slight overlapping between the first and second analyses)

brain. The part of subjectivity defined at level a) is not avoided, since this programme treats visually detected elementary signals. Nevertheless, the technique applied here seems to lead to interesting openings in the study of both the instantaneous and the sequential organisation of electrophysiological sleep patterns: inasmuch as it makes it possible to break from the *a priori* classification of sleep into stages, and to investigate whether the successive combinations of primary signals organize themselves into more or less stable or stationary structures, which in turn could define stages or validate *a posteriori* an already established classification.

Materials and Methods

Source of Data and Selection of Variables

The work presented here is concerned with the analysis of the first three cycles in the all night sleep of a normal four-year-old child. This particular sleep recording was chosen because of its classic cyclic structure, evident from visual analysis and from hypnogram representation (cf. Fig. 1b).

The paper recording, run at 15 mm/s, consisted of 16 channels:

12 EEG (time constant 0.3 s, 9 monopolar, 3 bipolar).

2 EOG (time constant 6 s, vertical and horizontal eye movements—E.M.—).

1 respiration (time constant 0.1 s).

1 EMG (time constant 0.1 s).

The visual analysis was carried out in 20 s epochs, each being one page of the recording.

For each of these epochs, the presence or absence—coded 1 or 0 respectively—of the following features was noted[1]:

Continuous occipital alpha	CA	Vertex spikes	VS
Discontinuous alpha	DA	Occipital spikes	OS
Continuous theta	CT	Rolandic spikes-right	RSR
Diffuse theta	DT	Rolandic spikes-left	RSL
Theta bursts	TB	Slow eye movements	SM
Delta bursts	DB	Rapid eye movements	RM
Spindles	SP	Twitches	TW
K complexes	KC		

The presence of delta rhythms was coded at two levels, according to increasing abundance, amplitude and diffusion:

Delta 1 D_1 Delta 2 D_2

The electromyographic activity, recorded from the chin, was coded according to the amplitude, at five levels:

Complete atonia	T_0	Average activity	T_3
Very feeble activity	T_1	Maximum activity	T_4
Feeble activity	T_2		

The respiration was coded as either regular RR or irregular IR.

We have been able to define a vector of which each of the 24 coordinates is of value 0 or 1, and which indicates the electrophysiological state of the sleeper during the 20 s of one page. If a time reference, which will be the number, in order, of the epoch is added, we can reduce 60 min of sleep to a table consisting of 180 rows and 25 columns.

To illustrate the three cycles of sleep studied here, we have used:

first the graphical presentation proposed by Salzarulo et al. (1975) of the simultaneous evolution with time of the above mentioned variables (Fig. 1a);

second, the hypnogram, drawn on the same time scale, with the criteria currently in use in our laboratory (Fig. 1b); this includes the four classical stages of NREM sleep (non rapid eye movement sleep, or slow sleep, or orthodox sleep), REM sleep (rapid eye movement sleep, or rapid sleep, or paradoxical sleep), and also the intermediate phases (IP) as defined by Lairy et al. (1968). The hypnogram was based not on the tables of detailed variables which served for Figure 1a, but on looking again at the record itself to determine, in a more holistic way, the beginnings and ends of the different "stages".

The hypnogram gives a very reduced representation of the phenomena. The comparison of the two graphs shows some gross correspondances between, for instance, D_1-D_2 and Stage IV, T_0-RM and REM sleep. It also shows clearly that what is recognized as one and the same "stage" on the hypnogram is not always characterized by the same variables. Figure 1a enables us to read the simultaneous evolution with time of the variables more clearly than from the tables of 0_s and 1_s supplied to the computer; however, to determine the significant groupings of variables, their redundancy from one cycle to another, etc., makes statistical treatment necessary.

Mathematical Methods

The mathematical method used, the analysis of correspondences proposed by Benzecri et al. (1973) has been successfully applied to a large number of cases in which the data were in analogue form. In common with all factorial analysis methods, it seeks, in a 24 dimensional space, the successive axes with respect to which the

[1] For definitions see Storm van Leeuwen et al. (1966) and Rechtschaffen and Kales (1968)

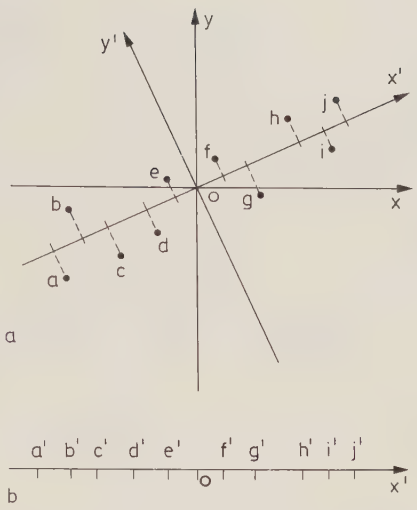

Fig. 2 a and b. Illustration of the general problem to be solved by the factorial analysis. It consists in finding the best approximation of a cloud of points by projecting it on a hyperplane whose dimension is inferior to that of initial space. In the case of this figure, **a**, the hyperplane is just a straight line. The projection of the cloud on the axis on which it is as little distorded as possible provides an approximate representation of the initial data, **b**. This representation facilitates the study of the structure of a cloud, with the drawback of loss of information

inertia of the cloud of points will be at a minimum i.e. the variance will be at a maximum. The following example (Fig. 2) should help to explain the idea underlying the mathematical theory: let there be a plane, with two cartesian axes Ox and Oy, in which is a cloud of points. The information attached to each point is the knowledge of its position in the plane, i.e. its two coordinates with respect to the axes Ox, Oy. In the diagram, it can be seen that the total information attached to the cloud is more or less equally shared between the two axes. However with the axes Ox', Oy' almost all the information is contained in the Ox' coordinates. This can be seen by projecting the cloud onto the axis; the projected cloud differs only slightly from the original. It can be said that the percentage of the variance with respect to Ox' is greater than that to Oy'. In representing the cloud by its projection on Ox' (1 dimensional), we have achieved a reduction of data, since now only one parameter is necessary for the definition of each point, whereas originally two were needed. The loss of information is minimal when the inertia of the cloud with respect to the axis of projection is at a minimum—the ideal situation is obviously that where the cloud of points is purely linear along the axis Ox'; its inertia with respect to this axis would then be zero. In the general case where there are more than two dimensions the axis of minimal inertia is called the 1st factor, the following orthogonal axis the 2nd factor, etc.

The plane formed by the 1st and 2nd factors serves as the main plane of projection and the cloud represented in it has a minimal loss of information. It is primarily this representation which interests us here.

The particular merit of the factor analysis of correspondances is its χ^2 metric and the possibility which it offers to represent in the same graph the items (the 20 s sleep epochs), and the characters (the 24 variables defined above). In effect, in this analysis the items and characters play symmetrical roles.

The graphs can be interpreted:

from the point of view of the items, in looking for their geographical groupings; items having similar characteristics are close

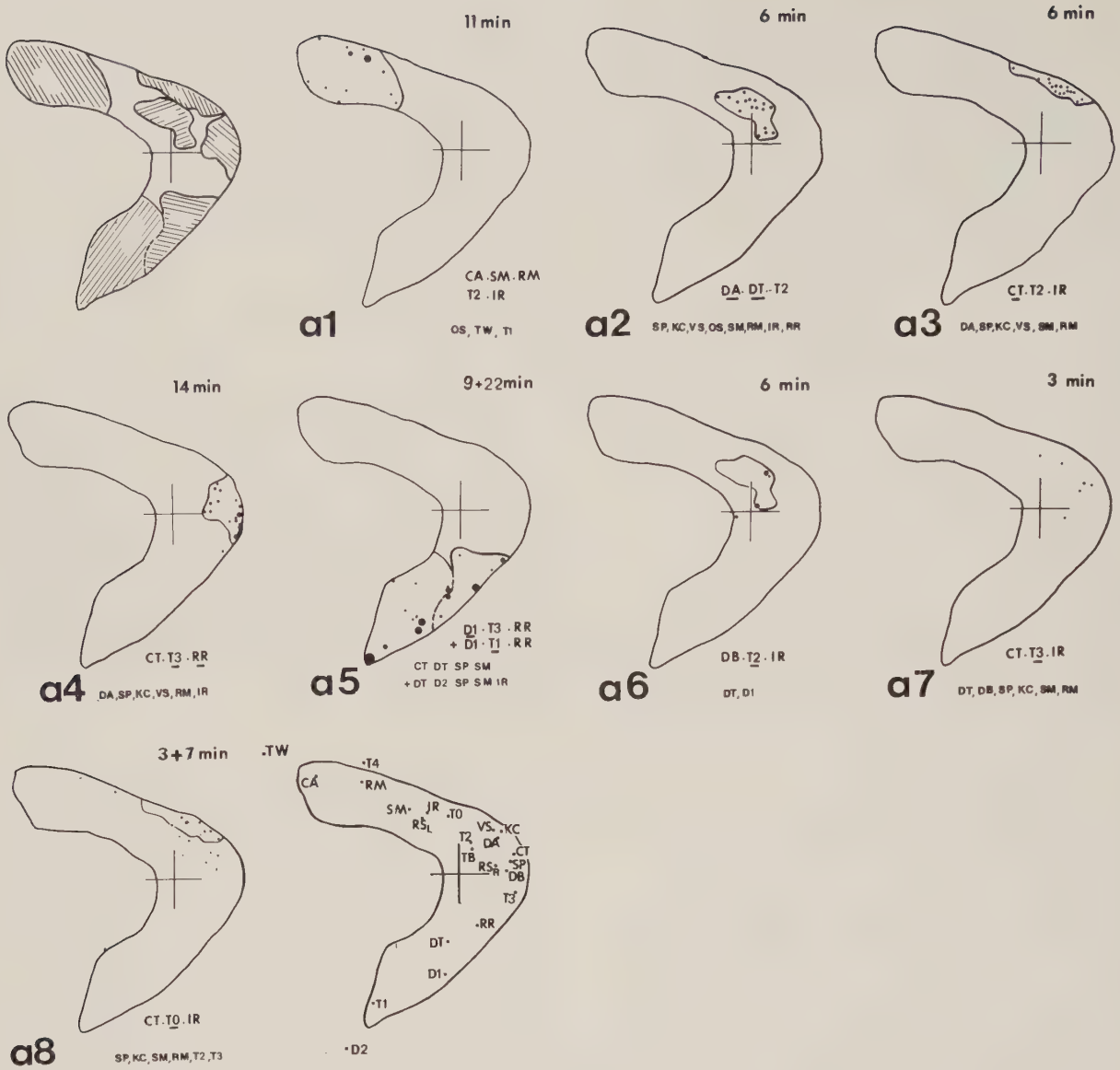

Fig. 3. Graphic results of the first analysis (first cycle). First graph, top left: zones of the whole cycle within the boomerang-shaped envelope, last graph, bottom right: respective positions of the variables graphs a1 to a8: successive zones or clouds of points during the cycle. The variables whose value unquestionably influences the position of points in the plane of projection are the following, in order of decreasing importance: T_1, CA, D_2, RM, D_1, SM, CT, RR, IR, OS, T_3, SP, DT. Variables DA, TB, DB, KC, VS, RSR, RSL, TW, T_0, T_2, T_4, remain out of the list; this explains that points characterized by primary and secondary variables which are different but of weak or null influence can group themselves in similar zones (cf. a2 and a6), and these zones thus are of little significance. Other zones, on the contrary, characterized by "strong" variables have a high significance (cf. a1, a3, a5, a8). The zone drawn on a5 includes two zones grouped together because of their temporal and spatial closeness

to each other in the graph. We shall try to find which values of the variables are typical of the groups shown;

from the point of view of the characters; those with strong correlations appear near to each other on the graph. The most significant points are situated on the convex face of the envelope of the cloud;

lastly, the simultaneous representation of the items and characters allow qualitative interpretation of the position of the items, with respect to the characters which define them. By this statistical method, an item will appear on the map at the center of gravity of the characters, the masses of which are their conditional frequencies.

Treatment-Results

Separate analysis was carried out for three sets of the initial data, corresponding approximately to the first three cycles of all night sleep. Our first aim being to test the performance of the method, the three sets treated were relatively short: 88, 120, and 99 min respectively, i.e. 264, 360, and 297 items; however, each of these sets covered a whole cycle of sleep, i.e. an NREM phase plus an REM phase, which thus

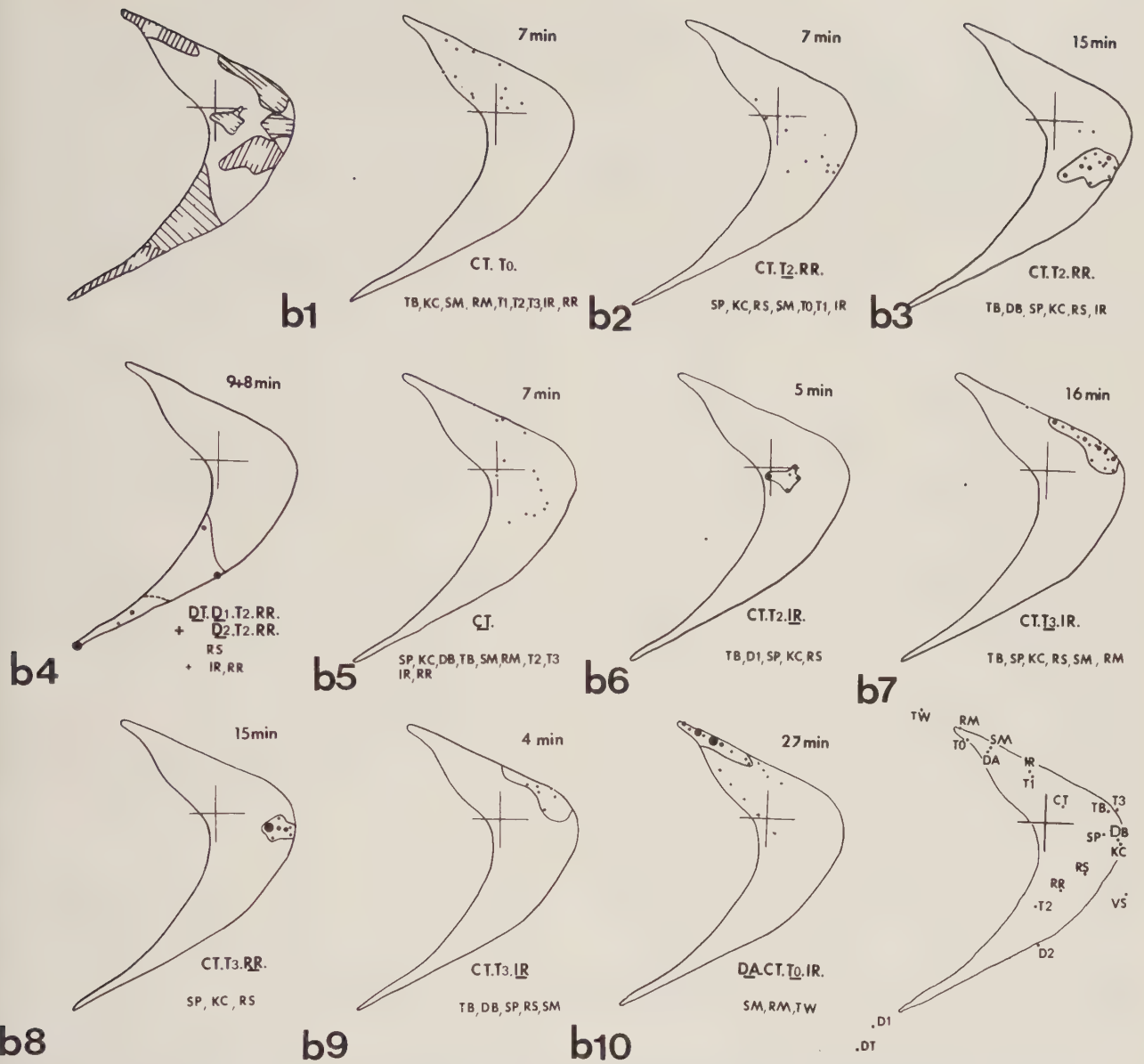

Fig. 4. Graphic results of the second analysis (second cycle). See legend Figure 3. The variables whose value unquestionably influences the position of points in the plane of projection are the following, in order of decreasing importance: D_1, DT, T_0, SM RM, DA, T_2, T_3, RR, SP, KC. Variables CA, CT, TB, DB, VS, OS, TSR, RSL, TW, D_2, T_1, T_4, IR, remain out of the list. The zone drawn on b4 includes two zones grouped together because of their temporal and spatial closeness

permited comparison of the three cycles with each other.

Each analysis gives, in the plane of the two first factors, a point for each original 20 s sequence; these together constitute the cycle.

To make clearer the presentation, as well as to illustrate the interesting phenomena, each cycle has been divided into shorter sequences, in which the representative points lie within a well defined zone (Figs. 3–5).

The first graph of each series shows the various zones of the whole cycle. In the following graphs, the contour of a zone is drawn whenever the period described in a certain graph has also served to define the particular zone. One can thus meticulously follow the course of the successive sequences and observe a reasonably continuous evolution of the representative points. The final graph of the series gives the respective positions of the variables.

The duration of each period is noted by the side of the corresponding graph. The chronological order of the periods has been respected in the figures, which must be read from left to right and from top to bottom. For each zone, we call "primary variables" those

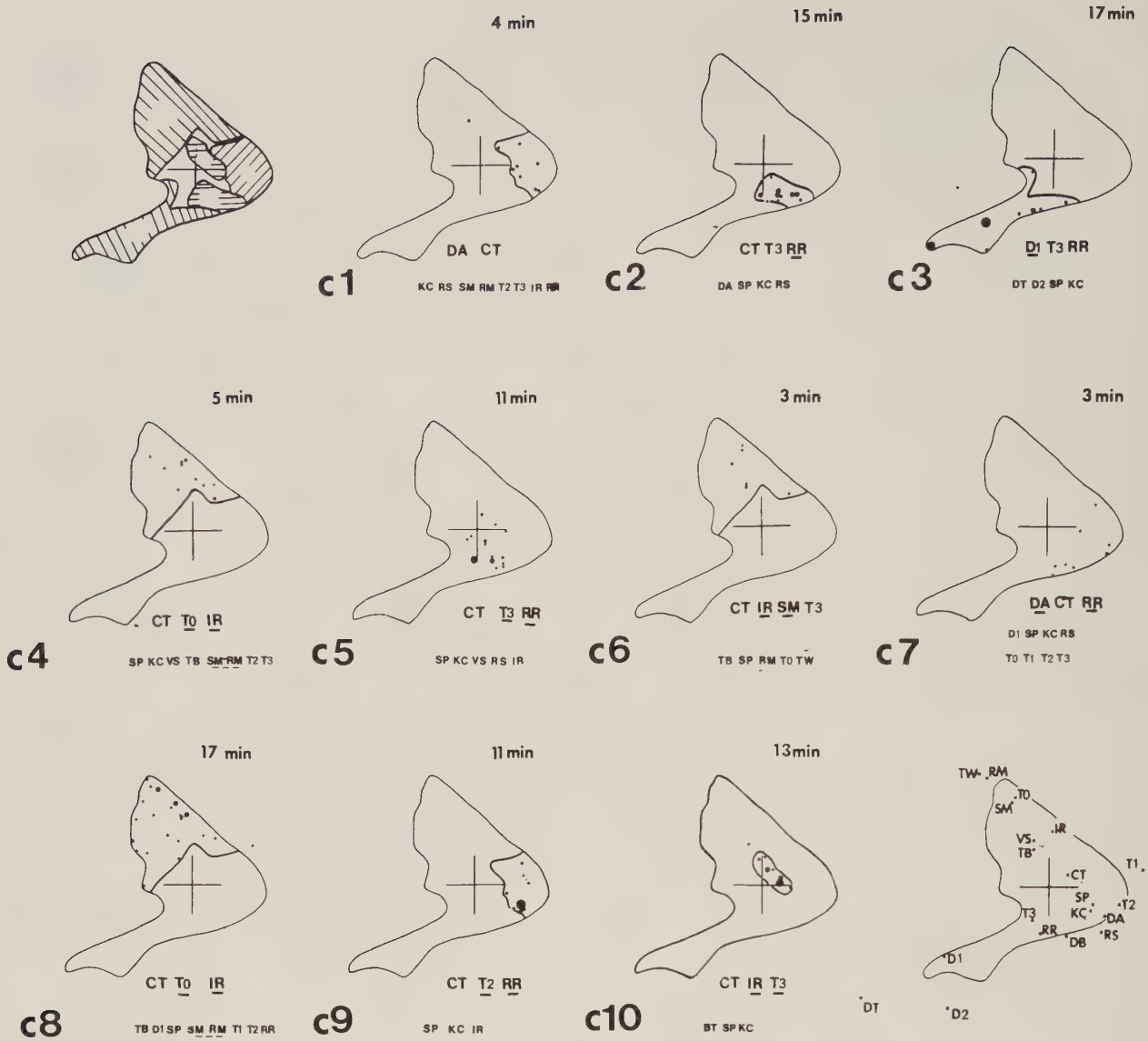

Fig. 5. Graphic results of the third analysis (third cycle). See legend Figure 3. The variables whose value unquestionably influences the position of points in the plane of projection are the following, in order of decreasing importance: D_1, DT, T_0, SM, RM, IR, RR, T_2, T_3, SP, KC, DA. Variables CA, CT, TB, DB, VS, OS, RSR, RSL, TW, D_2, T_1, T_4, remain out of the list

which have the value 1 for all the points in the zone, i.e. they characterize the corresponding period of sleep. These variables are noted in large letters by each graph. However, those variables having the value 1 for certain of the points only, are named "secondary variables"; they explain the different positions of the points inside each zone and indicate the electrophysiological fluctuations during the period in question. These are noted in smaller letters under the primary variables.

Further, the primary and the secondary variables explaining the passage from one zone to another are underlined.

General Results

The decrease of the eigen values is satisfactory in the three analyses. This means that the percentage of the variance explained by the successive factors decreases regularly. The order of importance of the factors proves to be well determined and there is no chance that a slight modification of the data would change the representation plane as would be the case if the 2nd and 3rd factors, for example, explained percentages equal or close to the variance. The percentages of the variance explained by the two first factors are respectively 28%, 31%, and 26%.

It should be noted that the enveloping curve of the representative points takes, for each cycle, the shape of a boomerang. This form depends on the method of analysis employed, and is generally known as the "Guttmann effect".

Characters (Variables); Comparison of the Structures of the Three Cycles

Looking at the last graph (bottom right) of Figures 3–5, obvious differences in structure of the three cycles appear, due to:

Differences in the factors. In other words, the variables which explain the position of the representative point in the projection plane are not the same from one cycle to the other. However, a closer resemblance between the 2nd and the 3rd cycles than between the 1st and 2nd cycles should be noted.

Changes in the relative positions of most of the variables.

However, aside from these differences, it can be noticed that there exist general groupings common to all three cycles: in the upper zone, the grouping (TW, RM, SM, IR), in the lower zone the grouping (D_1, D_2, DT, RR) and in the middle zone, the grouping (SP, KC, DB, CT, TB); in this latter zone, the proximity of SP and KC is noticeable for every cycle. This enables a common significance to be given to certain phenomena visible in the different figures.

Items (Sequences); Evolution with Time

The successive periods of sleep, represented by the successive graphs, a1 to a8, b1 to b10, c1 to c8 in Figures 3–5, show a pattern consisting of a descent towards the lowest zone followed by an ascent to the upper zone; the final period in the upper part of the boomerang is particularly long for cycles 2 and 3.

The extreme zones correspond reasonably well from one cycle to the next. The upper zones are characterized, for the second and third cycles, by the combination of the variables TW, RM, SM, T_0, IR; the first cycle differs from the two others in, essentially, the EMG and the continuous alpha rhythm.

The lower zones are characterized, for the three cycles, by the combination RR, D_1, D_2. However, the identification of these zones can only be partial, because of the differences in EMG and in several secondary variables.

No identification is possible for the medial zones; moreover, the number of these zones is not consistent, and the combinations of the variables change from one cycle to another. The studied phenomena are thus heterogeneous, and present new combinations for each cycle.

Table 1

Graph	Duration	Stage	Primary variables
c1	4	I II	Da CT
c2	15	II III	CT T_3 RR
c3	17	IV	D_1 T_3 RR
c4	5	II	CT T_0 RR
c5	11	II	CT T_3 RR
c6	3	II	CT T_3 IR
c7	3	IP	DA CT RR
c8	17	REM	CT T_0 IR
c9	11	II	CT T_2 RR
c10	13	II	CT T_3 IR

Comparison with the Visual Analysis

In all 3 figures, the same descending-ascending evolution of the representative points can be observed and compared to the ascending-descending slopes of the cycle as shown in the hypnogram.

More precise comparison of the figures representing the three cycles with the corresponding parts of the hypnogram indicates that Stages IV and REM only correspond in a very coherent way to the extreme zones of the boomerang (the highest and lowest respectively). Stage I, however, does not occur often enough to give its own particular zone. Stages II and III, and the IPs are dispersed among the medial zones without there being any clear correspondence between zone and stage. Also, changes of zones occur without there being a change of stage, and vice-versa. The third cycle for example, presents the two situations, the comparison of which is given in Table 1.

It is the modifications in the EMG and the respiration which are the primary cause of the diversity of the zones classed Stage II in the middle and at the end of the cycle. The presence of eye movements in the graphs c4 and c6 only further this heterogeneity of the stage classed II.

Discussion

Data Collection and Processing

Several points can be critized concerning our method.

As we stressed at the beginning of this paper, we have not managed to avoid all subjective errors since the data are visually collected. Although very detailed and painstaking, the method of visual collection of electrophysiological signals leaves out a large number of parameters such as the amplitudes of alpha and theta rhythms, the frequencies within the alpha, theta, delta ranges, etc.

Coding in a finite number of modalities contributes to render discrete the evolution with time of the representative points on the graphs. Thus, the passage

from one zone to another can be explained as the passage from one modality to another.

It is likely that a more accurate way of data quantification would give a more continuous evolution of the points.

Also, the choice of the duration of the elementary epochs, fixed at 20 s, has two consequences: first, the observed phenomena, i.e. the formation of the zones, are necessarily of much greater length than that of one elementary epoch; in other words, a "microstage" would pass unnoticed; for example, in graphs b6 and b7, an isolated point exists outside the zone. It is interesting to speculate as to what grouping would replace the two points if the elementary epochs had been shorter;

second, the transitory electrophysiological signals, called "phasic" sleep phenomena (such as RM, SM, SP, KC ...), whose actual duration in an elementary epoch is much less than 20 s, are given the same value as continuous "tonic" phenomena covering the 20 s of an epoch.

Finally, the statistical method used gives unequal weight to items and characters: an item gets the more weight as the combination which represents it is rich in 1_s; a character gets the more weight as the number of items of value 1 for this character is high. An improvement of the method, at the price of increased computing time, would consist in doubling the 0 and 1 Table (T) with its complementary Table in 1 and 0 ($\bar{T}$) and to build the double Table

T	$\bar{T}$
$\bar{T}$	T

Whatever its insufficiencies, the method used treats all the raw information gathered by the human eye in a more precise manner than the eye does, and consequently enables us to compare visual and automatic treatments.

Results

Two important points must be recalled:

First, the zones drawn on the graphs of Figures 3–5 were not obtained through computation, but only represent a convenient way to summarize the temporal evolution of the phenomena.

Second, as already stated, the principal planes defined for the three analyses only explain respectively 28%, 30%, and 26% of the variance. Taking into account the number of initial variables, these results will not surprise those who are familiar with the methods of factor analysis; however, one must consider the 70% of unexplained variance and examine the factors found by statistical analysis beyond the two first factors. Taking the 3rd cycle as an example, the third factor is almost confused with variable D_1 and explains 9.2% of the variance; the fourth factor is confused with T_1 and explains 7.4% of the variance; the fifth factor is confused with PVR and explains 7.3% of the variance. Thus, five factors are necessary to explain 50% of the variance, and thirteen to explain 90%.

As a matter of fact, the information provided by the knowledge of these variables is not completely lost in the projection on the plane of the two first factors. Their variations lead to fluctuations of the representative point within a given zone. A close confrontation of the graphs with the initial data can help in the interpretation of these phenomena; this is the reason why we have represented inside each zone, the primary and secondary variables, as a reminder of the initial data.

Let us now see how the results obtained fit with the classical notions of sleep cycles and sleep stages.

1. The reality of sleep cycles is strongly supported by the statistical analysis performed here. But it is also clear that the successive cycles of a given night's sleep are not strictly equivalent to each other. Thus, although there is a periodicity in alternating NREM and REM phases, the process of alternation is not as regular as was first assumed (Aserinsky and Kleitman, 1953).

2. The definition of sleep stages needs to be specified. If one accepts that a "stage" implies a relatively stationary combination of primary signals over a certain period of time, then each zone, as defined above, could be considered as representing a stage.

One must then recall that:

i) The number of zones drawn on Figures 3–5 is superior to the number of stages classically recognized;

ii) The stationary combinations which define the zones vary from one cycle to the other. It is most likely that another night sleep record of the same subject, or the night sleep record of another subject, would have provided stationary combinations different from those obtained here;

iii) the dispersion of these stationary combinations, due to the secondary variables, and the shifts from one to the other, lead to a relatively continuous representation of the phenomena, contrary to the classification into stages which is, by definition, discontinuous, as expressed by the horizontal and vertical lines on the hypnogram. A continuous representation is reminiscent of the one attained by Dirlich et al. (1973) by quite different mathematical procedures. It is also in agreement with the neurophysiological evidences of a continuous modulation

of neuronal activity of pontine units all over the sleep cycle as shown by Mc Carley and Hobson (1975). In any case a continuous representation of sleep cycles solves the difficulty, familiar to all electrophysiologists, of the criteria of stages and of their limits. An example is provided by the intermediate phases as shown on graphs a3 (Fig. 3), c4, and c6 (Fig. 5) where zones identical to the ones of REM sleep appear within NREM sleep, virtually as if REM were present during some phases of NREM sleep. Incidentally, one can note that the statistical method used here seems to be more accurate than visual analysis in identifying the intermediate phases. These remarks suggest that sleep should be considered as a most complex phenomenon, whose electrophysiological signals evolve continuously with time between a certain number of typical combinations through modalities which are never exactly the same.

Perspectives

The research presented here could be developped in two opposite ways.

1. One should consist in finding the same factors for all cycles of the all-night sleep record. This would allow a better comparison of the different cycles with each other since they would be represented on the same plane of projection. Of course, this would involve the drawback of a loss of precision for each individual cycle since the common plane of projection, optimal for all cycles taken together, would not be optimal for each cycle taken individually.

At a later stage one could foresee realizing an analysis (either cycle by cycle or considering the whole night record) on several records of the same subject or even of different subjects, in such a way as to establish whether a universal plane of projection exists despite the intra and inter-individual variability. If such a plane exists, one would only need to project the data on it to obtain a bidimensional description of sleep. The mathematical operation would then be simple and would be performed by a relatively simple and inexpensive programme. But the existence of such a plane, common to every type of sleep, is most questionable.

2. The other way to develop the method would be, on the contrary, to treat more variables and more precisely defined ones. The method tested here constitutes a first step towards the processing of sleep electrophysiological signals, freed from both human subjectivity and the *a priori* classification into stages. A further step, the collection of primary data by sophisticated automatic procedures, will permit multiplication of the number of signal parameters and of combinations of primary variables, and description of the temporal organization of the successive sleep cycles in conformity not with a model but with the physiological reality. If this step can be reached, it will fulfil Jeannerod's (1975) wish "Neuronal data are" (at present) ... "poorly related with paradoxical sleep and slow sleep considered as 'states'. A first methodological step to reconcile neuronal data with sleep would be to break the states into as many subroutines as possible. Such a reductionistic attitude ... may 'compatibilize' sleep phenomena with discrete neuronal changes ... This will offer an opportunity to reconstruct a new conceptual frame ... on a purely physiological basis."

References

Aserinsky, E., Kleitman, N.: Regularly occurring periods of eye motility and concomittant phenomena during sleep. Science **118**, 273—274 (1953)

Benzecri, J. P.: L'analyse des données. Paris: Dunod 1973

Dirlich, G., Friedrich-Freksa, C., Schulz, H.: A time-dependent model of the sleep EEG. In: Koella, W. P., Levin, P. (Eds): Sleep. Basel: Karger 1973

Jeannerod, M.: Changes in neuronal activity during sleep. Relevance to the sleep-center theory. In: Lairy, G. C., Salzarulo, P. (Eds.): The experimental study of human sleep: methodological problems. Amsterdam: Elsevier 1975

Lairy, G. C., Goldsteinas, L., Gennoc, A.: "Phases intermédiaires" du sommeil de nuit des malades mentaux. In: Wertheimer, P. (Ed.): Rêve et conscience. Paris: P.U.F. 1968

Loomis, A. L., Harvey, E. N., Hobart, G.: Cerebral states during sleep as studied by human brain potentials. J. exp. physiol. **21**, 127—144 (1937)

Mc Carley, R. W., Hobson, J. A.: Neuronal excitability modulation over the sleep cycle: a structural and mathematical model. Science **189**, 58—60 (1975)

Rechtschaffen, A., Kales, A.: A manual of standardized terminology, techniques and scoring system for sleep stages of human subjects. Washington: Public Health Serv., U.S. Gover. Print Off. 1968

Salzarulo, P., Pelloni, G., Lairy, G. C.: Semeiologie electrophysiologique du sommeil de jour chez l'enfant de 7 à 9 ans. Electroenceph. clin. Neurophysiol. **38**, 473—494 (1975)

Storm van Leeuwen, W., Bickford, R., Brazier, M., Cobb, W. A., Dondey, M., Gastaut, H., Gloor, P., Henry, C. E., Hess, R., Knott, J. R., Kugler, J., Lairy, G. C., Loeb, C., Magnus, O., Oller-Daurella, L., Petsche, H., Schwab, R., Walter, W. G., Widen, L.: Proposal for an EEG terminology by the Terminology Comitee of the International Federation for Electroencephalography and Clinical Neurophysiology. Electroenceph. clin. Neurophysiol. **20**, 306—310 (1966)

Received: September 27, 1976

D. Burger
Hôpital Henri Rousselle
1, rue Cabanis
F-75674 Paris/Cedex 14, France

Biol. Cybernetics 26, 141—150 (1977)

Biological Cybernetics

Modelluntersuchung zur Prüfung der Wertigkeit dynamischer Testverfahren für die Herz-Kreislauf-Regulation unter Verwendung determinierter Signale

K. Balla

Carl-Ludwig-Institut für Physiologie der Karl-Marx-Universität Leipzig (Direktor: Prof. Dr. sc. med. H. Drischel), DDR

Model Considerations for the Evaluation of Dynamic Test Methods of Cardiovascular Control Founded on Determinist Signals

Abstract. The clinical examination of the cardiovascular systems efficiency based on methods of control theory demands favourable input signals and suitable response characteristics. In this paper by means of modelling it was intended to find aspects, which should allow to evaluate several test methods with regard to their correspondence to specific claims. A control model used for this purpose represents the baroceptor control of systemic arterial pressure by physical work-load. Its alterations were considered in step, stair, ramp, and sinusoidal form. According to a judgement founded on theoretical and practical aspects, the aperiodic input changes prove to be advantageous. Especially the ramp test function seems to be suitable for selection of output components issuing from physical and mental parts of work-load.

1. Einleitung

Über die Wahl des Testsignals

Deterministische Testsignale, welche zur Untersuchung des Leistungsvermögens des Herz-Kreislauf-Systems üblicherweise verwendet werden, können periodisch oder aperiodisch sein (Wigertz, 1970; Tiedt u. Mitarb., 1972, 1975; Karlsson u. Wigertz, 1971). Eine solche Einteilung ist bedeutungsvoll, weil gerade nach der dabei zugrunde gelegten Eigenschaft eine scharfe Trennlinie zwischen verschiedenen miteinander konkurrierenden Möglichkeiten sowohl in den theoretischen Methoden der Systemanalyse als auch in der praktischen Erzeugung der Testsignale und der Auswertung der Systemantworten verläuft. Die Wahl der einen oder der anderen Möglichkeit muß sich aus der Suche nach dem zweckmäßigsten Weg ergeben, der bei einem konkreten Problem zum Ziele führt. Dies würde bedeuten, daß man einfache Testsignale verwendet, die eine wohldefinierte, gut erkennbare und quantitativ leicht auswertbare Auswirkung der Systemeigenschaften auf die Antwortfunktion ermöglichen.

Nach diesen Gesichtspunkten scheinen die aperiodischen Testsignale im Vorteil zu sein, die ja die Information über die Systemeigenschaften schon in der transienten Phase der Antwort auf die oben geforderte Art zum Ausdruck bringen.

Im Gegensatz zur theoretisch-analytischen Untersuchung, bei denen man mit idealisierten Verhältnissen zu tun hat, ist bei der Deutung experimenteller Untersuchungen eine hinreichend gute mathematische Approximation der physikalischen Gegebenheiten eine grundlegende Voraussetzung. In diesem Sinne sind solche Testsignale zu bevorzugen, deren mathematisches Vorbild zum mindestens bezüglich des Funktionswertes keine Unstetigkeiten aufweist. Dies ist bei der meist bevorzugten Sprungfunktion nicht der Fall. Der Anwender solcher Methoden hat nicht immer das notwendige Gefühl zu entscheiden, ob die für sprungförmig gehaltene Änderung in der Tat noch als eine solche angesehen werden kann. Strenggenommen ist eine solche Entscheidung an Fakten gebunden, die objektiv und im voraus unbekannt sind. Deshalb ist es berechtigt, sich von vornherein auf eine wohldefinierte stetige Änderung zu orientieren, die physikalisch realisierbar ist.

Die einfachste aperiodische Zeitfunktion, die einer solchen Forderung genügt, ist der lineare Anstieg (Rampenfunktion), die bei einem Zeitpunkt $t_0=0$ beginnt

$$f(t)=\begin{cases}0 & \text{für} \quad t\leqq t_0\\ At & \text{für} \quad t\leqq t_0\end{cases}, \tag{1}$$

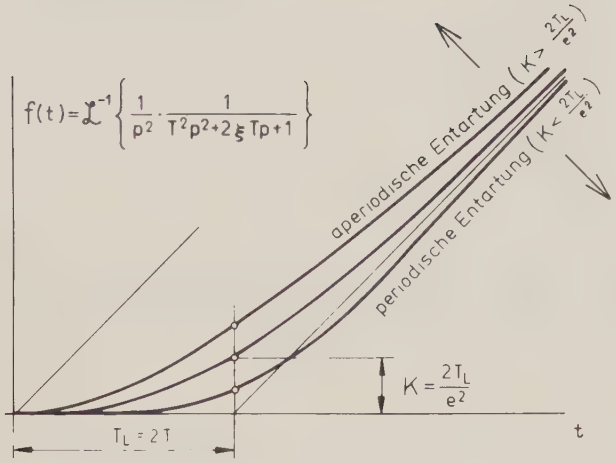

Abb. 1. Qualitativer Verlauf der Rampenantwort von linearen Systemen 2. Ordnung in Abhängigkeit der Systemeigenschaften

bzw. die daraus durch Begrenzung entstandene sog. Schrittfunktion

$$f(t)=\begin{cases}0 & \text{für} \quad t\leqq t_0\\ At & \text{für} \quad t_0\leqq t\leqq t_1\\ At_1 & \text{für} \quad t\geqq t_1\,.\end{cases} \tag{2}$$

Die Antwort eines Systems auf ein nach diesen Funktionen verlaufendes Eingangssignal gestattet ebenso seine Charakterisierung, wie dies mit der Impuls- bzw. Sprungantwort möglich ist.

Ein lineares Übertragungsglied 2. Ordnung wird oft als stark vereinfachtes Modell zur Beschreibung verschiedener biologischer Phänomene verwendet. Die Antwort dieses Übertragungsgliedes im Falle einer stoß- oder sprungförmigen Beeinflussung ist den Physiologen und den Klinikern wohlbekannt. Demnach werden im stabilen Arbeitsbereich zwei qualitativ gut abgrenzbare Verhaltensweisen unterschieden: Der periodisch bzw. aperiodisch gedämpft verlaufende Übergang in den neuen Gleichgewichtszustand (Drischel, 1966). Wird nun diesem Übertragungsglied ein rampenförmiges Eingangssignal gemäß (1) zugeführt, so werden diese Verhaltensweisen auch aus den hier erhaltenen Antworten gut erkennbar. Aus Abb. 1 kann man erkennen, daß die Antwortfunktion nach einer Übergangsphase sich asymptotisch einer Geraden annähert, deren Steigung mit der des Eingangssignals übereinstimmt und die gegenüber dem Eingangssignal um einen Betrag verzögert ist. Der Wert dieses Betrages kann unmittelbar als ein Maß für das Verzögerungsverhalten benutzt werden: Er hängt mit den Zeitkonstanten des Übertragungsgliedes definitiv zusammen. Der qualitative Verlauf der Annäherung der Asymptote durch die Antwortfunktion erlaubt eine Aussage darüber, zu welcher der beiden genannten Kategorien das System gehört. Erfolgt die Annäherung von oben, so liegt ein aperiodisch gedämpftes, andernfalls ein periodisch gedämpftes System vor.

Es bedeutet prinzipiell keine Schwierigkeit, die Rampenantwort von häufig auftretenden und erwarteten Systemtypen mit den verschiedensten Parameterkonfigurationen zu ermitteln und in Atlanten zusammengestellt als ein Hilfsmittel für die praktische Analyse zur Verfügung zu stellen. Ein ähnliches Verfahren wird auch in der Technik anhand der Gewichtsfunktionen praktiziert (Werner, 1966).

2. Theoretisches Kreislaufmodell zum Vergleich der Testverfahren

Die über die Hämodynamik vorliegenden physikalischen Kenntnisse ermöglichen die Bildung eines theoretischen Modells des Herz-Kreislauf-Systems. Es ist von vornherein wohlbekannt, daß dies nur auf der Basis einer Homomorphie erfolgen kann. Das im folgenden kurz dargelegte Modell zur Untersuchung des Testsignalproblems geht in seiner Konzeption auf Grodins (1959, 1963) und McAdam (1961) zurück. Es erfolgt hier vornehmlich die Untersuchung im geschlossenen Wirkungskreis der Barorezeptoren-Rückkopplung. Dieses Regelsystem dient als Grundmodell für die unterste Stufe in der Hierarchie der Herz-Kreislauf-Regulation. Bei der hier zu lösenden Aufgabe gilt es, die Zustandsänderungen dieses Subsystems aus der zu verrichtenden physischen Arbeit unter Berücksichtigung des damit verbundenen sympathischen Stimulus abzuleiten.

2.1. Modell des Subsystems der Eigenregulation

Für die folgende Behandlung wird eine Aufteilung des betrachteten Regelsystems wie üblich in Regelstrecke und Regler vorgenommen. Die Regelstrecke beinhaltet die beiden Herzhälften und den Körper- bzw. Lungenkreislauf. Hinsichtlich dieser Bestandteile werden folgende Idealisierungen gemacht:

1. Die für den Bluttransport notwendige Energie wird ausschließlich durch die aktive Kontraktion der Herzkammern geliefert.
2. Die Füllung des Herzens erfolgt passiv.
3. Die Wirkungsweise der beiden Herzhälften ist identisch.
4. Die Vorhöfe werden als Bestandteile der Venen angesehen.
5. Körper- bzw. Lungenkreislauf werden jeweils in drei Abschnitte konzentriert: In einen rein elastischen arteriellen bzw. venösen und einen rein resistiven peripheren Abschnitt.
6. Alle Bestandteile werden mit konstanten konzentrierten Parametern charakterisiert.

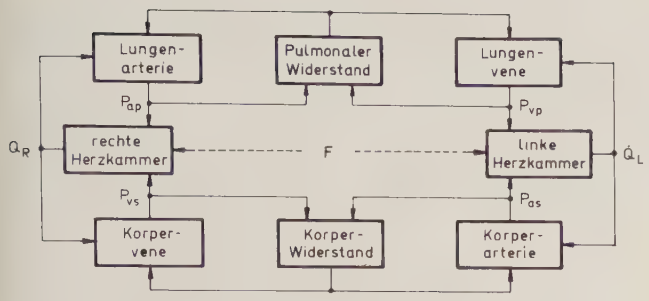

Abb. 2. Wirkungsbeziehungen in der Regelstrecke Herz-Gefäßsystem

Die mit diesen Voraussetzungen durchgeführte Modellbildung führt zu dem Gleichungssystem

$$\frac{d}{dt}\begin{bmatrix} P_{as} \\ P_{vs} \\ P_{ap} \\ P_{vp} \end{bmatrix} = \begin{bmatrix} \frac{-1}{C_{as}R_s} & \frac{1}{C_{as}R_s} & 0 & 0 \\ \frac{1}{C_{vs}R_s} & \frac{-1}{C_{vs}R_s} & 0 & 0 \\ 0 & 0 & \frac{-1}{C_{ap}R_P} & \frac{1}{C_{ap}R_P} \\ 0 & 0 & \frac{1}{1C_{vp}R_P} & \frac{-1}{C_{vp}R_P} \end{bmatrix} \begin{bmatrix} P_{as} \\ P_{vs} \\ P_{ap} \\ P_{vp} \end{bmatrix} +$$

$$+ \begin{bmatrix} 0 & \frac{1}{C_{as}} \\ \frac{1}{C_{vs}} & 0 \\ \frac{1}{C_{ap}} & 0 \\ 0 & \frac{-1}{C_{vp}} \end{bmatrix} \begin{bmatrix} \dot{Q}_R \\ \dot{Q}_L \end{bmatrix} \quad \text{mit} \qquad (3)$$

$$\dot{Q}_R = \frac{S_R C_R P_{vp}}{P_{as} + \frac{\exp(T_S/R_R C_R)}{\exp(1/FR_R C_R) - \exp(T_S/R_R C_R)}} F \quad \text{und} \quad (4)$$

$$\dot{Q}_L = \frac{S_L C_L P_{vs}}{P_{ap} + \frac{\exp(T_S/R_L C_L)}{\exp(1/FR_L C_L) - \exp(T_S/R_L C_L)}} F\,, \qquad (5)$$

das das dynamische Verhalten der Mittelwerte der wesentlichsten Zustandsgrößen des Herz-Kreislauf-Systems beschreibt. Die Wirkungsbeziehungen werden durch Abb. 2 veranschaulicht. Die Bezeichnungen haben folgende Bedeutung:

a) Zustandsgrößen

P_{as}: Druck in Körperarterie
P_{vs}: Druck in Körpervene
P_{ap}: Druck in Lungenarterie
P_{av}: Druck in Lungenvene
$\dot{Q}_R$: Herzzeitvolumen, rechts
$\dot{Q}_L$: Herzzeitvolumen, links
F: Herzfrequenz
T_S: Systolendauer.

b) Parameter — Dehnbarkeiten:

Körper-Arterie: $C_{as} = 1{,}0\ \mathrm{cm^3/mm\ Hg}$
Körper-Vene: $C_{vs} = 500{,}0\ \mathrm{cm^3/mm\ Hg}$
Pulm.-Arterie: $C_{ap} = 3{,}0\ \mathrm{cm^3/mm\ Hg}$
Pulm.-Vene: $C_{vp} = 100{,}0\ \mathrm{cm^3/mm\ Hg}$
rechter Ventrikel: $C_R = 50{,}0\ \mathrm{cm^3/mm\ Hg}$
linker Ventrikel: $C_L = 20{,}0\ \mathrm{cm^3/mm\ Hg}$

Wandspannungen:

rechter Ventrikel: $S_R = 7{,}0$ mm Hg
linker Ventrikel: $S_L = 50{,}0$ mm Hg.

Widerstände:

Körper: $R_S = f_R(P_{as})$
Lunge: $R_P = 0{,}06\ \mathrm{mm\ Hg\ cm^{-3}}$
rechter Ventrikel: $R_R = 0{,}027\ \mathrm{mm\ Hg\ cm^{-3}}$
linker Ventrikel: $R_L = 0{,}0175\ \mathrm{mm\ Hg\ cm^{-3}}$.

Die Werte der Parameter entsprechen den Angaben von Milhorn (1966).

Durch gegenregulatorische Beeinflussung der mit den obigen Zustandsgleichungen beschriebenen Regelstrecke des Herz-Kreislauf-Systems mittels Rückführungen, deren Ursprung selbst innerhalb der Grenzen dieses Systems liegt, wird auf der untersten Ebene eine Autonomie verwirklicht. Solche Beeinflussung erfolgt durch Veränderung der Herzfrequenz und des peripheren Körperwiderstandes in Abhängigkeit vom arteriellen Blutdruck im Körperkreislauf entsprechend den Differentialgleichungen

$$\tau_{RS}\frac{dR_S}{dt} + R_S = f_R(P_{as}) \qquad (6)$$

und

$$\tau_F\frac{dF}{dt} + F = f_F(P_{as})\,. \qquad (7)$$

Die Abbildungen 3 u. 4 zeigen die statischen Charakteristiken $R_S = f_R(P_{as})$ bzw. $F = f_F(P_{as})$. Für die Zeitkonstanten wurden die Werte $\tau_{RS} = 5{,}0$ s und $\tau_F = 1{,}0$ s angenommen.

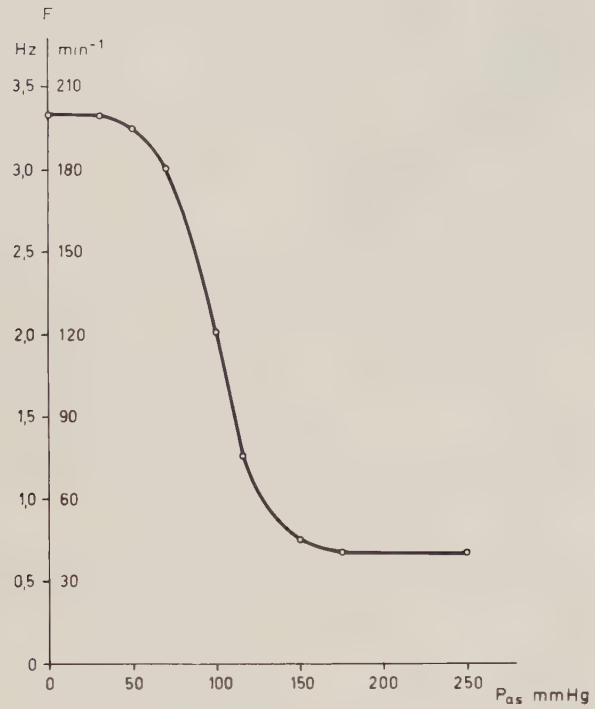

Abb. 3. Statische Kennlinie des Reglers für die Rückkopplung arterieller Druck-Herzfrequenz (nach McAdam)

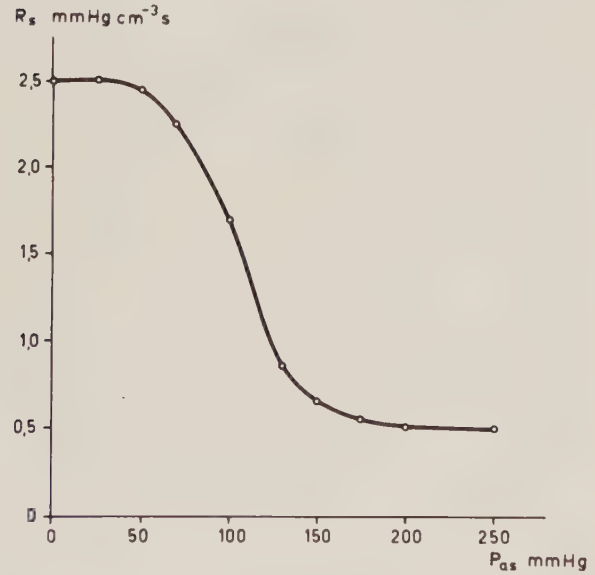

Abb. 4. Statische Kennlinie des Reglers für die Rückkopplung arterieller Druck-Körperwiderstand (nach McAdam)

2.2. Beeinflussung des Subsystems der Barorezeptoren-Regelung des Blutdrucks durch Arbeitsleistung

Der Wirkungsmechanismus der störenden Beeinflussung des sich im stationären Zustand befindenden autonomen Herz-Kreislauf-Systems wird im Falle einer submaximalen physischen Belastung mit aerobem Stoffwechsel folgenderweise berücksichtigt:

1. Proportional zur geleisteten Arbeit erfolgt über höhere Zentren eine positiv chronotrope Beeinflussung der Herztätigkeit.

2. Entsprechend der Tatsache, daß unter den genannten Bedingungen zwischen O_2-Verbrauch und Stoffwechsel eine lineare Beziehung besteht, kann für die Belastung der Sauerstoffbedarf als Bezugsgröße verwendet werden. Aus ihm werden

2a) die Senkung des peripheren Gefäßwiderstandes infolge Dilatation der Wandmuskulatur und

2b) die Erhöhung des Schlagvolumens durch Veränderung der Kontraktilität unter Einfluß des Sympathikus abgeleitet.

3. Der mit der Verrichtung der Arbeit verbundene psychische Effekt wird durch eine vorübergehende Erhöhung des Sympathikotonus berücksichtigt, die durch eine mit Beginn der Arbeitstätigkeit sprungartig einsetzende nervale Belastung im Interesse der Einhaltung der Arbeitsbedingungen ausgelöst werden könnte.

Jede dieser Einwirkungen wird für die Modellbetrachtung mittels dynamischer Übertragungsglieder quantitativ erfaßt.

Zu 1. Arbeitsleistung → Herzfrequenz

$$F = F_0 \left(1 + \frac{k_{WF}}{\tau_{WF} p + 1} W_{ph}\right), \tag{8}$$

F_0: Herzfrequenz entsprechend dem unbeeinflußten Eigenverhalten gem. Abbildung 3

$k_{WF} = 0{,}007\,\mathrm{W}^{-1}$,
$\tau_{WF} = 28\,\mathrm{s}$.

Die Erfassung des Übertragungsverhaltens in dieser Form entspricht der Arbeit von Pickering (1969), der Wert der Zeitkonstanten τ_{WF} der von Luczak u. Raschke (1975). Die Konstante $k_{WF} = \Delta F / F_0 W_{ph}$ wurde auf Grund der von Schmidt (1973) angegebenen Meßergebnisse ermittelt.

Zu 2. Arbeitsleistung → Sauerstoffbedarf

$$B_{O_2} = \frac{k_{O_2}}{\tau_W p + 1} W_{ph}, \tag{9}$$

B_{O_2}: Sauerstoffbedarf, ml/s
W_{ph}: physische Belastung, W
k_{O_2}: 0,275 ml/Ws
τ_W: 26 s.

Die Approximation des Verhaltens durch ein Verzögerungsglied mit den obigen Parameterwerten entspricht den Angaben von Luczak u. Raschke (1975), die sich auf Messungen von Stegemann (1971) und Grimby u. Mitarb. (1966) beziehen.

Zu 2a) Sauerstoffbedarf → Schlagvolumen

$$V_S = V_{S0} + k_{WS} \cdot B_{O_2}, \tag{10}$$

V_{S0} : Schlagvolumen in Ruhe, ml
k_{WS}: 1,235 s.
Der Wert von k_{WS} ergibt mit k_{O_2} in (9) eine Erhöhung des Schlagvolumens von 0,34 ml/W (Luczak u. Raschke, 1975).

Zu 2b) Sauerstoffbedarf → peripherer Widerstand

$$R_S = \frac{R_{S0}}{1 + k_{WR} \cdot B_{O_2}}, \tag{11}$$

R_{S0} : Körperwiderstand entsprechend dem unbeeinflußten Eigenverhalten gem. Abbildung 4,
k_{WR}: 0.005 s/ml.
Die Festlegung einer umgekehrt proportionalen Bewertung zwischen Sauerstoffbedarf und Körperwiderstand entspricht den physiologischen Gegebenheiten. Die Bestimmung des Koeffizienten k_{WR} erfolgte aufgrund folgender Überlegung:

Aus dem für den Körperkreislauf geltenden Zusammenhang

$$\frac{1}{R_S}(P_{as} - P_{vs}) = \dot{Q}_L = F V_S \tag{12}$$

kann unter Berücksichtigung von $P_{as} \gg P_{vs}$ für die Herzfrequenz eine Näherung

$$F \approx \frac{P_{as}}{V_S R_S} \tag{13}$$

entnommen werden. Diese für die Regelstrecke geltende Gerade bestimmt zusammen mit der Kennlinie des Reglers (Abb. 3) den Arbeitspunkt des geschlossenen Systems. In Abb. 5 werden mit ausgezogenen Linien die Verhältnisse für den Fall dargestellt, in dem das System sich ohne Arbeitsbelastung im stationären Zustand befindet. Bei Belastung stellt sich ein neuer Arbeitspunkt ein, wobei die Kennlinien sowohl vom Regler als auch von der Strecke Änderungen erfahren. Der Umstand, daß der Arbeitspunkt im belasteten Zustand sowohl einer Herzfrequenz- als auch einer Blutdruckerhöhung entsprechen muß, liefert eine Bedingung zur Festlegung der in (11) enthaltenen Konstante k_{WR}. Diese Bedingung kann aufgrund der in Abb. 5 dargestellten Verhältnisse und von (13) unter Berücksichtigung der Auswirkung der Änderung des Schlagvolumens und des Körperwiderstandes gemäß (10) bzw. (11) in der Form

$$\frac{F_0}{P_{\max}} \leqq \frac{1 + k_{WR} B_{O_2}}{R_{S0} V_{S0} \left(1 + \frac{k_{WS}}{V_{S0}} B_{O_2}\right)} \leqq \frac{F_{\max}}{P_{aso}} \tag{14}$$

angegeben werden. Hieraus folgt mit Heranziehung von (9) und mit $F_{\max} = F_0 + \Delta F$ sowie $P_{\max} = P_{aso} + \Delta P$

$$\frac{1}{1 + \frac{\Delta P}{P_{aso}}} \leqq \frac{1 + k_{WR} k_{O_2} W_{ph}}{1 + \frac{k_{WS} k_{O_2}}{V_{S0}} W_{ph}} \leqq 1 + \frac{\Delta F}{F_0}. \tag{15}$$

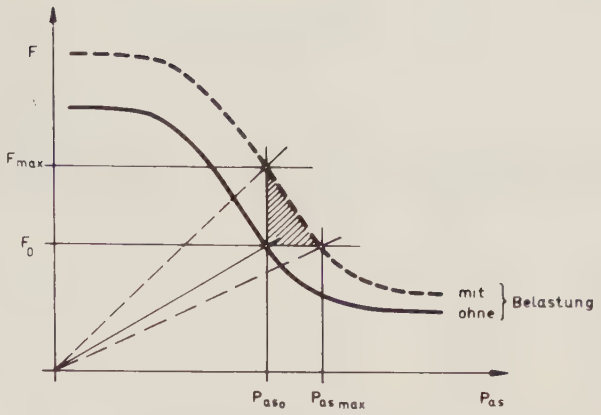

Abb. 5. Gebiet möglicher Systemzustände in der $P_{as} - F$-Ebene

Nimmt man bei der vorgesehenen maximalen Belastung $W_{ph_{\max}} = 100$ W die Werte $\Delta F/F_0 = 0{,}7$ und $\Delta P/P_{aso} = 0{,}25$ sowie ein Schlagvolumen $V_{S0} = 100$ ml an, so ergibt (15) unter Benutzung der weiter oben eingeführten Werte der auftretenden Konstanten die Relation

$$0{,}0025 < k_{WR} < 0{,}01 \tag{16}$$

auf deren Grund die Festlegung $k_{WR} = 0{,}005$ s/ml erfolgte.

Zu 3. Arbeitsstatus → Herzfrequenz

$$F = F_0 \left[1 + \frac{k_{SF} p}{(\tau_{PF} p + 1)^2} W_{ps}\right], \tag{17}$$

$$W_{ps} = \begin{cases} 0 & \text{falls} \quad W_{ph} = 0 \\ 1 & \text{falls} \quad W_{ph} \neq 0 \end{cases}$$

$k_{SF} = 9$ s
$\tau_{PF} = 30$ s .

Übertragungsverhalten und Parameterwerte wurden aufgrund von weiter unten genannten Meßergebnissen an gesunden Probanden ermittelt.

Den Ausgangspunkt für eine Computersimulation des oben aufgestellten Modells bildet das in Abb. 6 gezeigte Blockdiagramm.

Der Umfang und Charakter der Simulationsaufgabe machte den Einsatz eines Digitalrechners in Verbindung mit einer Simulationssprache notwendig. Verwendet wurde die am Rechner BESM-6 zur Verfügung stehende Simulationssprache DIALOG zur Berechnung der Reaktion kontinuierlicher dynamischer Systeme auf verschiedenartige Störungen (Kraus, 1972).

3. Ergebnisse der Modelluntersuchung

3.1. Untersuchung mit aperiodischen Testsignalen

Am Anfang der Modelluntersuchungen galt es festzustellen, ob das Modellverhalten den an gesunden

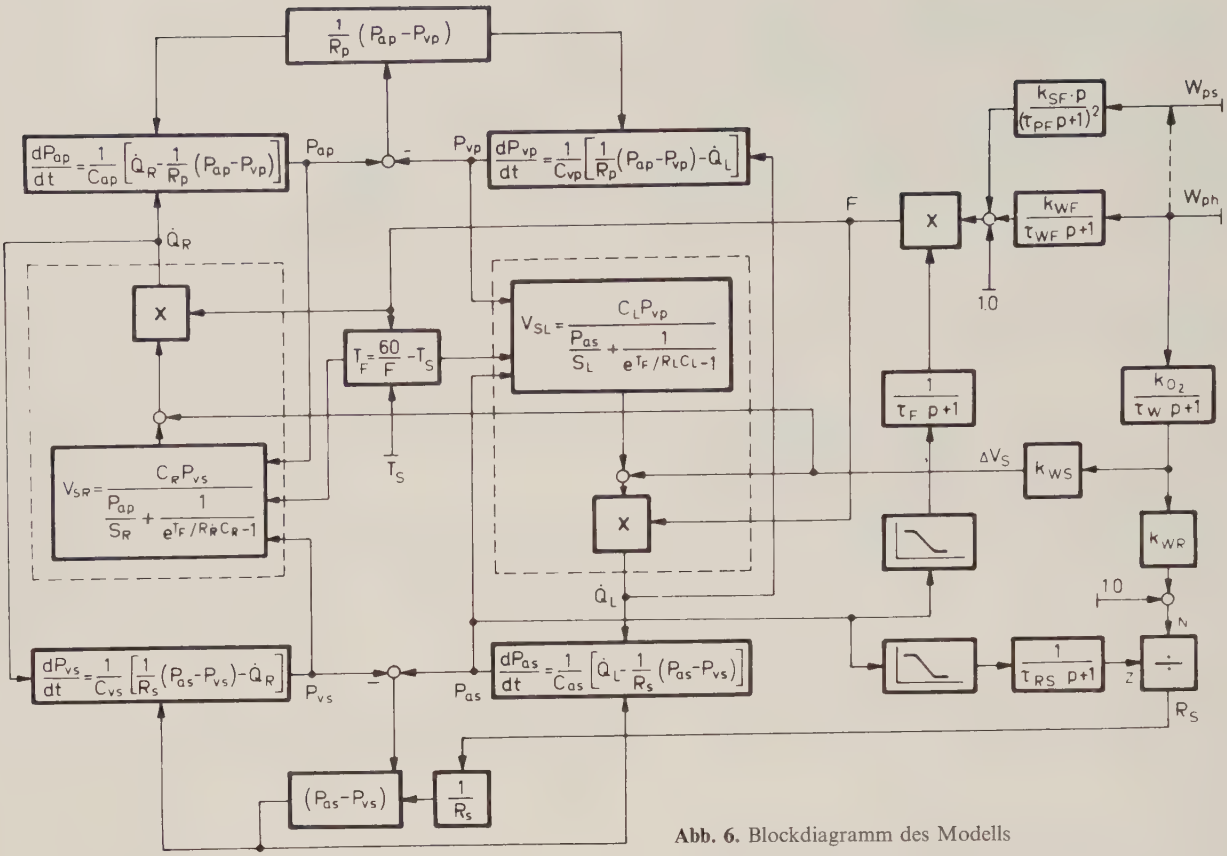

Abb. 6. Blockdiagramm des Modells

Menschen ermittelten durchschnittlichen Verhältnissen entspricht. Der dazu erforderliche Vergleich wurde aufgrund von Meßergebnissen vorgenommen, die an der Medizinischen Klinik der Karl-Marx-Universität Leipzig von Doz. Dr. Urbaczek und Dr. Schauer durchgeführt wurden. Es handelte sich dabei um aperiodische Belastungen, die in Abb. 7 angegeben werden. Der Vergleich bezog sich auf die Größen Herzfrequenz und mittlerer arterieller Blutdruck.

Die Kurvenverläufe in Abb. 8 lassen erkennen, daß eine Übereinstimmung der Meßergebnisse mit den errechneten Werten der Modelluntersuchung mit Ausnahme der Herzfrequenz bei der vita-maxima Belastung im Streubereich gewährleistet wurde. Bei dieser Belastung liegt jedoch der gemessene Ruhewert selbst gegenüber dem bei Gesunden allgemein für gültig angesehenen 70–75 Schläge/min um etwa 10 Schläge/min zu hoch. Von dieser Verschiebung angesehen, stimmt der qualitative Verlauf der berechneten und der experimentell ermittelten Kurven auch in diesem Fall überein.

Aus den experimentell in relativ großen Zeitabständen ermittelten Werten bei der sprungförmigen Belastung kann über die insbesondere in der Initialphase interessierenden zeitlichen Verlaufsform der Antwortkurven nur wenig ausgesagt werden. Bei diesen Messungen verfolgte man in erster Linie das Ziel, den stationären Endwert der registrierten Größen zu erfassen.

Gute Übereinstimmung liefern die mit rampenförmiger Belastung erzielten Ergebnisse, insbesondere nachdem die anfänglichen Erhöhungen der Antwortkurven im Modell durch entsprechende Beeinflussung des Sympathikotonus Berücksichtigung fand. Ähnliche Erhöhungen sind auch bei den Meßergebnissen der vita-maxima-Belastung andeutungsweise erkennbar. Die Erhöhungen in den Antwortkurven der rampenförmigen Beslastung sind in allen drei Fällen verschiedener Steilheit der Leistungszunahme in guter Näherung ungefähr gleich groß. Diese Unabhängigkeit von der Größe und dem zeitlichen Verlauf der Arbeitsbelastung läßt vermuten, daß es sich hier um Vorgänge handelt, deren Ursache allein die Veränderung des Tätigkeitszustandes ist, die auf die beteiligten nervalen Instanzen wie eine Sprungerregung wirkt. Ohne diese müßte die Rampenantwort einen streng monotonen Verlauf zeigen, vorausgesetzt, daß in dem durch die physische Belastung ausgelösten Regulationsvorgang kein stark ausgeprägtes differenzierendes Verhalten vorherrscht. Dagegen spricht jedoch die quasi-Unabhängigkeit von der Steigung der rampenförmigen Belastung und ins-

besondere das Fehlen einer dementsprechend stark ausgeprägten überschießenden Reaktion bei den sprungförmigen oder sonstigen, einer unstetigen Änderung entsprechenden Belastungsformen.

Anhand dieser Tatsachen erweist sich die rampenförmige Belastungsform als geeignet, objektive Anteile der Antwortreaktion von denen zu unterscheiden, deren mögliche nervale Ursache mit der Belastung nicht ergotrop verknüpft ist.

3.2. Auswirkung von Parameteränderungen auf die Systemcharakteristiken bei aperiodischen und periodischen Testsignalen

Zur Untersuchung der Auswirkung von Änderungen in der Beschaffenheit des Herz-Kreislauf-Systems wurde ein Vergleich zwischen rampenförmigen und sinusoidal verlaufenden Testsignalen am Modell durchgeführt. Dazu wurde eine willkürliche Vergrößerung des Wertes der Zeitkonstante τ_{WF} auf das Anderthalbfache vorgenommen.

In den Rampenantworten kam dieser Eingriff durch eine Zunahme der in Abb. 1 mit T_L bezeichnete Verzögerung der Antwortkurven zum Ausdruck. Die konkreten Werte der Zunahme zeigt Abb. 9. Hieraus ist ersichtlich, daß der relative Anteil der Zunahme mit dem der Parameteränderung übereinstimmt. Es wurde ferner gefunden, daß die Verzögerung T_L bei zunehmender Steigung der Belastungszunahme abnimmt. Dies stimmt mit dem von Karlsson u. Wigertz (1971) an gesunden Menschen ermittelten Befund überein. Dieser Effekt bietet die Möglichkeit, mittels Belastungen verschiedener Steilheit Aussagen über die Linearitätseigenschaften des Herz-Kreislauf-Systems zu gewinnen.

Die Auswirkung der gleichen Parameteränderung auf den Frequenzgang zeigt Abb. 10. Im Gegensatz zur Rampenantwort jedoch, woraus unmittelbar eine Vergrößerung der Trägheit des Systems quantitativ entnommen werden kann, ist aus den Ortskurven lediglich die Tatsache einer Änderung erkennbar, deren Präzisierung mit weiterem Aufwand verbunden ist.

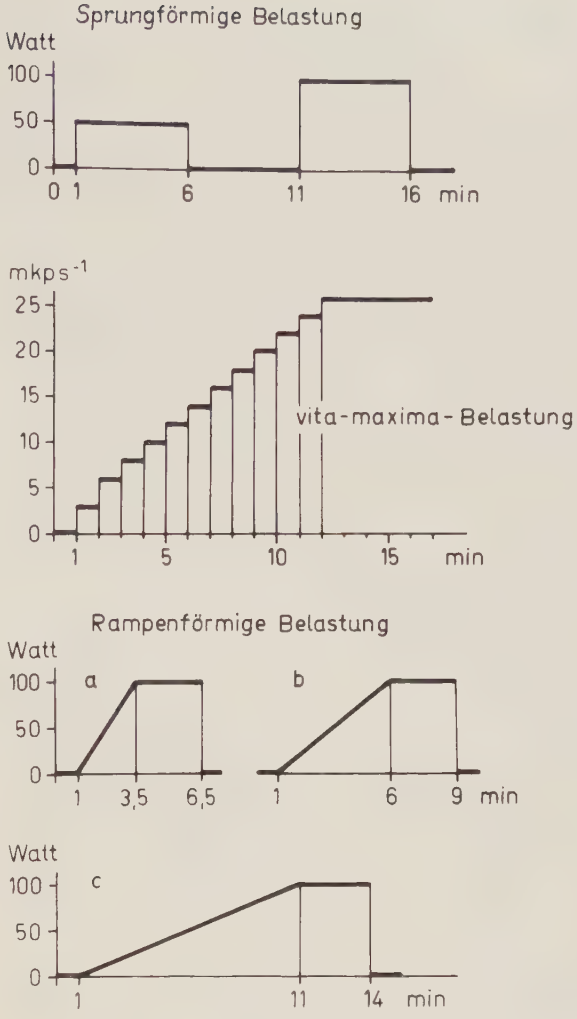

Abb. 7. Verlauf der verwendeten aperiodischen Testsignale

4. Diskussion

Die klinische Untersuchung des Leistungsvermögens des Herz-Kreislauf-Systems unter Zuhilfenahme regelungstheoretischer Betrachtungsweisen wirft das Problem der Festlegung eines geeigneten Testsignalverlaufs für die Belastung auf und fordert die Entscheidung darüber, welche Charakteristiken zur Beurteilung der Systemeigenschaften verwendet werden sollen.

Unter Beschränkung auf determinierte Testsignale steht zur Beantwortung dieser Fragen die Möglichkeit der Wahl zwischen periodischen oder aperiodischen Testsignalen bzw. Zeit- oder Frequenzcharakteristiken zur Verfügung. Der heutige Stand der experimentellen Systemanalyse verfügt über eine Vielzahl von Verfahren, die jeder getroffenen Wahl gerecht werden können, doch es kann eine Entscheidung darüber, unter welchen Bedingungen sich die einzelnen Verfahren am vorteilhaftesten einsetzen lassen, nur unter Berücksichtigung der spezifischen Verhältnisse des Anwendungsgebietes gefällt werden.

Es kann kaum erhofft werden, daß diese Verhältnisse sich eindeutig und vollständig formulieren lassen. Es können jedoch einige Aspekte genannt werden, deren Beachtung als Minimalforderung von einem Testverfahren verlangt werden muß. Für ein Testsignal würde dies bedeuten, daß es mit vertretbarer Genauigkeit einfach realisierbar und reproduzierbar, beliebig dosierbar hinsichtlich Leistungshöhe und Leistungsdauer und gut verträglich auch für Kranke ist.

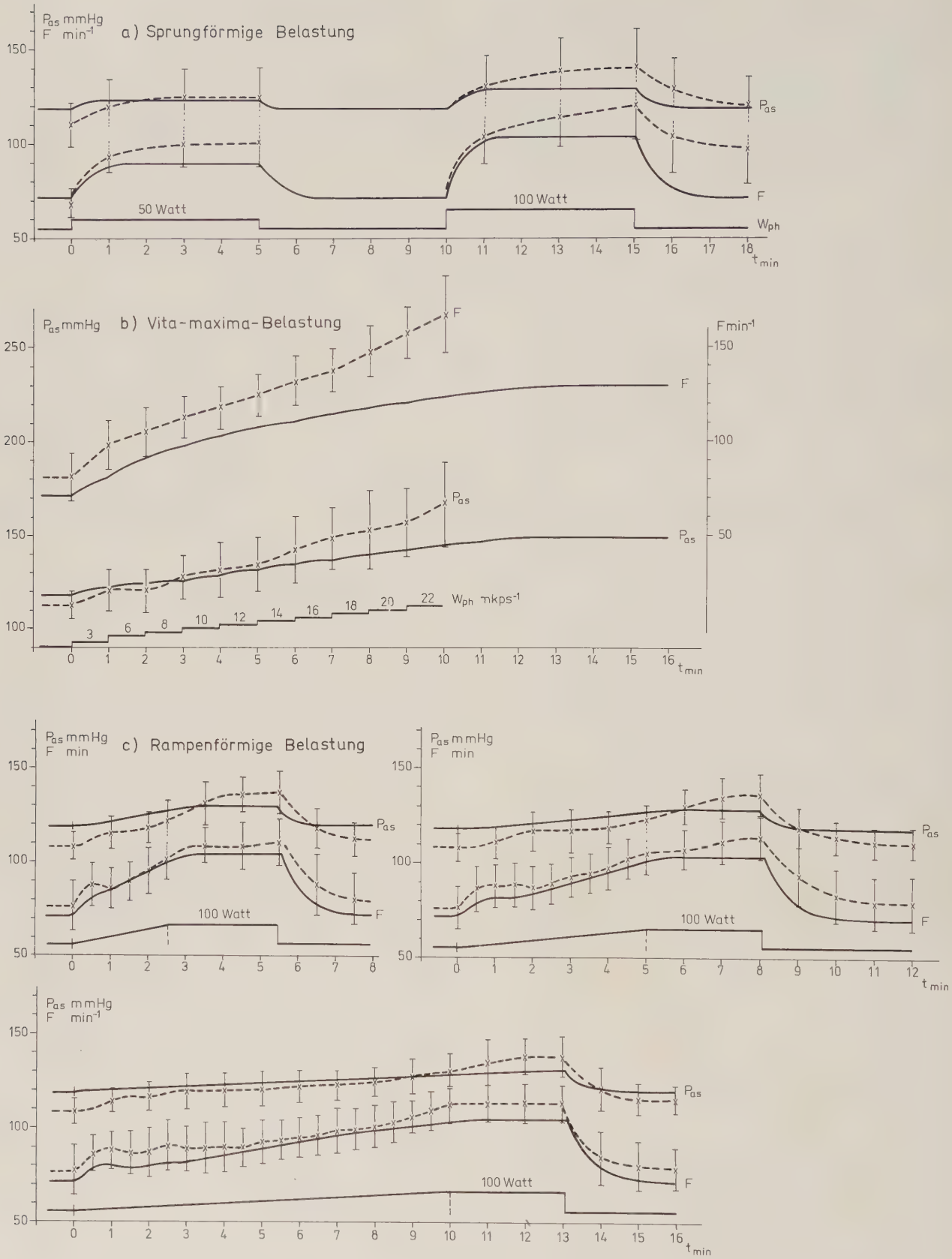

Abb. 8. Errechnete und experimentell ermittelte Ergebnisse

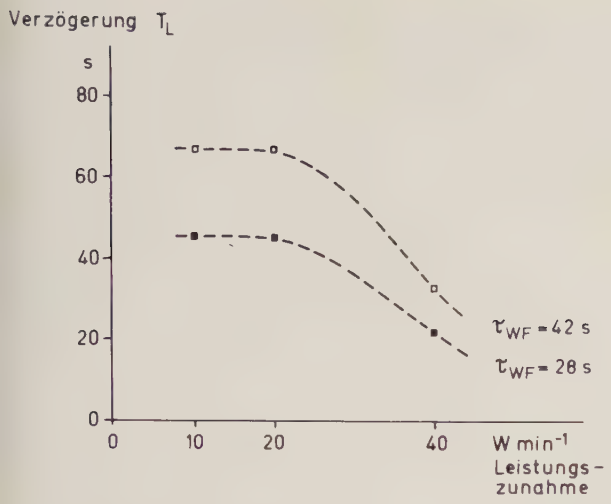

Abb. 9. Abhängigkeit der Verzögerung der rampenförmigen Antwort von der Steilheit der Belastung

Von den Systemcharakteristiken kann gefordert werden, daß sie eine anschauliche Interpretierbarkeit und eine schnelle und unaufwendige Auswertung erlauben, die Abweichungen der Systemeigenschaften von der Norm deutlich zum Ausdruck bringen und sowohl über das kinetische als auch über das statische Verhalten unmittelbar informieren.

Die vorangehende Abhandlung hat Ergebnisse geliefert, die es ermöglichen, eine Einschätzung der möglichen Arten von Testverfahren nach der Erfüllung dieser Forderungen vorzunehmen.

Periodische Testsignale, so wie sie in der Kreislaufforschung aufgefaßt werden, d. h. harmonisch veränderliche periodische Zeitfunktionen können mit Hilfe besonderer Vorrichtungen erzeugt werden. Für einen Test ist die Amplitude von vornherein festgelegt; die Dauer muß mindestens die von einer Periode betragen oder länger als die transiente Phase sein. Damit ist die Dosierbarkeit stark beeinträchtigt. Will man die Untersuchung mit einer Reihe von solchen

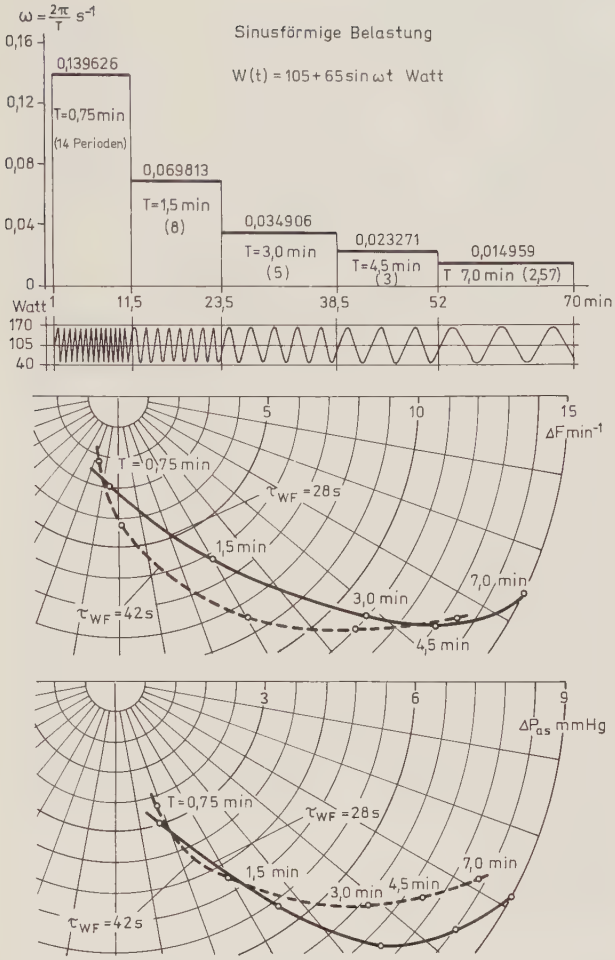

Abb. 10. Auswirkung von Parameteränderung auf den Frequenzgang

Signalen unterschiedlicher Frequenz mit dem Ziel der Ermittlung des Frequenzganges durchführen, so nimmt die Gesamtdauer der Untersuchung beträchtlich zu. Die erhaltene Systemantwort kann unmittelbar nur für den stationären Zustand Information liefern.

Tabelle 1. Gegenüberstellung der möglichen Klassen von dynamischen Testverfahren der Herz-Kreislauf-Untersuchung

		I periodische TS-Zeitcharakteristik	II periodische TS-Frequenzcharakteristik	III aperiodische TS-Zeitcharakteristik	IV aperiodische TS-Frequenzcharakteristik
Testsignal	Realisierbarkeit/ Aufwand	++	+	+++	+++
	Dosierbarkeit	+	+	+++	+++
	Verträglichkeit	++	+	+++	+++
Ergebnisdarstellung	Interpretierbarkeit/ Aufwand	++	+	+++	+
	Parameterempfindlichkeit	++	+++	++	+++
	Aussagefähigkeit über Dynamik	++	++	+++	++

Geeignet gewählte aperiodische Testsignale können sowohl die Forderung nach einfacher Realisierbarkeit als auch nach der Dosierbarkeit in beiden genannten Hinsichten erfüllen. Denkt man die aperiodischen Testsignale als durch Integration aus dem Diracschen Stoß generierte Funktionen, so ist das einfachste, der Bedingung der Realisierbarkeit gut entgegenkommende, aber auch allen weiteren Forderungen genügende aperiodische Testsignal der lineare Anstieg.

Hinsichtlich Systemcharakteristiken kommen die auf ein festgelegtes Eingangssignal gelieferte Ausgangsantwort und der Frequenzgang in Betracht. Da sie miteinander verknüpft sind, werden sie beide die Systemeigenschaften auf die eine oder die andere Art widerspiegeln. Entscheidend im vorliegenden Fall sind die Anschaulichkeit und die Möglichkeit einer unmittelbaren Deutung. Wie es aus den durchgeführten Untersuchungen hervorgeht, kommen diese letzteren bei der Zeitcharakteristiken besser zum Ausdruck. Sie sind außerdem gut geeignet, auf einfache und schnelle Art Vergleiche mit vorgegebenem Normverhalten anzustellen.

In Tab. 1 wird versucht, eine Gegenüberstellung der vier möglichen Grundvarianten von Testverfahren aufgrund einer guten (+ + +), mittelmäßigen (+ +) und mäßigen (+) Erfüllung der gestellten Forderungen vorzunehmen.

Literatur

Drischel, H.: On the dynamics of cybernetic systems of the body. In: Progress in biocybernetics, Vol. III, pp. 41—81. Amsterdam-New York: Elsevier Publ. Congr. 1966

Grodins, F.S.: Control theory and biological systems. New York: Columbia University Press 1963

Grodins, F.S.: Integrative cardiovascular physiology: a mathematical synthesis of cardial and blood vessel hemodynamics. Quart. Rev. Biol. **34**, 93 (1959)

Karlsson, H., Wigertz, O.: Ventilation and heart-rate responses to ramp-function changes in work load. Acta physiol. scand. **81**, 215—224 (1971)

Kraus, H.: DIALOG — eine Simulationssprache zur digitalen Modellierung dynamischer Systeme. messen-steuern-regeln **15**, 75—80 (1972)

Luczak, H., Raschke, F.: Regelungstechnisches Kreislaufmodell zur Integration arbeitsphysiologischer und rhythmologischer Einflüsse auf die Momentanherzfrequenz: Arrhythmie. Biol. Cybernetics **18**, 1—13 (1975)

Milhorn, H.T.: The application of control theory to physiological systems. Philadelphia-London: Saunders 1966

McAdam, W.E.jr.: An analog simulation of the mammalian cardiovascular system. M. S. Thesis, Dept. of Elect. Eng., Northwestern University, 1961

Pickering, W.D., Nikiforuk, P.N., Merriman, J.E.: Analogne computer model of the human cardiovascular control. system. Med. Biol. Eng. BME **7**, 401—410 (1969)

Schmidt, F.L.: Herzschlagfrequenz und Leistung. Basel-München-Paris-London-New York-Sydney: Karger 1972

Stegemann, J.: Leistungsphysiologie. Stuttgart: Thieme 1971

Tiedt, N., Fritzsch, Ch., Wohlgemuth, B., Wohlgemuth, P.: Ein Verfahren zur sinusförmigen Belastungsänderung auf dem Fahrradergometer. Acta biol. med. germ. **28**, 193 (1972)

Tiedt, N., Wohlgemuth, B., Wohlgemuth, P.: Dynamik des Herzfrequenzverhaltens und Leistungsbeurteilung bei sinusförmiger Belastungsänderung. Med. Sport **7**, 208 (1972)

Tiedt, N., Wohlgemuth, B., Wohlgemuth, P.: Dynamic characteristics of heart-rate responses to sine-function work-wad patterns in man. Pflügers Arch. ges. Physiol. **335**, 175—187 (1975)

Werner, G.-W.: Auswertung graphisch vorliegender Gewichtsfunktionen. messen-steuern-regeln **9**, 375—380 (1966)

Wigertz, O.: Dynamics of ventilation and heart rate in response to sinusoidal work load in man. J. appl. Physiol. **29**, 208 (1970)

Eingegangen am 2. Oktober 1976

Dr.-Ing. K. Balla
Carl-Ludwig-Institut für Physiologie
der Karl-Marx-Universität
Liebigstr. 27
DDR-701 Leipzig

Biol. Cybernetics 26, 151—158 (1977)

Biological Cybernetics

Some Remarks on Organization and Structure

E. R. Caianiello*
Theoretical Physics Institute, University of Alberta, Edmonton, Alberta, Canada

Abstract. Self-organizing systems are defined as able to change their structure, according to need, within specific equivalence classes. Once hierarchical levels and their value functions are assigned, requirements of invariance under transformations within an equivalence class can be used as a principle to determine the population of each level. This program is carried out in complete detail, as an example, for a particular class of systems (called "modular"), for which it is shown that a full Thermodynamics can be constructed. Modular systems are compared with linguistic, monetary, and military organizations; they are found to describe exactly the empirical data available on monetary circulation over the world, and to offer other perhaps suggestive indications. The emerging picture is that of a development, for any such system, which alternates phases of evolution (changes of level occupation numbers) with phases of revolution (changes of level structure within the given equivalence class).

I. Introduction

1. The view is here taken that the search for general principles governing the formation and change of structures in systems of the most varied sorts (biological, social, economical, linguistic, military, physical...) may be, at this time, a legitimate object of scientific enquiry; that such principles, if any, should be very few indeed, because of their assumed universal character; that the major difficulty in the task proposed may be expected to lie in the discrimination between the obvious (as any such principle is wont to be *a posteriori*) and the evident, which is readily seen but not as readily recognized to be most often of a specific rather than general nature.

Any such endeavor can only be a study of models (stemming from motivations that need interest only the author), the cruder at the inception the better; also, overly general definitions turn out to be, more often than not, wishful thinking or mathematical traps. The discussion that follows adheres strictly to these premises, by being a discourse on models rather than on things, narrowed by definitions as strict as possible. This constraint will not be maintained in the last Part, where some comparisons with known facts are made and others are proposed as objects of theoretical and experimental research.

2. The concept of "system" is taken as primitive. Although "large" systems with "complex interactions" among their elements ("element" is also of course a primitive concept) are our main interest, these added qualifications, easily confusing, are not needed and better kept away at this stage.

Two examples will be useful to fix ideas and render most of the following intuitive:

a) given an alphabet A of M letters, consider all possible strings of letters, of any length (up to a maximum, if so desired): they form the *semigroup* generated by A. Again, consider all possible sequences of such strings: this is the *monoid* A^* generated by A;

b) given a number system (e.g. decimal) consider the semigroup obtained as in a) with $A \equiv (0, 1, \ldots, 9)$, $M = 10$: this contains all integer numbers (up to a maximum, if so desired). A^* will be formed by all possible sequences of numbers (no connection with the operations of arithmetics is implied).

We restrict from now on, *by definition*, our attention only to systems composed of a *discrete*, however large, number of elements. The rounding off of a number into the nearest integer will be *understood without further mention*, as a necessary approximation in the application of theory: e.g. $\sqrt{10} \equiv 3$, if it denotes number of cells, coins or people.

Each string of a) or number of b) is, by our definition, a system; so are the corresponding semigroups, or the closely allied monoids. The relation is that of "system" to "ensemble" in statistical physics;

* On leave of absence from Laboratorio di Cibernetica, CNR, Naples, Italy

both concepts will be necessary for us, but the word "system" will be used indiscriminately to cover *both* instances; the context will make it clear when the discussion applies to both, or only to one situation.

3. A definition of "structure" will not be attempted in general (it would have no less traps than that of "randomness", and would be useless for our purposes); we shall rather confine our attention to a particular class of systems *(hierarchical systems*, HS*)* and more in detail to a subclass of them *(hierarchical modular systems*, HMS*)*, to be defined in Part II. We shall say that a HS or a HMS (or whatever other system we may have decided to define unambiguously at any time) *have structure* or *are structured;* whenever the word "structure" is used, it must be so understood.

A HMS will be seen to behave much like Example b) in the previous section, the "module" corresponding to the arithmetical base $M(=10)$.

4. A structured system may be subject to change in the course of time. We distinguish two types of behavior in this respect, which are best described first on an example. Suppose the system is isomorphic with a set of numbers; the first type of change has to do with changes of these numbers, we may call it "evolution"; the second with a change of the structure itself, which in this example corresponds to a change of the base of the number system (to provide isomorphism with the new situation of the system); we call this a "revolution" (we are not considering the "wrecking" of the system, which one is of course at freedom to call "revolution" as well).

A change of structure is therefore a "revolution". We shall be concerned mostly with this type of change and shall restrict (arbitrarily) the use of the appellative "self-organizing" to systems which can change spontaneously their structure (besides evolving) so as to meet new situations. We emphasize that our use of words is merely technical, and that a literal reading might prove as misleading as it might appeal as suggestive. (To resort to facile analogies, the warming up of water is for us an "evolution", its boiling a "revolution"; the clustering of spins into domains, and again the alignment of the latter into a magnet, and generally all phase transitions of physics, are revolutions; likewise the depolarization of a neuronal membrane, or the sudden transition from the all-white to the all-black state in some U.S. neighborhood once a critical black/white ratio is reached.)

Structure emerges as a quantification into the discrete of the continuum or indefinite; a change of structure must be a change among integer values, so that a criterion of stability is thereby provided to self-organizing systems against arbitrarily small perturbations.

5. Part II contains the necessary preliminary postulations and definitions, as well as a description of what a non-structured system may be expected to gain by acquiring a hierarchical structure.

Emphasis is then placed on how one may best characterize structures (assumed as *given*, the mechanism of their formation is *not* the object of investigation), and parameters pertaining to them, so as to judge their efficiency in performing specific tasks. This is done in Part III, on the particular case of HMS's, which are amenable to a complete mathematical treatment; they are expected to play a relevant role in further analyses of this nature, both as conceptual tools and as approximating devices.

In Part IV it is shown that a full thermodynamics (not only an "entropy", but also a "temperature", an "energy", etc.) can be developed for HMS's.

Part V is devoted to a first, by necessity preliminary comparison with some realistic situations. HMS's are seen to have a distribution law which coincides strikingly with that empirically determined by experts from available data on the monetary circulation in the world's countries; the agreement of it with the standard military chain of command is also intriguing. A brief discussion of further possibilities, as well as limitations, of the present approach is finally given.

II. Definitions and Remarks

1. Bose-Einstein and Boltzmann Counting

Elements will be regarded as *identical*, non distinguishable, when in a collection of them their identity is *irrelevant for the purpose at hand.* Thus, any two groupings into a same "state" of the same number n of infantrymen to form a squad, or of 100-dollar bills to form a same total (if one is not interested in forgery and serial numbers), etc., are indistinguishable for the general officer, or the tax collector, conceived here as physical "Observers".

We pose no *a priori* restriction on the values that n, the number of identical elements of some sort, may assume; given n, the number W of *different* states that can be formed with them is clearly $W=n+1$ ($n=0$ is included). This is the counting of Bose-Einstein statistics (we do not treat here, though we do not exclude, situations in which Gentile or Fermi counting may be appropriate).

Whenever non-identical elements are involved, e.g. coins of different denominations when this is important, Boltzmann counting will apply.

2. Information and Level Formation

Since we are going to utilize quantities that are familiar in Thermodynamics, our notation and symbols will conform to physical usage and terminology. This is of course only a matter of conceptual convenience, the reader need not feel so constrained.

We need first to get some notion on the function of hierarchical levels in a system. This is best seen on an example; of the host that might be quoted, the simplest is perhaps that of a monetary system. We ask whether any reason can be found for the fact that all such systems (in less than primitive societies) are always quantified into discrete units of different denominations and values, rather than being "continuous" (as would be the use, say, of gold by weight, any weight; "evident" reasons, such as the certification of exact weight imprinted by the royal mint of ancient Lydia, or many others to be found in history, would be misleading for our purposes). We assume to have at the start only an indefinite amount of coins, or tokens, of a same unit value (we are restricted to discrete systems: this is here no limitation, only a simplification).

Plot (Fig. 1) on the horizontal axis the number of different possible states (sums of money) $W=n+1$, on the vertical the corresponding entropy (or information: no distinction is here necessary)

$$S=K\lg W=K\log(1+n).$$

The logarithmic growth of S (nearly linear for small n, increasingly slower for higher n), well typifies our correspondingly increasing awkwardness in handling the system when n grows, whatever we may want to do or know about it (Von Neumann, 1958): doubling n nearly doubles S for small n, while for large n an enormous increase is necessary to double the information S.

Suppose that, at this point, the system is restructured into a new one, in which identical "clusters" of unit coins, each containing M elements, are formed; a cluster is a bag of unit coins, or, equivalently, a second type of coin. We can now form a definite total in more ways, if it exceeds $M-1$; suppose we use n_1 unit coins and n_2 coins of the second type, and put them down one at a time, starting with the unit coins. The latter being distinguishable from the former, we have

$$W=(1+n_1)(1+n_2)$$
$$S=K\lg(1+n_1)+K\lg(1+n_2).$$

Curve *1* of Figure 1 changes into Curve *2*, which has a kink, and separates from *1* to form a new logarithmic arc *which is again nearly linear for small* n_2, as soon as the new coins start being used. *The introduction of a new value, or level, keeps the information nearly linear within a broader range* (n_1, n_2). Another way of looking at Curve *2* is to imagine its second arc as deriving from a contraction by a scaling factor $1/M$ of the subjacent portion of the horizontal axis. We may then want, associating information with value, that

$$S=K\lg[(1+n_1)(1+n_2)]=K\lg(1+n_1+Mn_2):$$

this occurs only if $n_1=M-1$, that is, we must not use unit coins unless necessary.

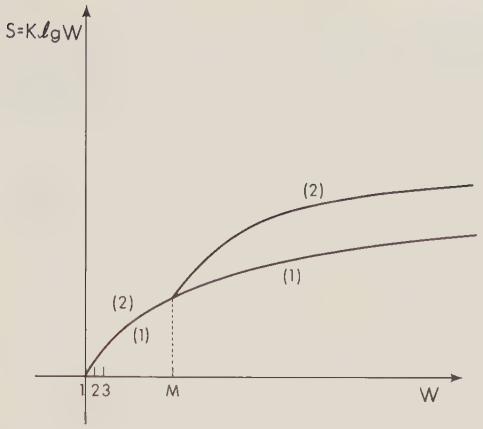

Fig. 1. Information growth with clustering

The latter remark is not trivial, it is rather typical of questions that arise once one starts in this field. We need not comment upon it here, as the issue will become evident from the sequel. We have thus seen that, informationwise, we can cope with the same ease with any system of identical elements (that is, staying always nearly linear) provided these systems are organized into levels, the elements of which are identical clusters of those of the level below, and that such clusters be treated as, or replaced by, new elements, identical among themselves but not with those of levels below or above.

3. Clustering

We have thus a cue for regarding clustering, and then the identification of a cluster as a new element of a different nature than its components, as a typical process of level and structure formation; also, a hierarchical arrangement of elements, clusters, clusters of clusters, etc., appears as a rather natural mechanism to achieve this effect.

We note that an element, by becoming a part of a cluster of the next higher level, *loses* many of its features and *acquires* the new function of member of the cluster. All examples we can draw, from collective motions to biology to army life, substantiate this view.

4. Definition of Hierarchical System

We are now ready for a definition which will suffice for our present purposes. Greater generality would be only detrimental at this stage.

Consider a system composed of elements of levels $0, 1, 2, \ldots, L(\leqq\infty)$. The elements at each level are indistinguishable among themselves, distinguishable from those at other levels. Let there be n_h elements in the level h $(h=0, 1, \ldots, L)$.

The *total number of elements* is

$$N=\sum_{h=1}^{L} n_h. \qquad (1)$$

Such arrangement we call a *partition* of the elements of the system.

Attach now to each level h an (integer) *value* v_h; the *total value of the system* (we assume for simplicity that there is only one value function) is

$$V=\sum_{h=0}^{L} n_h v_h ; \tag{2}$$

the *average value of an element* of the system is then

$$\langle v\rangle=\frac{\sum_{h=0}^{L} n_h v_h}{\sum_{h=0}^{L} n_h}. \tag{3}$$

We recall that we have convened to term "self-organizing" a system which can organize itself by the partitioning process into one or another hierarchical structure. This definition may be readily generalized to any other given specification of structure.

We further require that the value function be such that

$$\frac{v_h}{v_{h-1}}=\text{integer}>1, \text{ any } h;\ v_0=1 \text{ (in suitable units)}. \tag{4}$$

If, in particular, (4) reduces to

$$\frac{v_h}{v_{h-1}}=\frac{v_{h-1}}{v_{h-2}}=\ldots=\frac{v_1}{1}=M, \tag{5}$$

we call the system *modular* (HMS), and M the *module* or *base* of the HMS and of the corresponding partition.

5. Hierarchical Partitions

We are now concerned with relations among different partitions of a same self-organizing system. We call a partition π_b a *refinement* of a partition π_a if it has more levels than π_a and retains *all* the levels of π_a (which stay invariant under π_b).

A *hierarchical modular partition* $\pi_b^{(\mathrm{mod})}$ is therefore a refinement of a previous $\pi_a^{(\mathrm{mod})}$ if, and only if:

$$M_b=M_a^{1/p}, \quad p \text{ integer } >1. \tag{6}$$

From now on our interest will be confined to HMS's. After (6), we shall call for short any $\pi_b^{(\mathrm{mod})}$ a *p-refinement* of $\pi_a^{(\mathrm{mod})}$.

6. Hierarchical Modular Systems

They have many interesting properties, which the reader may easily consider by himself. We notice here only the following: provided the number of elements employed at each level is always $v_h<M$, any (integer) value v (not exceeding the total value of the system) can be expressed *in a unique way* in terms of elements of the system:

$$v=v_H M^H+\ldots+v_0 M^0. \tag{7}$$

This property is far from trivial; it can be elaborated upon in several ways to lead again to a definition, or to other properties, of HMS's. The proof is immediate, if we choose M as the basis of a number system (decimal, binary, or whatever) so as to write $M=10$: then (7) becomes

$$v=v_H v_{H-1}\cdots v_0 \tag{8}$$

and uniqueness becomes evident because all possible values v can be expressed, provided $v_h<M$ (which is a minimal requirement) by means of *strings* (8), which are *isomorphic with the numbers of ordinary arithmetics in base M*; the figures v_h retain their arithmetic meaning, level corresponds to position.

III. Hierarchical Modular Systems

1. It is important to make a clear-cut distinction between two orders of questions:

a) those pertaining to specific assignments of values to the levels of a HS or of a HMS (in the latter case to M^h); these, as well as the number $L+1$ of levels, are in the present work assumed to be given *a priori* (their discussion is expected to be specific for each system, and therefore beyond our scope; we shall return to this point in Part V);

b) those which relate to the distribution n_h of the N elements of the system among its levels, $h=0, 1, 2, \ldots, L$, once their number and values are known; this distribution will reflect the way the system *adapts* to an *external* requirement.

We expect that general properties may be derived from a study of b) in typical instances, i.e. models. As an example of the method, we shall give a complete discussion of HMS's.

2. As long as a self-organizing HS stays "isolated", it has no reason (from what was said thus far) to prefer any particular choice of n_h. If, however, it is in "interaction with the universe" this cannot be expected to be the case any more. We shall adopt for handling this problem the following principle: to assume that the system, which is in a given situation as assigned under a), is however at freedom to change it by any *refinement* of its original hierarchical partition. This principle assumes, in other words, that the "universe" is not interested into what partition the system chooses to organize itself; its interaction with the system is of a *global* nature, to be expressed therefore by requiring that the value of some *mean* quantity of the system be imposed from its outside (the universe).

We have here a requirement of invariance under a class of transformations (the refining partitions); this is important also because additional requirements (see Part V) may impose refinements of structure. We note, however, that (on purpose) we have said very little

about HS's in general, as it carries more conviction in a first work to discuss completely a single, though restricted instance, than only to touch upon a variety of cases. We shall therefore from now on concentrate on HMS's, for which our definitions are complete; pleasingly enough, remarkable computational simplifications will be seen then to occur.

3. The principle just stated requires that the average value of an element of a HMS stay invariant under any p-refinement of the HMS

$$M \to M^{1/p}; \tag{9}$$

then

$$L \to pL \tag{10}$$

and it is wanted that $(n_h \equiv n_h^{(1)})$:

$$\langle v \rangle = \frac{\sum_{h=0}^{L} n_h^{(1)} M^h}{\sum_{h=0}^{L} n_h^{(1)}} = \frac{\sum_{h=0}^{pL} n_h^{(p)} M^{h/p}}{\sum_{h=0}^{pL} n_h^{(p)}}. \tag{11}$$

We also note that a HMS possesses a natural *invariant* under (9): the ratio of the maximum number of states to the module:

$$w = \frac{M^{L+1}}{M} = \frac{(M^{1/p})^{pL+1}}{M^{1/p}} = M^L. \tag{12}$$

We want to determine $n_h^{(p)}$ so that, for given L, M, (11) stays valid for any p. This task, otherwise formidable, turns out to be surprisingly simple for modular systems.

Take first $L=1$ and set

$$n_h^{(p)} = n_0^{(p)} f(M^{h/p}), \quad \text{with} \quad f(1)=1; \tag{13}$$

write (11) for $p=1$ and 2:

$$\frac{1+f(M)\cdot M}{1+f(M)} = \frac{1+f(\sqrt{M})\cdot\sqrt{M}+f(M)\cdot M}{1+f(\sqrt{M})+f(M)} \tag{14}$$

whence

$$f(M) = M^{-1/2} \tag{15}$$

and

$$n_1^{(2)} = n_0^{(2)} M^{-1/4}, \quad n_2^{(2)} = n_0^{(2)} M^{-1/2}. \tag{16}$$

Try now to generalize (16) into

$$n_h^{(p)} = n_0^{(p)} M^{-h/2p}. \tag{17}$$

Substitution into (11) leads, after (12), to:

$$\langle v \rangle = \frac{\sum_{h=0}^{pL} M^{h/2p}}{\sum_{h=0}^{pL} M^{-h/2p}} \equiv \sqrt{w} \equiv M^{L/2}, \tag{18}$$

independent of p. The modular nature of the system is of course crucial in determining the simplification which leads to (18), and proves (17) to be indeed the correct solution of our problem.

We add from now on the further restriction that our HMS be such that:

$$N = n_0^{(p)} \sum_{h=0}^{pL} M^{-h/2p};$$

this is not in anyway necessary, may be easily removed and is made only to shorten the discussion to barest essentials. Then, in conclusion:

$$n_h^{(p)} = N \frac{1-M^{-1/2p}}{1-M^{-1/2p-L/2}} \cdot M^{-h/2p} \tag{19}$$

is the distribution law that secures the wanted invariance of $\langle v \rangle$ under p-refinements.

In the following we need not consider values of p other than 1; in a HMS there is no way of knowing a "past history" of levels. Note that, in particular:

$$n_h = \frac{n_{h-1}}{\sqrt{M}}. \tag{20}$$

IV. Thermodynamics of HMS's

1. Given a *HMS* with distribution law (we remind that N has been assumed, for short, to be a constant)

$$p_h = \frac{n_h}{N} = \frac{1-M^{-1/2}}{1-M^{-1/2-L/2}} \cdot M^{-h/2} \qquad (h=0,1,\ldots,L) \tag{21}$$

we can regard p_h as expressing a frequency, or a probability scheme, to which we may associate an information, or entropy, in the familiar way:

$$S = -K \sum_{h=0}^{L} p_h \lg p_h. \tag{22}$$

A change of variables will clarify the form without altering the content. Write:

$$\beta = \frac{1}{KT}, \tag{23}$$

$$\frac{E_0}{L} = \varepsilon_0, \tag{24}$$

$$\varepsilon_h = \varepsilon_0 h, \tag{25}$$

$$M = e^{2\beta\varepsilon_0}, \tag{26}$$

and set then

$$Z = \sum_{h=0}^{L} e^{-\beta\varepsilon_h} = \frac{1-M^{-\frac{L+1}{2}}}{1-M^{-1/2}}, \tag{27}$$

$$\psi = \lg Z. \tag{28}$$

Then (21) is rewritten in the well familiar form

$$p_h = \frac{1}{Z} e^{-\beta\varepsilon_h} \tag{29}$$

and (22) becomes

$$S = K\psi + \frac{1}{T}\langle \varepsilon \rangle, \tag{30}$$

where

$$\langle \varepsilon \rangle = \sum_{h=0}^{L} p_h \varepsilon_h = \varepsilon_0 \sum_{h=0}^{L} h p_h = -\frac{\partial \psi}{\partial \beta}, \tag{31}$$

corresponds clearly to the average energy of Thermodynamics and means here, to within a factor ε_0, the *average order*, or *length*, of a level. For instance, should we attribute to each word, conceived as a string of h code letters, an "energy ε_h", this energy would come proportional to h. We recover thus, from our premises, a concept which has been used sometimes by mathematical linguists (see Part V). The *variance* is given by

$$\sigma^2(\varepsilon) = \frac{\partial^2 \psi}{\partial \beta^2}. \tag{32}$$

We note finally, from (18) and (23)–(26), that

$$\lg \langle v \rangle = \frac{E_0}{KT}. \tag{33}$$

2. Our principle of invariance under p-refinements of the average value of a HMS leads thus ($N = \text{const}$) to the Boltzmann statistics (29). The quantities (25) $\varepsilon_h = \varepsilon_0 h$ that correspond to the usual energies are *not*, however, connected with the value, but only with the order of the levels. To have found a formal definition of energy, however remote our starting point, is significant, because we can then develop for any such HMS the full formalism of Thermodynamics.

We choose to do so with the "subjective" interpretation of probability by means of which Jaynes (1957) has connected Information Theory and Statistical Mechanics (Rothstein, 1951). Although this is not necessary (we could just call $N\langle \varepsilon \rangle = $ total energy), it may allow a freer transition between Information Theory and Physics, according to opportunity and without formal changes. To do so, we have only to remark that the average energy per element of the system is given by (31) and that (Tribus, 1961) we can regard

$$dQ_r = \sum_{h=0}^{L} dp_h \cdot \varepsilon_h \tag{34}$$

and

$$dW_r = \sum_{h=0}^{L} p_h d\varepsilon_h \tag{35}$$

as the (reversible) heat and work, so that

$$d\langle \varepsilon \rangle = dQ_r - dW_r \tag{36}$$

is (one way of formulating) the first principle of Thermodynamics for our HMS. Next, if ε_h (through ε_0, h or both) is dependent on some external parameters X_k [which act upon the system: $\langle \varepsilon \rangle = \varepsilon(\beta, X_k)$], then one can define forces

$$(F_k)_h = -\frac{\partial \varepsilon_h}{\partial X_k} \tag{37}$$

so that, for a change dX_k

$$dW_r = -\sum p_h d\varepsilon_h = -\sum_{h,k} \left(p_h \frac{\partial \varepsilon_h}{\partial X_k} \right) dX_k = \sum_k \langle F_k \rangle dX_k \tag{38}$$

and from (27) and (28):

$$\langle F_k \rangle = \frac{1}{\beta} \frac{\partial \psi}{\partial X_k}.$$

Also:

$$dS = K d\psi + K\beta d\langle \varepsilon \rangle + K\langle \varepsilon \rangle d\beta = K\beta d\langle \varepsilon \rangle + K\beta \sum_k \langle F_k \rangle dX_k \tag{39}$$

and, for reversible processes:

$$dS = K\beta dQ_r + K\beta \left(\sum_k \langle F_k \rangle dX_k - dW_r \right) = K\beta dQ_r, \tag{40}$$

or

$$dS = \frac{dQ_r}{T}. \tag{41}$$

The discussion is omitted, because it is amply done in the references cited in this Section, and otherwise, if things are done in the traditional way, is standard.

By analogy with physics, two different HMS's 1 and 2 will be said to be *in equilibrium* (0^{th} law) if they have the same "temperature" T, or β (23), *to which we must now add the further requirement that* $\langle v \rangle$ *be the same for both*; from (33):

$$T^{(1)} = T^{(2)}, \tag{42}$$

$$E_0^{(1)} = \varepsilon_0^{(1)} L^{(1)} = E_0^{(2)} = \varepsilon_0^{(2)} L^{(2)}. \tag{43}$$

If $\varepsilon_0^{(1)} = \varepsilon_0^{(2)}$, then (43) imposes that, besides having the same "temperature", the two systems have also the same number of levels; if $\varepsilon_0^{(1)}, \varepsilon_0^{(2)}$ are some integers, there will be obvious connections with refinements.

V. Concluding Remarks

1. Invariance within an Equivalence Class

We may now try to give a general formulation to the method which has been here applied *in extenso* only to a sub-class ($N = \text{const}$) of HMS's. Asking no questions as to "why", but only as to "how", we take as initial data a description of the levels, and of the value functions attached to them, of the system (these define its "structure"). In so doing, one is naturally led to consider transformations, such as the p-refinements for HMS's, which change the system into an "equivalent" one, both as regards its interaction with, i.e. response to, its "universe" (as measured by average values) and the type of its structure (e.g. modularity must be retained). The specification of such transformations can be regarded as part of the initial data: what one defines is really an *equivalence class*, within which a self-organizing system

can freely move. (A mathematical study linking structures with structure-preserving transformations is of course called for.)

Such transformations within its equivalence class will actually take place and change the structure of the system during its development (e.g., because forced by external influences, or by the growth of the number of individuals in a population model, or of the volume of trade in an economical model...); this fact is *not* considered here, because to some extent *specific* of each system.

All our attention was focused in this work on finding a general criterion that might allow the determination of the population of each level, once the initial data are given. As such we have proposed, and applied to HMS's, a "principle of invariance of response under allowed structural transformations": "response" or "interaction" is measured through mean values, "allowed transformations" are in our example the p-refinements. That is, the "universe" does not know nor care about which class a self-organizing system chooses to settle in, within equivalence.

2. Mathematical Linguistics

The present research stems from work done in mathematical linguistics (Caianiello and Capocelli, 1971), aiming at an *inductive* study of the hierarchical organization of a language; the Example I-1a) is carried over from it. We take, in this respect, HMS's only as a very first step, meant for formulating questions more than answering them.

It is however significant to find, even so, a natural connection between "energy" and "word length", such as was postulated by Mandelbrot (1954) in his attempt to find an explanation of the so called "Zipf's law" (1949); proceeding further as he does, we would immediately obtain the same result, for any HMS and not only for somewhat idealized languages. This we refrain from doing, as we feel that Herdan's criticism (Herdan, 1962) is not to be taken lightly.

3. Monetary Systems

HMS's should be regarded as the crudest possible models of self-organizing systems, especially with the (unnecessary) restriction that the number of elements stay constant under refinements. It was therefore rather surprising to find a realistic situation which is described by them quite satisfactorily. The evidence is provided by an interesting study made by Hentsch (1973) (former president of the "Association suisse des analystes financiers"), in which a penetrating analysis is made of monetary circulation in the various countries of the world, in the attempt to find some regularities; data are reported by this Author for the 1969 circulation in Switzerland, and the 1971 circulation in Switzerland, France, Holland, Germany, and USA; the results he discovers are said to hold for all countries. They all reduce, in our notation, to the law

$$n_h v_h \propto \sqrt{v_h}\,, \tag{44}$$

which exactly coincides with (17), when $p=1$ and $v_h = M^h$. Various fractional powers of 10 are studied, notably

$$10^{1/3} \to 1,\ 2.15,\ 4.64,\ 10,\ 21.5,\ 46.4,\ 100,\ \ldots \tag{45}$$

which, after rounding off to nearest integer, should be well familiar to the reader.

Even more interesting, perhaps, is the fact that the law (44) (which is generally followed within one, at most two variances) is occasionally not respected; Hentsch shows that this happens either because some country lacks some value of the sequence (45) [and computes that everything would go back to (44) otherwise], or because of external causes [the graph for Swiss circulation in 1969 deviates in excess from (44) for the values 0.5, 1, 2, and 5 francs, which were coined in silver; in 1971 silver was no longer in circulation, and the corresponding graph follows (44)]. The simplification in formula (18) was also noted by this Author.

The explanation of this behavior, once it is ascertained empirically that a monetary system is a HMS (M need not of course be necessarily $10^{1/3}$), becomes quite obvious in our perspective. A monetary system is not just a game, it interacts with the "universe" of all that can be exchanged with money; the requirement (18) and the principle of invariance under p-refinements mean here simply that the average value of the monetary token must equal the average value, or cost, of anything that may be bought or sold, from needle to skyscraper: this "universe", we repeat, "does not know nor care" about what module a country may choose for her monetary system.

4. Human Society and Military Structures

Some considerations on human societies cannot be avoided in discussing this subject; we shall do so in the crudest possible manner, by considering as the only basic factor common to any form of society the necessity that its members have of *communicating* among themselves in order to undertake any activity that may be termed social. Of communication we observe that it takes *time*, in amounts which increase with the complexity of the task to be agreed upon or commanded; and that *rational* communication becomes the less efficient, the larger the group with which an individual has to communicate. Aside from one-level societies, which may be termed anarchic and are found only in very small groupings, all others are hierarchical (which does *not* mean authoritarian).

The crudest model one may make is then, again, a HMS where, treating all individuals and tasks as equal, the module M denotes the (assumedly constant) number of individuals who are communicating with, or controlled by, an element of the next higher level.

This model may be compared with the chain of command typical of military organizations. Within this writer's experience (not altogether negligible, thanks to the second world war!), $M \cong 10$ can be very nearly taken as the module (unless otherwise required for technical reasons). But then one is immediately struck by the systematic appearance of the number 3 (3 leaders: 1 sergeant and 2 corporals, for a squad of 10 soldiers; 3 squads to a platoon, 3 platoons plus one squad to a company; and so on). If we now look at (20), we find that $\sqrt{10} \cong 3$ is just what a HMS would require in this case.

This can only be an argument proposed for discussion: it would be interesting to know from experts how things stand, in case there are armies or similarly schematizable societies where M is significantly $\neq 10$; as well as to know how levels were developed in the course of history.

Another such modular society was that of the Incas—except that, at the highest echélon, one finds 4 instead of 10 (higher decisional responsibilities, or something to do with the cardinal points?).

Of the myriads of questions that come to mind only two will be formulated here as examples; both are based upon the crude assumptions that M is a *biological* constant and that no other factors are involved. When the number of individuals increases, M cannot change, so there is the need for p-refinements, or "revolutions" (no blood is meant!); the dynamics of this phenomenon requires the intervention of splitting forces, or "social tensions", which it should not be difficult to estimate in models using the Thermodynamics of HMS's: can this be an acceptable explication, in lieu of more "evident" others? Next: a computer is not bound by so small a value of M; can we make models to evaluate, albeit crudely, a reasonable if not optimal structure for a society based on man-machine symbiosis?

5. Conclusion

The reader will have noticed that several things have *not* been stated in this work, although seemingly "evident": such as that level formation is a consequence of entropy maximization (the argument in II-2 can be readily construed to this effect); or that it is due to the increased working efficiency of structured systems (army vs. crowd); or that it comes from a balance between "organizing" and "disorganizing" agents, as it happens with all equilibria (these statements are not contradictory). We have avoided the issue altogether as a matter of methodology, it not being yet clear to us to what extent they are "specific" and to what "general".

The dynamical development of a system, i.e. of a model, through phases of evolution and revolution as defined here, will have to be studied, as a consequence of intrinsic or extrinsic changes (e.g. in a HMS of N and/or V), and the corresponding dynamical concepts clarified. The work of Part IV should help in this task.

There may be questions for the biologist: e.g., can biological hierarchies be connected with the requirement that the total, or average, mass of food (or of particular substances) used up in a hierarchy be dependent only on the "universe of supply"? Not to mention physics, where yet another outlook on phase transitions would not cause much surprise.

Another issue that comes to mind is the following: a hierarchical system interacting with another *acts as a template* for it: *structure forces structure* upon the environment. Formula (43) is only one among a host of cases that can be thus studied.

In conclusion, we feel that our attempt is "exposed to destruction", in Mendeleev's sense, in so many ways, that we find it stimulating to present it for this very reason.

Acknowledgment. The author expresses his sincerest thanks to Dean K. B. Newbound and to Prof. H. Umezawa for their warm hospitality, as well as his appreciation for having provided him with an environment which has rendered the writing of this work possible.

References

Caianiello, E. R., Capocelli, R.: Structural analysis of hierarchical systems. Proc. 3rd Int. Joint Conf. Pattern Recognition, Nov. 1976, Coronado, California

Hentsch, J. C.: La circulation des coupures qui constituent une monnaie. J. Soc. Stat. Paris **4**, 279 (1973)

Herdan, G.: The calculus of linguistic observations, Chapter VI. s'Gravenhage: Mouton Co. 1962

Jaynes, E. T.: Information theory and statistical mechanics. Phys. Rev. 106, 620 (1957)

Mandelbrot, B.: Structure formelle des textes et comunications. Deux etudes. World **10**, 1 (1954)

von Neumann, J.: The computer and the brain. New Haven: Yale University 1958

Rothstein, J.: Information measurement and quantum mechanics. Science **114**, 171 (1951)

Rothstein, J.: Information organization as the language of the operational viewpoint. Phil. Sci. **29**, 406 (1962)

Tribus, M.: Information theory as the basis for thermostatics and thermodynamics. J. Appl. Mech. Tr. ASME, Sér. E **28**, 1 (1961)

Zipf, G. K.: Human behaviour and the principle of least effort. Cambridge, MA.: Addison Wesly 1949

Received: October 14, 1976

Prof. E. R. Caianiello
Laboratorio di Cibernetica del CNR
Via Toiano 2
I-80072 Arco Felice (Napoli), Italy

Biol. Cybernetics 26, 159—167 (1977)

Biological Cybernetics

A Model of a Human Neuromuscular System for Small Isometric Tensions

R. D. Traub
IBM Thomas J. Watson Research Center, Yorktown Heights, NY, USA

Abstract. A model is constructed of the motor units in the human first dorsal interosseus (FDI) muscle. Each motorneuron is simulated using a pseudo-steady-state model that omits the membrane capacity and the events underlying the action potential. Properties of individual twitches in the corresponding muscle units are based on the data of Milner-Brown et al. for the FDI, while the transduction between steady firing rate and percentage of maximum tension in a muscle unit is based on the work of Rack and Westbury on the cat soleus muscle. Since we are concerned only with small isometric tensions, we ignore effects due to muscle spindles and to recurrent inhibition. The model allows one to to determine, by simulation, the tension-time functions produced by different "programs" of input to an entire pool of 120 motorneurons. Thus, for example, in order to produce tension rising linearly with time, it suffices to deliver to each neuron in the pool a non-linearly rising conductance; the conductance can be the same for all neurons in the pool, but can NOT be scaled in proportion to the surface area of the respective neurons. The input may be delivered to any part of the neuron's dendritic tree, as long as the electrotonic distribution of input is the same for all the neurons. For a linearly rising force produced in this way, most of the motorneurons yield similar slopes for their frequency-force curves, as observed by Milner-Brown et al. To produce tensions greater than about 1 kg, mechanisms not included in this model must come into play, i.e. perhaps introduction of phasic motorneurons. The most important data needed to improve this model are sets of isometric frequency-force curves for muscle units of different twitch tensions.

Introduction

The purpose of this paper is to construct a model of the tonic motor units comprising the human first dorsal interosseus (FDI) muscle. In doing so, we shall attempt to synthesize data on muscle (derived from the work of Milner-Brown et al. and Rack and Westbury, etc.) with a motorneuron model developed by the author (Traub, 1977); the latter model in turn synthesizes data of Kernell, Henneman, and others.

The model allows one to test, via simulation, the isometric muscle tension produced for a given set of inputs to an entire pool of motorneurons. For a particular motorneuron at a particular time, its input is specified by the excitatory and inhibitory synaptic conductance changes across the different electrotonic regions of its membrane. A set of inputs to the entire pool of motorneurons at a number of different times is called an *input program* to the pool.

We shall use the FDI model to explore how the size principle applies quantitatively to a given muscle. In particular, we examine different input programs to the motorneuron pool, testing the resulting patterns of recruitment and change in firing rate with increasing force, to check for consistency with data of Milner-Brown et al. (1973a–c). Certain input programs are consistent with these data while others are not. Our results suggest certain inferences about the "wering" of the anterior horns of the spinal cord.

The human first dorsal interosseus muscle is chosen because of the availability of both anatomical data on its total number of motor units, and also electromyographic data on the distribution of force thresholds and other properties of the individual motor units.

We shall consider only *slowly changing, small isometric* tensions. "Slowly changing" means that at each time the motorneuron and its muscle fibers are taken to be in a steady state of regular firing and contraction respectively. [Thus, the catch phenomenon in muscle (Burke and Edgerton, 1975) and the effects of bursts, doublets, etc. from the motorneurons are excluded, as is motorneuronal adaptation.] "Small" means "up to about 1 kg", as compared to the maximum tension of 4–6 kg which the FDI can exert (Milner-Brown et al.,

Table 1. Motor unit parameters

Number of motor units	120
Threshold h in g of motor unit i	1000–469 log (i)
Twitch tension w in g for unit of threshold h	$h/200$
Contraction time c in ms for unit of threshold h	70–20 log ($h/20$)
Relaxation half-time r in ms of unit of threshold h	55–15 log ($h/20$)
Average force in g per twitch per ms	$w(c/2-r/\log(0.5))$
Fusion frequency (impulse/s)	$20+h/20$

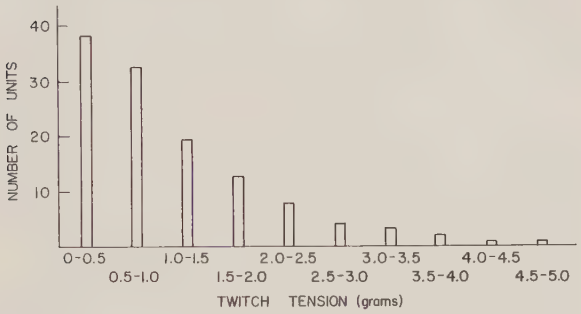

Fig. 1. Distribution of twitch tensions among the muscle units

1973a). At these "small" tensions, we can assume that, in a steady state, the force is produced solely by the activity of tonic motorneurons. We also exclude from consideration recurrent (Renshaw) inhibition and sensory feedback of all kinds onto the motorneurons, either from Golgi tendon organs (which might be important at large tensions) or from muscle spindles; for although the length of the latter may not change during an isometric contraction, $\alpha-\gamma$ coactivation might still produce feedback onto the motorneuron pool that is some function of the tension in the muscle. The practical reasons for the above restrictions are as follows: 1) we avoid the integration of differential equations, since, as will be seen, in the steady state the input-output relations of both motorneurons and muscle units can be expressed by straightforward functions; and 2) by not allowing feedback, we avoid having to consider time explicitly. These two factors allow a great reduction in the complexity of the model, which nevertheless serves to capture some important aspects of the organization of this particular neuro-neuromuscular system.

Construction

Properties of the Muscle Units

Following the terminology of Burke and Edgerton (1975), we shall call the set of muscle fibers in a particular motor unit a *muscle unit*; the motor unit then consists of a muscle unit plus a motorneuron.

Feinstein et al. (1955) estimated that there were 119 motor units in the human FDI. We have therefore used 120 motor units in our model. Note that Feinstein et al.'s estimate is for the *total* number of motor units, whereas our model is concerned only with *tonic* motor units. However, the estimate of Feinstein et al. is based on counting the number of axons in a nerve with extensive branching, and may therefore be too small.

In one of their studies of the FDI, Milner-Brown et al. (1973b) had their subjects develop a force just adequate to activate a given motor unit. The *threshold force of activation* (TFA) could thus be measured. The following properties were then determined as functions of the TFA: twitch tension, contraction time (i.e. time to reach the peak of a twitch), and relaxation half-time for a twitch. [See Figures 3 and 4 of Milner-Brown et al. (1973b).] We have used these figures as follows (Table 1): 1) We take the twitch tension as 1/200 the TFA; 2) the contraction time in ms we take as 70–20 log (TFA/20); and 3) the half-relaxation time in ms we take as 55–15 log (TFA/20). We approximate a twitch as rising linearly to its peak and then decaying exponentially. Thus, we can determine the average tension produced at low frequencies for a motor unit of known TFA.

The most important consequence of the above is this: the TFA of a motor unit and its ability to generate tension correspond; the larger the TFA, the greater the contribution of tension.

Finally, Milner-Brown et al. (1973b) give the distribution of twitch tensions throughout the entire FDI; from this one can easily determine the overall distribution of TFA's. We approximate this distribution by assigning to motor unit i a TFA in grams of 1000–469 log (i). The resulting distribution of TFA's is shown in Figure 1 and in Curve A of Figure 8. We emphasize that this "TFA" is an "*a priori* TFA". It remains to be shown that an input program exists such that motor units are recruited at the correct force levels, i.e. so that the TFA in the simulation equals the "*a priori* TFA". This is the major check of consistency of the model.

We must now determine the mean tension produced by each muscle unit for any given steady stimulating frequency. Here, we are forced to extrapolate from the cat. We shall proceed in two steps:

(A) The data of McPhedran et al. (1965) on the cat soleus muscle (see their Fig. 9) demonstrate that

1) motor units have different fusion frequencies (i.e. frequencies at which maximum tetanic tension is developed);

2) in that particular muscle, no units fuse at frequencies of 10/s although some do at frequencies of 20/s;

3) almost all units fuse at frequencies of 50/s.

We shall assume that the fusion frequency of an FDI motor unit is a monotone increasing frequency of its TFA. (Note that motor units with a small TFA are themselves small, because twitch tension is proportional to TFA.) Our reasoning is that 1) small muscle units are driven by small motorneurons; and 2) small motorneurons have, in their primary range, flatter conductance-frequency curves than large motorneurons, and therefore attain lower maximum frequencies. Thus, the fusion frequency of a small motor unit should be less than the fusion frequency of a large motor unit.

In particular, we shall assume that the fusion frequency is equal, in impulses per second (ips), to 20+TFA/20. Thus, the smallest units are assumed to fuse at about 20 ips and the largest units at about 70 ips.

(B) Rack and Westbury (1969) give the isometric tension for the *entire* cat soleus muscle stimulated (asynchronously through multiple filaments) at various steady frequencies (see their Fig. 7). Note that their curve is not defined at frequencies below 3 ips.

Let T denote tension for a muscle unit or collection of muscle units, and f denote frequency. Rack and Westbury's Figure 7 then defines a function Φ defined by $T=\Phi(f)$. We shall use a slightly modified function Φ in which the discontinuity at 3 ips is removed. Let f_1 denote the fusion frequency for the soleus muscle as a whole (about 35 ips).

We now assume that the frequency-tension response of each muscle unit behaves as a linearly distorted version of Φ: distorted in the vertical axis according to the tetanic tension of the unit, and distorted in the horizontal axis according to the fusion frequency. Thus, if T_{tet} denotes tetanic tension, f_{fus} denotes fusion frequency, and T_{max} denotes the maximum value which Φ assumes, then the tension T of a given motor unit at frequency f will be

$$(T_{tet}/T_{max})\times\Phi(f\times f_1/f_{fus}).$$

We assume further that for each muscle unit T_{tet} is proportional to the average force unit time of a single twitch. This average force is, in turn, a function of contraction time, peak twitch tension and relaxation half-time, all of which themselves are functions of TFA. The tension-frequency curve of a particular motor unit (TFA=166 g) is illustrated in Figure 2.

We have thus defined the frequency-tension response of all the muscle units in the model.

Figure 3 illustrates the ratio of tetanus tension to twitch tension for the entire set of muscle units. This curve would be flat but for the fact that the twitches of the different units do not all have the same time course. The range of values in the curve is from about 5.7 to about 10.8. Note that in McPhedran et al., study of the cat soleus (see McPhedran et al., 1965, p. 75), the range

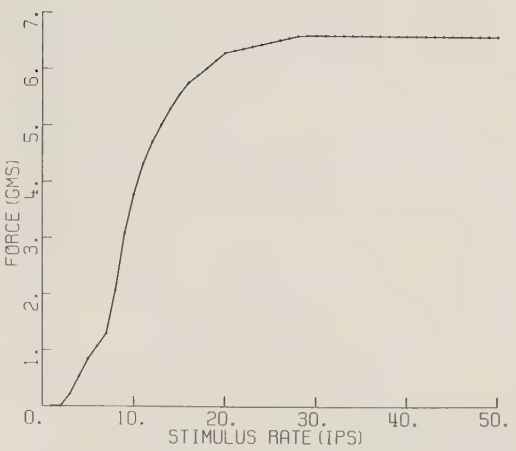

Fig. 2. Tension in a single muscle unit (TFA=166 g) as a function of steady stimulating rate

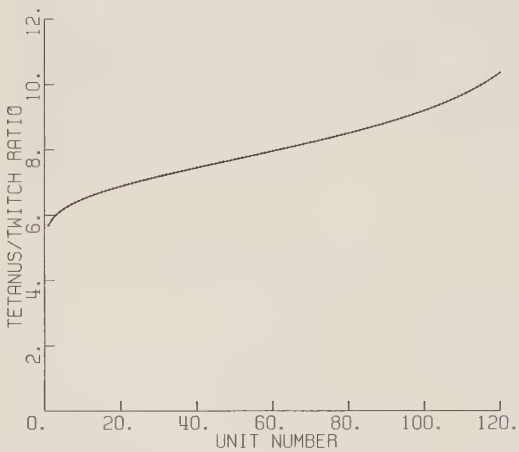

Fig. 3. Ratio of tetanus tension to twitch tension for the different muscle units

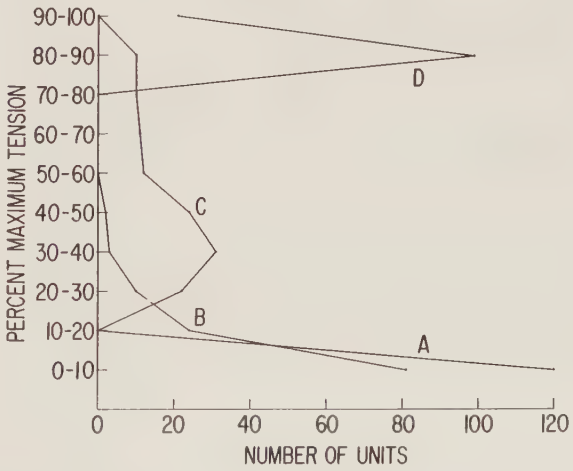

Fig. 4. Percentage of maximum tension developed by the different muscle units at various steady stimulating rates. *A*: 5 ips, *B*: 10 ips, *C*: 20 ips, *D*: 50 ips

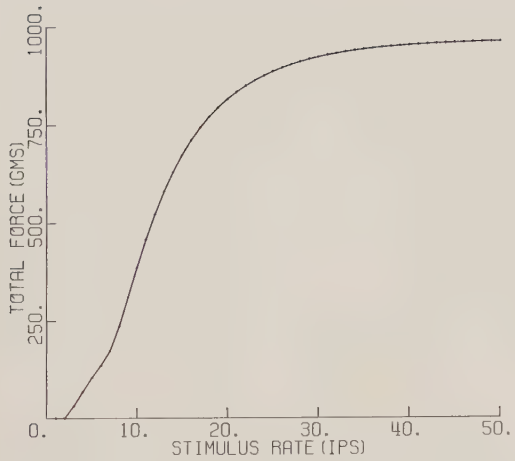

Fig. 5. Total muscle tension as a function of steady stimulating rate (all muscle units stimulated at same rate)

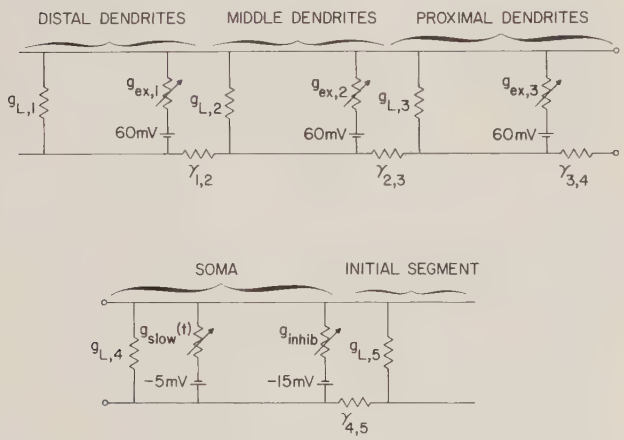

Fig. 6. Electric circuit representation of steady-state motorneuron model

of tetanus to twitch ratio was 6.4 for the smallest muscle unit to 10.1 for the largest.

Figure 4 is a set of histograms for the model population of FDI motor units, with 4 different steady stimulating frequencies. The histograms are qualitatively similar to Figure 9 of McPhedran et al. (1965).

Figure 5 represents the tension of the entire FDI muscle (i.e. the sum of the tensions of the individual motor units) when all units together are stimulated at the same frequency. The curve has a shape similar to Figure 2. Thus, our assumptions relating the frequency-tension curves for the individual units to the frequency-tension curve of an entire muscle are self-consistent.

Properties of the Motorneurons

In a previous paper (Traub, 1977), models of tonic motorneurons of different size were constructed. We shall briefly summarize how this was done.

It was assumed that the soma-dendritic tree could be transformed into a cable by the method of Rall (1962), and that the neuron as a whole could be represented as a non-homogeneous cable (Dodge and Cooley, 1973). The soma and initial segment membranes contained Hodgkin-Huxley-like sodium and potassium conductances. In addition, the soma contained a "slow potassium" conductance which was activated during an action potential and then decayed approximately exponentially with time; this slow potassium conductance was found to determine the interspike intervals during firing in the "primary" range.

We further assumed that all motorneurons shared intensive membrane properties: capacitance/cm^2, leakage conductance/cm^2, sodium and fast and slow potassium conductance densities; and that all motorneurons had the same electrotonic length (1.3) and Hodgkin-Huxley rate functions—*except* for the time constant of inactivation of the slow potassium conductance, denoted $1/\beta_q$. Simulations demonstrated that β_q must depend on the size of the motorneuron; the reason being that, although small motorneurons have lower current and conductance thresholds for the onset of repetitive firing than large motorneurons, the *slope* of the current-firing rate curve ($f-I$ curve) is *less* for a small motorneuron.

The behavior of the motorneuron was then determined by three basic parameters: input resistance (R_{input}), axon conduction velocity, and β_q. The first two parameters determine the geometry of the cell and the last one essentially defines the dynamics of the slow potassium conductance.

With a choice of these three parameters, all other parameters of the neuron were defined. The resulting non-homogeneous cable was then compartmentalized, generally into 5 compartments: distal dendrites, middle dendrites, proximal dendrites, soma and initial segment. The dynamic behavior of this model was obtained by integration of the differential equations describing the electrical circuit equivalent to the compartmentalized cylinder. The model displayed action potentials of appropriate time course, repetitive firing, and an $f-I$ curve with primary and secondary ranges. Inputs to the model were either injected currents, or excitatory or inhibitory synaptic conductances. An excitatory synaptic conductance connected a 60 mV battery across the membrane of one or more of the dendritic compartments, while an inhibitory synaptic conductance connected a -15 mV battery across the soma membrane.

In the idealized case of steady repetitive firing to *constant* synaptic input conductances, the following further simplifications were made to produce the *steady-state* model: 1) membrane capacity and Hodgkin-Huxley events underlying the action potential were

ignored; 2) the soma slow potassium conductance was turned on fully and instantaneously with an action potential and then decayed exponentially in time with time constant $1/\beta_q$; 3) the motorneuron fired an action potential when the initial segment voltage reached a fixed threshold—but this turned out to be equivalent to the soma reaching a fixed threshold. The equivalent electrical network for the steady-state model is shown in Figure 6.

The advantage of the steady-state model is that we can write the firing frequency f as an explicit function of the input conductances. If P is a certain polynomial in the input synaptic conductances (P being determined by the parameters in the equivalent electrical circuit and the voltage threshold), then

$$f = -\beta_q / \log P \quad \text{if} \quad P > 0$$
$$f = 0 \quad \text{otherwise}$$

This avoids the computation associated with integrating differential equations.

This steady-state model predicted steady firing rates accurately at rates less than about 50 ips. At higher rates, it is not possible to ignore membrane capacity and the duration of the action potential becomes non-negligible in comparison with the interspike intervals.

It is this steady-state motorneuron model which is used in this paper.

It remains to define the basic parameters (R_{input}, axon conduction velocity and β_q) for our entire population of motorneurons in terms of the TFA of the corresponding motor units. Note that the axon conduction velocity is used only to scale the dimensions of the initial segment; since time is not included explicitly in the model, we do not use the conduction velocity per se. We know that 1) large motor units (i.e. large TFA) correspond to large motorneurons (i.e. small input resistance); 2) large motorneurons have axons with large conduction velocity; 3) large motorneurons have a small slow potassium time constant.

We therefore take (Table 2), for the motorneuron belonging to a motor unit of TFA $= h$,

$$R_{\text{input}} = 2.5 - h/600 \ (\text{M}\Omega)$$
$$\text{axon conduction velocity} = 100 - 10\,(R_{\text{input}} - 1) \ (\text{m/s})$$
$$\text{slow potassium time constant} = 13.3 + 6.7\,R_{\text{input}} \ (\text{ms}).$$

Thus, as TFA ranges from 0 to 1000 g, R_{input} ranges from 2.5 to 0.83 MΩ, axon conduction velocity from 85 to 102 m/s, and slow K time constant from 30 to 19 ms.

Finally, we assume a voltage threshold of 8 mV for all of the motorneurons.

Table 2. Parameters for motorneuron in motor unit of threshold h g

Input resistance R_{input} (MΩ)	$2.5 - h/600$
Voltage threshold (mV)	8
Axon conduction velocity (m/s)	$100–10\,(R_{\text{input}} - 1)$
Slow potassium time constant (ms)	$13.3 + 6.7\,R_{\text{input}}$

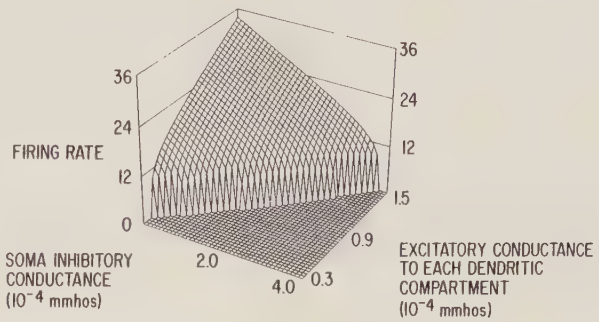

Fig. 7. Steady firing rate of model of a single motorneuron as a function of soma inhibitory conductance and dendritic excitatory conductance (same excitatory conductance on each dendritic compartment). Motorneuron is the one that connects to muscle unit of Figure 2, TFA = 166 g; $R_{\text{input}} = 2.2$ MΩ, $\beta_q = 0.0276$, conduction velocity = 87.8 m/s

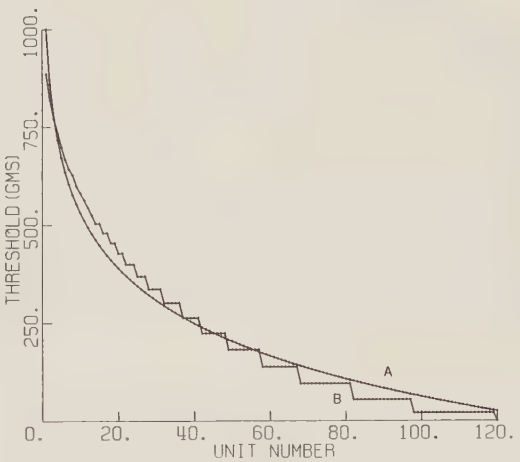

Fig. 8. Threshold force of activation (TFA) for the different muscle units. *A*: *a priori* TFA's. *B*: TFA's observed during simulation with the "basic program". See text

Figure 7 illustrates the steady firing behavior for the motorneuron corresponding to motor unit of TFA = 166 g.

We have now determined all the basic parameters of the neuromuscular model.

The "Basic Program" and Self-consistency of the Model

One of the experiments performed by Milner-Brown et al. (1973c) was the following: a human subject was directed to produce an isometric FDI force that fol-

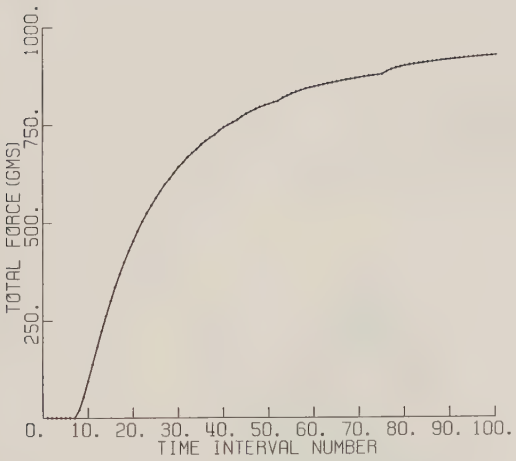

Fig. 9. Total muscle tension for each time interval with the "basic program". See text

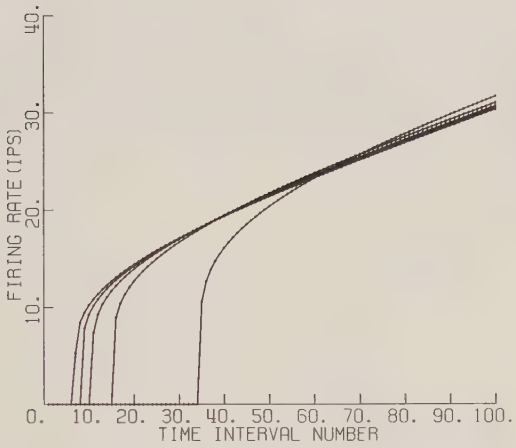

Fig. 10. Firing rates for 5 different motorneurons during "basic program". From left to right, curves correspond to motorneurons connecting to muscle units of TFA = 25, 83, 166, 307, and 672 g respectively

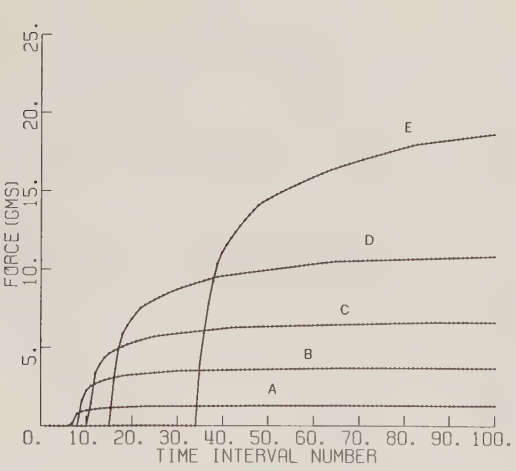

Fig. 11. Tension developed in the muscle units connecting to motorneurons of Figure 10. "Basic program". TFA's are *A*: 25 g, *B*: 83 g, *C*: 166 g, *D*: 307 g, *E*: 672 g

lowed a triangular function of time displayed on an oscilloscope screen; the subject's actual produced force was simultaneously displayed on the screen, so that the difference between desired force and produced force could be used to aid in the control. Milner-Brown et al. then observed the following: 1) independently of TFA, single motor units began to fire at 8.4 ± 1.3 ips and increased their firing rate 1.4 ± 0.6 for each 100 g increase of force; 2) during slow increases in voluntary force, the firing rate tended to plateau.

We idealize this experiment by assuming the subject develops a force ramp, not necessarily linearly in time, sufficiently slowly so that at each time we may apply the steady-state models described above. We ask, then, if there exists a "program" of inputs to the motorneuron pool, defined on suceeding time intervals, which produces a rising force and which recruits motor units at their correct TFA's. For such a program, we can then determine at what rates motor units begin to fire, and how they increase their rate with increasing force. From this program, it is a simple matter to compute inputs which cause the muscle force to rise linearly in time, although this adds no new information.

A conclusion of our earlier paper was that the size principle can arise if input is distributed to a pool of motorneurons so that the same conductance changes are induced on electrotonically equivalent portions of all the neurons in the pool. For this reason, we take as our "basic program" the following: 1) at each time interval, the same excitatory conductance is delivered to all 3 dendritic compartments of all 120 motorneurons; 2) at time interval i, this conductance in mmhos is $3 \times 10^{-5} + i \times 10^{-6}$ on each compartment; 3) there is no inhibition. (Note that 1 mmho = 10^{-3} mhos.)

Figures 8 through 12 illustrate the results of this "basic program". Figure 8, Curve *A*, shows the *a priori* threshold force of activations used in the basic construction, while Curve *B* shows the actual force thresholds for this program. The curves generally agree, although the smaller units (high unit numbers) are recruited at forces somewhat too small. Modulo this minor error, the model is seen to be basically consistent.

Figure 9 illustrates the total force for each time interval. The force "saturates" at about 900 g, showing that this model *does not* apply to forces this large or larger; reasons for this will be discussed later. (A separate computation shows that with all muscle units maximally stimulated, the total force is 963 g.) This figure can be used to find a sequence of inputs that will cause the total force to rise linearly with time (up to a peak of less than 900 g).

Figure 10 shows the firing rates of selected units at each time interval, the curves corresponding, from left to right, to units of TFA 25, 83, 166, 307, and 672 g re-

spectively. The minimum firing rate is not rigorously defined, but if we estimate it to be where the "elbow" of the curves are, the minimum rates will be 8–10 ips. If we were to graph all of the curves for all of the motor units, most would be toward the left side of the figure, because the distribution of motor units is skewed toward those with small TFA. Note that with this "basic program", the fusion frequency of the larger motor units (i.e. about 70 ips) is not approached, the entire operating range of firing rates being here about 8–30 ips.

Figure 11 illustrates the force produced by the same motor units of Figure 10. Most of the motor units eventually produce their maximum tension with this input program.

Finally, Figure 12 illustrates firing rate as a function of force for these same 5 motor units. Recall again that, were we to draw curves for all of the motor units, most of the curves would fall to the left of Curve *C*. The slopes of the linear parts of the curves shown, in ips per 100 g, are: *A* 1.2, *B* 1.4, *C* 1.7, *D* 2.1, *E* 5.3. Thus, for most of the units over most of the range considered, the slope of the force-frequency curve is in the range of 1.4 ips per 100 g observed by Milner-Brown et al. (1973c). The exceptions occur with larger units and larger forces. Note that the firing rates do not plateau with this "input program"; this may be a result of our omission of feedback.

Figure 13 illustrates force as a function of time interval for two similar programs, one consisting of input only to proximal dendrites and the other of input only to distal dendrites. This demonstrates that "pure distal" and "pure proximal" programs can be constructed that will cause total tension to rise linearly; however, both of these programs exaggerate the tendency of small units to be recruited at force levels that are too small.

Another conceivable program would deliver input to all motorneurons in proportion to their surface area: Let $S(i)$ denote the area of motorneuron number i. The program which we shall consider delivers to all dendritic compartments of motorneuron i during time interval j (in mmhos):

$$(10^{-4}+8j\times 10^{-7})\times S(i)/S(1).$$

The results of this program are shown in Figure 14. Note that the largest units are recruited at the smallest forces and vice versa. Thus, a program of input proportional to surface area seems unlikely (if the assumptions of our model are at all reasonable).

Input-output Relations of the Neuromuscular System

Figure 15 illustrates the isometric tension developed in the FDI muscle when all motorneurons in the pool receive the same excitatory conductance (equally distributed among the dendritic compartments) and also the same inhibitory conductance. The surface in Figure 15 resembles a smoothed version of the corresponding surface for a single motorneuron (Figure 7), although the muscle surface is rounded and flattened due to "saturation".

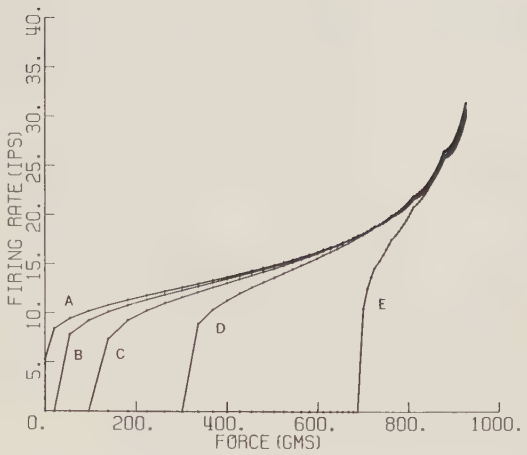

Fig. 12. Firing rate in the motor units of Figures 10 and 11 as a function of total muscle tension. "Basic program". TFA's as in Figure 11

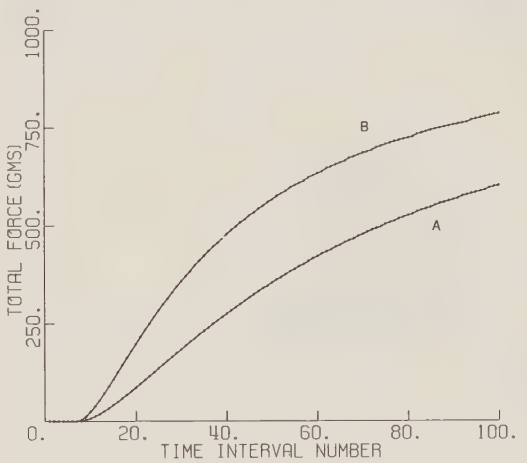

Fig. 13. Result of "input programs" restricted to specific dendritic compartments. *A*: input to distal dendrites only. *B*: input to proximal dendrites only. Further details in text

Discussion

Our model of the isometric FDI neuromuscular system suggests 1) a plausible distribution of parameters (R_{input}, etc.) for the motorneuron pool; and 2) an input program (the "basic program") to the motorneuron pool that yields motor unit TFA's close to our "*a priori* TFA's" (actually based on the observations of Milner-Brown et al.).

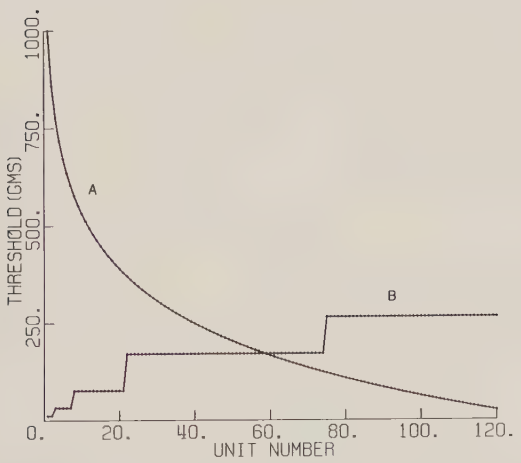

Fig. 14. Threshold force of activation (TFA) for the different muscle units. *A*: *a priori* TFA's. *B*: TFA's observed during simulation in the case where, during each time interval, excitatory conductance on any given motorneuron is proportional to surface area of that motorneuron. Further details in text

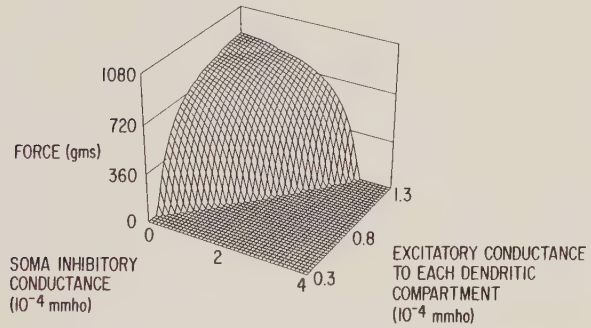

Fig. 15. Total muscle tension as a function of steady-state excitatory and inhibitory synaptic conductances on motorneurons. All motorneurons receive same stimulus. Excitatory conductance equally divided among dendritic compartments

However, the model does not yield forces greater than 963 g even when all the muscle units are maximally stimulated. This suggests either 1) the distribution of tonic motorneurons used contains too few large motorneurons; and/or 2) phasic motorneurons, not included in this model, are important at forces greater than about 1 kg. Our steady-state assumptions will not apply to phasic motorneurons.

Note that the "basic program" can not be used universally. Thus, Tanji and Kato (1973), studying isometric tensions in human abductor digiti minimi, found that motor units recruited at low tensions developed higher firing rates than motor units recruited at large tensions. This suggests a role of inhibitory feedback on the large motorneurons. This finding of Tanji and Kato also suggests that our assumption concerning the lower fusion frequency of small muscle units vis a vis large ones needs to be checked experimentally [see (4) below].

If the CNS does use the "basic program", then one function of the spinal interneurons might be to "decode" commands from the brain so as to induce equivalent conductance changes on all the motorneurons. Thus, if the mean density of synapses is the same for motorneurons of different size, this requires that the synapses on small motorneurons be stimulated at higher frequency than the synapses on large motorneurons; the spinal interneurons might perform this function.

We shall now discuss some of the assumptions and limitations involved in our construction.

1) We postulated a relation between motorneuronal parameters (input resistance and slow K inactivation) and motor unit TFA. Note that TFA is defined in terms of a human performing voluntary actions. Conceivably, our postulated relation could be tested in a trained primate.

2) We ignore feedback from afferent receptors and from Renshaw cells. Such feedback might be expected to lower the firing rates of the larger motorneurons, as suggested in the observations of Tanji and Kato noted above. To include this feedback requires data on Renshaw, γ-motorneuronal and Ia activity during fine voluntary movements, presumably in primates. It also will significantly increase the complexity of the simulation algorithms. Nevertheless, an extension in this direction is essential for real understanding of motor control.

3) We ignore the effects of motorneuronal bursts, doublets, etc., and of history-dependent response in muscle fibers. We ignore phasic motorneurons and restrict our attention to isometric contractions. Here is required a quantitative understanding of how individual motor units respond to arbitrary physiological loads and neuronal inputs, a very difficult matter indeed. Again, even with such an understanding, the computation will become orders of magnitude more difficult.

4) We derive the frequency-force function for the different-sized motor units by extrapolating data from the whole cat soleus muscle. Experimental complete frequency-force curves for individual cat or primate motor units of different size can, in principle, be obtained. This data would increase the accuracy of the model without adding to its complexity.

References

Burke, R.E.: On the central nervous system control of fast and slow twitch motor units. In: Desmedt, J.E. (Ed.): New developments in electromyography and clinical neurophysiology, Vol. 3, pp. 69—94. Basel, Karger 1973

Burke, R.E., Edgerton, V.R.: Motor unit properties and selective involvement in movement. Exercise Sport Sci. Rev. **3**, 31—81 (1975)

Dodge, F.A., Jr., Cooley, J.W.: Action potential of the motorneuron. IBM J. Res. Dev. **17**, 219—229 (1973)

Eccles, R.M., Phillips, C.G., Chien-Ping, W.: Motor innervation, motor unit organization and afferent innervation of M. Extensor Digitorum Communis of the baboon's forearm. J. Physiol. **198**, 179—192 (1968)

Feinstein, B., Lindegard, B., Nyman, E., Wohlfart, G.: Morphologic studies of motor units in normal human muscles. Acta Anat. **23**, 127—142 (1955)

Kernell, D.: The limits of firing frequency in cat lumbosacral motoneurons possessing different time course of afterhyperpolarization. Acta Physiol. Scand. **65**, 87—100 (1965)

Kernell, D.: Input resistance, electrical excitability and size of ventral horn cells in cat spinal cord. Science **152**, 1637—1640 (1966)

McPhedran, A.M., Wuerker, R.B., Henneman, E.: Properties of motor units in a homogeneous red muscle (soleus) of the cat. J. Neurophysiol. **28**, 71—84 (1965)

Milner-Brown, H.S., Stein, R.B., Yemm, R.: The contractile properties of human motor units during voluntary isometric contractions. J. Physiol. **228**, 371—390 (1973a)

Milner-Brown, H.S., Stein, R.B., Yemm, R.: The orderly recruitment of human motor units during voluntary isometric contractions. J. Physiol. **230**, 359—370 (1973b)

Milner-Brown, H.S., Stein, R.B., Yemm, R.: Changes in firing rate of human motor units during linearly changing voluntary contractions. J. Physiol. **230**, 371—390 (1973c)

Milner-Brown, H.S., Stein, R.B., Lee, R.G.: Pattern of recruiting human motor units in neuropathies and motor neurone disease. J. Neurol. Neurosurg. Psychiat. **37**, 665—669 (1974)

Rack, P.M.H., Westbury, D.R.: The effects of length and stimulus rate on tension in the isometric cat soleus muscle. J. Physiol. **204**, 443—460 (1969)

Rall, W.: Theory of physiological properties of dendrites. Ann. N.Y. Acad. Sci. **96**, 1071—1092 (1962)

Tanji, J., Kato, M.: Firing rate of individual motor units in voluntary contraction of abductor digiti minimi muscle in man. Exp. Neurol. **40**, 771—783 (1973)

Traub, R.: Motorneurons of different geometry and the size principle. Biol. Cybernetics **25**, 163—176 (1977)

Received: November 11, 1976

Dr. Roger D. Traub
IBM Thomas J. Watson Research Center
Yorktown Heights, NY 10598, USA

Biol. Cybernetics 26, 169—174 (1977)

Biological Cybernetics

Funktionsschema zur Beschreibung der subjektiven Bewertung von Schalländerungen

W. Suchowerskyj
Lehrstuhl für Elektroakustik der Technischen Universität München, BRD

Model of the Subjective Evaluationof Sound Variations

Abstract. Periodic changes of different sound parameters can be compared using the strength of the fluctuation sensation as common criterion. The model porposed describes the relation between the fluctuation sensation and the sound changes. The first stage of the model, which detects level differences within critical bands produced by the parameter changes in the sound spectrum, is followed by a weighting, squaring and summing network, providing at its output a signal proportional to the subjective fluctuation strength. This model is applied to predict equivalent parameter variations, i.e. variations which produce the same fluctuation strength, e.g. equivalent changes of sound pressure level and of cut-off frequency of filtered noise. The predictions of the model are in good agreement with corresponding experimental results. The model can also be applied to describe subjective differences between steady sounds.

1. Einführung

Überschwellige Änderungen der physikalischen Parameter von akustischen Signalen lassen sich auch dann subjektiv miteinander vergleichen, wenn sie zu Änderungen verschiedenartiger Hörempfindungen führen. Versuchspersonen können z. B. angeben, ob der Tonhöhen- oder der Lautstärkeunterschied zwischen aufeinanderfolgenden Sinustönen subjektiv größer erscheint (Terhardt, 1968a), und sie können diese Unterschiede relativ zu einem Standard durch Zahlenangaben schätzen (Carvellas u. Schneider, 1972). Dadurch ist es möglich, die subjektive Bewertung von Schalländerungen systematisch zu untersuchen und quantitativ zu beschreiben (Suchowerskyj, 1975, 1976, 1977a, b). Im folgenden wird ein Funktionsschema vorgeschlagen, das es erlaubt, Schalländerungen hinsichtlich ihrer subjektiven Bewertung abzuschätzen und in eine Rangfolge zu bringen. Solche Abschätzungen können beispielsweise bei der Behandlung von Problemen der Informationsübertragung durch akustische Signale und bei der Klassifikation von Sprachlauten Verwendung finden.

Der Umstand, daß Änderungen verschiedenartiger Hörempfindungen miteinander verglichen werden können, läßt auf die Existenz eines übergeordneten Entscheidungskriteriums schließen. Solch ein Kriterium ist z. B. die „Schwankungsstärke". Langsame periodische Schalländerungen rufen die Empfindung „Schwankungsstärke" hervor (Zwicker, 1962; Terhardt, 1968b). Diese ist psychophysikalisch skalierbar (Terhardt, 1968c). Der Vergleich von periodischen Änderungen verschiedener Schallparameter erfolgt demnach mit Hilfe des gemeinsamen Kriteriums „Schwankungsstärke".

Experimente zur subjektiven Bewertung von Schalländerungen wurden so durchgeführt, daß zu jeder Änderung eines bestimmten physikalischen Schallparameters diejenige Änderung eines anderen Parameters ermittelt wurde, die im Mittel subjektiv gleich groß erschien (Suchowerskyj, 1977b). Solche Änderungen wurden als *äquivalent* bezeichnet. Die Zusammenhänge zwischen einander äquivalenten Parameteränderungen wurden in Form von *Äquivalenzfunktionen* angegeben. Die vor allem mit verschiedenen Rauschspektren angestellten Versuche führten im wesentlichen zu folgenden Ergebnissen:

1. Periodische Änderungen verschiedener physikalischer Parameter eines Schalles sind subjektiv äquivalent, das heißt, sie erzeugen die gleiche subjektive Schwankungsstärke, wenn sie die gleiche Anzahl von Unterschiedsschwellen umfassen.

2. Bei breitbandigen Schallen setzt sich die subjektive Schwankungsstärke aus Beiträgen verschiedener Teile des Schallspektrums zusammen.

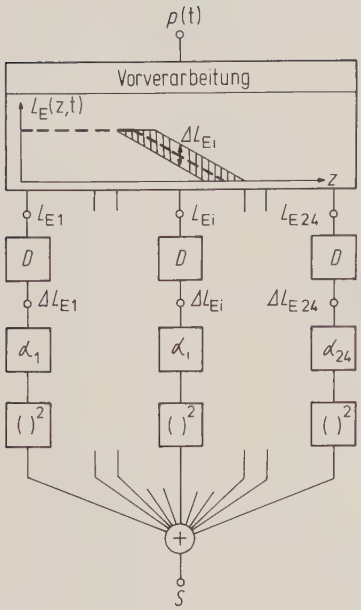

Abb. 1. Funktionsschema für den Zusammenhang zwischen dem Schalldruck $p(t)$ und der subjektiven Schwankungsstärke S. Erläuterungen im Text

3. Beiträge hochfrequenter Spektralanteile werden subjektiv stärker bewertet als Beiträge tieffrequenter Teile.

Wenn es gelingt, die Zusammenhänge zwischen den Änderungen des Schallspektrums und der daraus resultierenden Schwankungsstärke allgemein zu formulieren, so lassen sich diejenigen Bedingungen voraussagen, unter denen periodische Schalländerungen als subjektiv äquivalent beurteilt werden. Nachstehend wird ein Funktionsschema der subjektiven Schwankungsstärke beschrieben, mit dessen Hilfe Äquivalenzfunktionen für periodische Schalländerungen berechnet werden können. Die berechneten Äquivalenzfunktionen werden mit experimentell ermittelten Daten verglichen. Abschließend wird gezeigt, daß mit diesem Funktionsschema auch die Beurteilung von diskontinuierlichen Parameteränderungen zwischen aufeinanderfolgenden stationären Schallen beschrieben werden kann.

2. Das Funktionsschema

Das in Abb. 1 dargestellte Funktionsschema dient der zusammenfassenden Darstellung der Beziehungen zwischen dem Schallreiz und der Empfindung Schwankungsstärke. Eine Vorverarbeitungsstufe transformiert die Zeitfunktion $p(t)$ des Schalldrucks in ein zeitabhängiges Erregungspegel-Tonheitsmuster $L_E(z, t)$. Diese Transformation berücksichtigt im wesentlichen das spektrale Auflösungsvermögen des Gehörs. Das Erregungspegel-Tonheitsmuster wird aus Messungen der Mithörschwelle hergeleitet. Der Zusammenhang zwischen Schallspektrum und Erregungspegel ist an anderer Stelle bereits ausführlich beschrieben (Zwicker, 1958; Maiwald, 1967; Zwicker u. Feldtkeller, 1967). Als Beispiel ist in Abb. 1 der Erregungspegel L_E eines Tiefpaßrauschens als Funktion der Tonheit z dargestellt (gestrichelt). Eine Einheit der Tonheitsskale z (1 Bark) entspricht der Breite einer Frequenzgruppe, die wiederum eine Grenze des spektralen Auflösungsvermögens des Gehörs repräsentiert. Im hörbaren Frequenzbereich lassen sich 24 Frequenzgruppen lückenlos aneinanderreihen. Die quantitativen Beziehungen zwischen Tonheit z und Frequenz f können aus den beiden Abszissenskalen in Abb. 2a entnommen werden.

Das Erregungspegel-Tonheitsmuster wird an 24 äquidistanten Stellen der Tonheitsskale abgenommen und in 24 Kanälen weiterverarbeitet. Aus der Zeitfunktion des Erregungspegels L_{Ei} bei der Tonheit z_i wird mit Hilfe eines Diskriminators die Pegelschwankung ΔL_{Ei} gewonnen. ΔL_{Ei} ist die Differenz zwischen Maximal- und Minimalwert der periodischen Zeitfunktion $L_{Ei}(t)$ des Erregungspegels. Diese Größe wird mit einem von der Tonheit z abhängigen Faktor α_i bewertet und anschließend quadriert. Die Summe der 24 Ausgangssignale ergibt die subjektive Schwankungsstärke S:

$$S = \sum_{i=1}^{24} (\alpha_i \Delta L_{Ei})^2 \,. \tag{1}$$

Die einzelnen Funktionen des Schemas beruhen auf folgenden Erkenntnissen.

1) Aus experimentellen Untersuchungen ergab sich, daß die subjektive Schwankungsstärke aus Beiträgen verschiedener Teile des Schallspektrums gebildet wird, ebenso wie die Hörempfindungen Lautheit und Rauhigkeit. In Analogie zu einem gemeinsamen Funktionsschema der Lautheit und der Rauhigkeit (Vogel, 1975), bei dem sich das Erregungspegel-Tonheitsmuster $L_E(z)$ als geeignete Zwischengröße erwiesen hat, wurde auch hier eine Verarbeitung in frequenzgruppenbreiten Bändern angenommen.

2) Die Skalierung der subjektiven Schwankungsstärke von amplitudenmodulierten Sinustönen ergab, daß die Schwankungsstärke dem Quadrat des Modulationsgrades m proportional ist (Terhardt, 1968c). Andererseits ist die Pegelschwankung ΔL amplitudenmodulierter Töne bis zu Modulationsgraden von etwa 60% dem Modulationsgrad proportional (vgl. Zwicker u. Feldtkeller, 1967) und das Gehör kann den Pegeländerungen bei kleinen Modulationsfrequenzen recht gut folgen (Zwicker, 1976; Fastl, 1976). Die Wahl des quadratischen Zusammenhangs zwischen Schwankungsstärke und Pegelschwankung erscheint demnach als sinnvoll.

3) Der Bewertungsfaktor α berücksichtigt, daß Pegelschwankungen in hochfrequenten Spektralbereichen stärker bewertet werden als in tieffrequenten Bereichen. Ein solches Verhalten des Gehörs ist auch aus Mithörschwellenmessungen bekannt: Bei breitbandigem Rauschen nimmt die innerhalb einer Frequenzgruppe eben wahrnehmbare Pegeländerung, das sogenannte Schwellenmaß ΔL_s, von hohen nach tiefen Frequenzen um etwa den Faktor 2,2 zu (Scholl, 1961; Zwicker u. Feldtkeller, 1967). Das Schwellenmaß ΔL_s gehorcht in guter Näherung der Beziehung

$$\Delta L_s(z) = 2{,}2\,\mathrm{dB} - 0{,}05\,\frac{\mathrm{dB}}{\mathrm{Bark}}\,z\,. \tag{2}$$

Der Bewertungsfaktor α wurde für Rauschen versuchsweise festgelegt zu

$$\alpha(z) = \frac{1}{\Delta L_s(z)}\,. \tag{3}$$

Um die Berechnung der subjektiven Schwankungsstärke zu vereinfachen, ist es zweckmäßig, das Aufsummieren von Teilbeträgen gemäß (1) durch eine Integration über der Tonheit z zu ersetzen. Entsprechend (1) gilt dann für die subjektive Schwankungsstärke

$$S = \int_0^{24\ \mathrm{Bark}} \alpha^2(z)\,\Delta L_E^2(z)\,dz/\mathrm{Bark}\,. \tag{4}$$

3. Die Berechnung subjektiv äquivalenter Schalländerungen

Mit Hilfe der in Abschnitt 2 getroffenen Vereinbarungen läßt sich in vielen Fällen der Zusammenhang zwischen den Änderungen des Schallspektrums und der daraus resultierenden subjektiven Schwankungsstärke algebraisch formulieren. Um die Bedingungen zu ermitteln, unter denen periodische Änderungen zweier verschiedener Parameter eines Schalles subjektiv äquivalent erscheinen, d. h. die gleiche subjektive Schwankungsstärke erzeugen, sind zunächst die beiden mathematischen Ausdrücke für die Schwankungsstärke aufzustellen und anschließend gleichzusetzen. Dieses Vorgehen wird im folgenden anhand eines Beispieles erläutert, bei dem das rechnerische Ergebnis mit entsprechenden Versuchsergebnissen verglichen werden kann.

In Abb. 2a ist schematisch das Spektrum eines breitbandigen Rauschens dargestellt, welches sich aus einem Tiefpaßrauschen (durchgezogen) und einem Hochpaßrauschen (gestrichelt) zusammensetzt. Aufgetragen ist der Anregungspegel L_A, d. h. der Pegel der in jeweils eine Frequenzgruppe fallenden Intensität des Rauschens, als Funktion der Tonheit z. Der Erregungspegel L_E kann für den vorliegenden Zweck

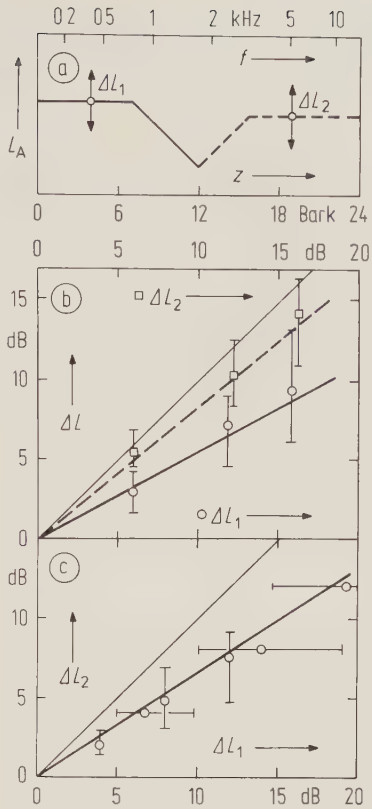

Abb. 2. a Anregungspegel L_A eines breitbandigen Testschalles, zusammengesetzt aus einem Tiefpaßrauschen (durchgezogen) und einem Hochpaßrauschen (gestrichelt), als Funktion der Tonheit z bzw. der Frequenz f. Die Pegel der beiden Rauschanteile wurden entweder allein (ΔL_1, ΔL_2) oder gemeinsam (ΔL) mit 4 Hz Modulationsfrequenz variiert. **b** Äquivalente Pegelschwankung ΔL des gesamten Rauschens als Funktion der Pegelschwankung ΔL_1 des tieffrequenten Anteils (Kreise, durchgezogene Gerade) und als Funktion der Pegelschwankung ΔL_2 des hochfrequenten Anteils (Quadrate, gestrichelte Gerade). **c** Äquivalente Pegelschwankung ΔL_2 des hochfrequenten Rauschanteils als Funktion der Pegelschwankung ΔL_1 des tieffrequenten Rauschanteils. Die eingetragenen Meßwerte sind Zentralwerte und Quartile der aus jeweils 288 Aussagen von 6 Versuchspersonen gewonnenen psychometrischen Funktionen. Die dargestellten Äquivalenzgeraden wurden mit Hilfe des Funktionsschemas berechnet

mit ausreichender Näherung gleich dem Anregungspegel L_A gesetzt werden. Die beiden spektralen Hüllkurven schneiden sich bei der Tonheit 12 Bark, d. h. beide Teilgeräusche bedecken jeweils dieselbe Anzahl von Frequenzgruppen.

Bei den Experimenten wurden die Pegel der beiden Rauschanteile einzeln oder gemeinsam mit 4 Hz moduliert (Suchowerskyj, 1977b). Es wurde ermittelt, unter welchen Bedingungen periodische Pegeländerungen des tieffrequenten Rauschanteils (ΔL_1), des hochfrequenten Rauschanteils (ΔL_2) und des gesamten Rauschspektrums (ΔL) zu subjektiv gleich großen Schwankungsstärken führten. Abbildung 2c zeigt bei-

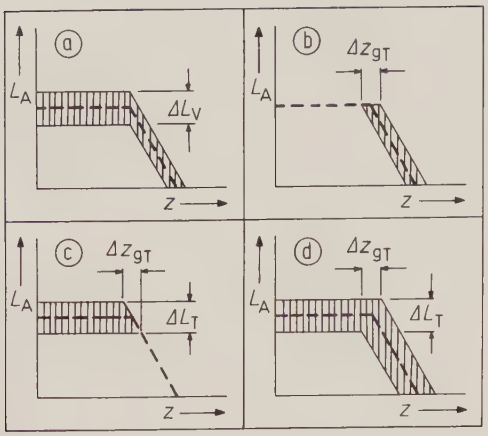

Abb. 3a—d. Anregungspegel L_A eines Tiefpaßrauschens als Funktion der Tonheit z (gestrichelt). Schraffierte Bereiche: Extremwerte des Anregungspegels bei Modulation des Pegels **a**, der Grenzfrequenz **b**, und bei gleichzeitiger Modulation des Pegels und der Grenzfrequenz in Gegenphase **c** oder in Phase **d**

spielsweise die Ergebnisse für den Vergleich der tief- und der hochfrequenten Pegeländerungen ΔL_1 bzw. ΔL_2. Im Gebiet oberhalb der dick durchgezogenen Geraden führen überwiegend die Pegeländerungen ΔL_2, darunter die Pegeländerung ΔL_1 zu einer subjektiv größeren Schwankungsstärke. Die Gerade stellt eine Grenze dar, bei der die beiden Pegeländerungen im Mittel als subjektiv äquivalent beurteilt werden. Sie wird deshalb als *Äquivalenzgerade* bezeichnet. Die Meßwerte liegen deutlich unterhalb der dünn eingetragenen Winkelhalbierenden $\Delta L_2 = \Delta L_1$. Um die gleiche subjektive Schwankungsstärke zu erzeugen, muß also die Pegelschwankung ΔL_1 des tieffrequenten Rauschanteils wesentlich größer sein als eine Pegelschwankung ΔL_2 des hochfrequenten Rauschanteils. Auf entsprechende Weise lassen sich die in Abb. 2b dargestellten Ergebnisse für den Vergleich von ΔL mit ΔL_1 bzw. ΔL_2 interpretieren.

Die in Abb. 2 dargestellten Äquivalenzgeraden wurden mit Hilfe des Funktionsschemas folgendermaßen berechnet: Bei Modulation des gesamten Rauschspektrums ist die Erregungspegelschwankung ΔL_E im gesamten Tonheitsbereich konstant gleich der Pegelschwankung ΔL. Mit (4) gilt also für die Schwankungsstärke

$$S = \Delta L^2 \int_0^{24\ \text{Bark}} \alpha^2(z)dz/\text{Bark} . \tag{5}$$

Bei Modulation des tieffrequenten Rauschanteils ist ΔL_E im Bereich zwischen 0 und 12 Bark konstant gleich ΔL_1 und darüber gleich Null. Somit gilt in diesem Fall:

$$S_1 = \Delta L_1^2 \int_0^{12\ \text{Bark}} \alpha^2(z)dz/\text{Bark} . \tag{6}$$

Analog dazu ist für die Schwankungsstärke S_2 bei Modulation des hochfrequenten Rauschanteils eine Integration zwischen 12 und 24 Bark durchzuführen.

$$S_2 = \Delta L_2^2 \int_{12\ \text{Bark}}^{24\ \text{Bark}} \alpha^2(z)dz/\text{Bark} . \tag{7}$$

Durch Gleichsetzen von (5) und (6) erhält man nach numerischer Auswertung der Integrale:

$$\Delta L = 0{,}56\,\Delta L_1 \tag{8}$$

und entsprechend

$$\Delta L = 0{,}83\,\Delta L_2 , \tag{9}$$

$$\Delta L_2 = 0{,}67\,\Delta L_1 . \tag{10}$$

Die aus Abb. 2 ersichtliche Übereinstimmung dieser berechneten Äquivalenzgeraden mit den Meßergebnissen ist als erste Bestätigung für die Richtigkeit der dem Funktionsschema zugrundeliegenden Annahmen zu werten.

4. Weitere Beispiele

Anhand einiger weiterer Beispiele soll geprüft werden, ob das in Abschnitt 2 vorgeschlagene Funktionsschema zutreffende Voraussagen über die subjektive Bewertung von Schalländerungen liefert. Hierzu werden die experimentellen Daten aus mehreren mit Tiefpaß- und Hochpaßrauschen durchgeführten Versuchsreihen den berechneten Äquivalenzbeziehungen gegenübergestellt. Einzelheiten der Berechnungen sind an anderer Stelle ausführlich beschrieben (Suchowerskyj, 1976), ebenso Methodik und Versuchsergebnisse (Suchowerskyj, 1977b).

Die Versuchsbedingungen seien anhand der in Abb. 3 dargestellten Spektren (vgl. Abb. 2a) erläutert. Aus gleichmäßig anregendem Rauschen (vgl. Zwicker u. Feldtkeller, 1967) wurde ein Tiefpaßrauschen ausgeschnitten, dessen Pegel und Grenzfrequenz unabhängig voneinander mit 4 Hz moduliert werden konnten. Den Versuchspersonen wurden nacheinander ein Test- und ein Vergleichsschall dargeboten. Bei dem Testschall war entweder nur die Grenzfrequenz (b) oder gleichzeitig Grenzfrequenz und Pegel moduliert, und zwar in einer Versuchsreihe gegenphasig (c), in einer zweiten Versuchsreihe gleichphasig (d). Bei dem Vergleichsschall wurde immer nur der Pegel moduliert (a). Die Versuchspersonen hatten anzugeben, welcher der beiden Schalle die größere subjektive Schwankungsstärke aufwies. Bei dem in Abb. 3c dargestellten Fall wurde das Verhältnis der Pegel- und der Grenzfrequenzänderungen so gewählt, daß im Bereich der Filterflanke keine Änderungen des Anregungspegels L_A auftraten. Die Bedingung hierfür ergab sich aus dem Dämpfungsanstieg des verwendeten Filters (11 dB/Bark).

Die Meßergebnisse sind gemeinsam in Abb. 4a dargestellt. Die eingetragenen Äquivalenzgeraden wurden gemäß (4) berechnet. Aufgetragen ist die äqui-

valente Pegelschwankung ΔL_V des Vergleichsschalles als Funktion der Pegelschwankung ΔL_T bzw. der Grenzfrequenzschwankung des Vergleichsschalles, umgerechnet in eine Tonheitsdifferenz Δz_{gT}. Zum Vergleich ist dünn durchgezogen die Winkelhalbierende $\Delta L_V = \Delta L_T$ eingetragen. Kreise symbolisieren die Ergebnisse für konphase Modulation des Pegels und der Grenzfrequenz (gestrichelte Gerade, vgl. Abb. 3d), Quadrate für gegenphasige Modulation (strichpunktierte Gerade, vgl. Abb. 3c). Die Dreiecke repräsentieren die Resultate für Testschalle, bei denen nur die Grenzfrequenz moduliert war (Abb. 3b). In diesem Fall kann die Skale für ΔL_T als die durch Δz_{gT} erzeugte Schwankung des Anregungspegels im Bereich der Filterflanke gedeutet werden.

Bei der Berechnung der Äquivalenzgeraden war zu berücksichtigen, daß die Frequenzbereiche oberhalb derjenigen Stelle, bei der der Anregungspegel die Ruhehörschwelle unterschreitet, keine Beiträge zur resultierenden Schwankungsstärke liefern. Außerdem wurde die Schwankung ΔL_E des Erregungspegels unterhalb bzw. oberhalb der Grenzfrequenz jeweil als konstant angenommen. Die berechneten Äquivalenzgeraden stimmen mit den Meßergebnissen recht gut überein. Pegeländerungen nur unterhalb der Grenzfrequenz (strichpunktierte Äquivalenzgerade) oder nur oberhalb der Grenzfrequenz (durchgezogene Gerade) erzeugen eine geringere Schwankungsstärke als Pegeländerungen des gesamten Spektrums (Winkelhalbierende). Bei stärkerer Modulation im Bereich der Filterflanke nimmt die Schwankungsstärke weiter zu (gestrichelte Äquivalenzgerade).

Die entsprechenden Ergebnisse für Hochpaßrauschen sind in Abb. 4b dargestellt. Hier bleibt die Filterflanke bei konphaser Modulation unmoduliert. Daher liegen die entsprechenden Meßergebnisse (Kreise) unterhalb der Winkelhalbierenden. Der Einfluß der Phasenlage ist bei dem Hochpaßrauschen trotz gleicher Grenzfrequenz wesentlich geringer als beim Tiefpaßrauschen. Da der Bewertungsfaktor mit zunehmender Frequenz ansteigt, sind bei Hochpaßrauschen die Beiträge zur Schwankungsstärke aus dem Bereich der Filterflanke (unterhalb der unteren Grenzfrequenz) geringer und die Beiträge aus dem Gebiet oberhalb der Grenzfrequenz größer. Das verdeutlicht auch die geringe Steigung der Äquivalenzgeraden für die Testschalle, bei denen nur die Grenzfrequenz moduliert war (Dreiecke). Auch hier stimmen die berechneten Äquivalenzgeraden mit den Meßergebnissen gut überein.

Neben den Versuchen mit kontinuierlichen, periodischen Schalländerungen wurden auch Experimente mit diskontinuierlichen Unterschieden zwischen aufeinanderfolgenden, stationären Schallen durchgeführt (Suchowerskyj, 1977a). Den Versuchspersonen wurden dabei je zwei Paare von Schallen dargeboten, die sich jeweils bezüglich eines anderen Parameters unterschieden. Die Versuchspersonen hatten anzugeben, welches der beiden Paare subjektiv den größeren Unterschied aufwies. Diese Experimente führten zu quantitativ vergleichbaren Ergebnissen. Es liegt daher nahe, das in Abschnitt 3 beschriebene Verfahren zur Berechnung subjektiv äquivalenter Schalländerungen auch für den Fall diskontinuierlicher Unterschiede zwischen aufeinanderfolgenden Schallen anzuwenden.

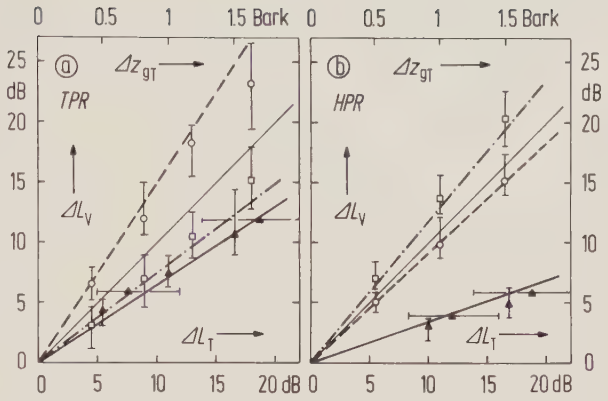

Abb. 4a u. b. Äquivalente Pegelschwankung ΔL_V eines Vergleichsschalles als Funktion der Schwankung der Grenzfrequenz des Testschalles, umgerechnet in Tonheitsschwankungen Δz_{gT} (Dreiecke, durchgezogene Gerade), und als Funktion der Pegelschwankung ΔL_T bei gleichzeitiger Modulation des Pegels und der Grenzfrequenz des Testschalles gemäß Abb. 3 in Phase (Kreise, gestrichelte Gerade) oder Gegenphase (Quadrate, strichpunktierte Gerade) bei Tiefpaßrauschen **a** und Hochpaßrauschen **b**, jeweils mit der Grenzfrequenz $f_g = 1{,}25$ kHz. Meßwerte für 6 Versuchspersonen wie Abb. 2. Die dünnen Linien sind die Winkelhalbierenden $\Delta L_V = \Delta L_T$. Die eingetragenen Äquivalenzgeraden wurden mit Hilfe des Funktionsschemas berechnet

In Abb. 5 ist das Ergebnis solcher Versuche mit Hochpaßrauschen dargestellt. Aufgetragen ist der äquivalente Pegelunterschied ΔL des einen Schallpaares als Funktion des Grenzfrequenzunterschiedes Δf_g des anderen Schallpaares, umgerechnet in eine Tonheitsdifferenz Δz_g. Kreise symbolisieren die Meßwerte bei einem Bezugspegel von $L_0 = 60$ dB und bei der Grenzfrequenz $f_{g0} = 1$ kHz, Quadrate die Ergebnisse für $L_0 = 52$ dB und $f_{g0} = 700$ Hz. Die berechneten Äquivalenzgeraden stimmen mit diesen Ergebnissen gut überein. Bei dem Hochpaßrauschen mit der Grenzfrequenz $f_{g0} = 700$ Hz ist wegen des geringeren Pegels der über der Ruhehörschwelle liegende Bereich der Filterflanke kleiner als bei dem Rauschen mit $f_{g0} = 1$ kHz. Der Flankenbereich liegt außerdem bei tieferen Frequenzen. Aus diesen beiden Gründen werden nach dem Funktionsschema die Pegelunterschiede im Flankenbereich des Hochpaßrauschens bei 700 Hz geringer bewertet als bei 1 kHz. Die Äquivalenzgerade für $f_{g0} = 700$ Hz (gestrichelt) verläuft daher flacher als die Äquivalenzgerade für $f_{g0} = 1$ kHz. Dieses Beispiel mag verdeutlichen, daß mit Hilfe des vorgeschlagenen Funktionsschemas auch die Bewertung von Unterschieden zwischen aufeinanderfolgenden Schallen beschrieben werden kann.

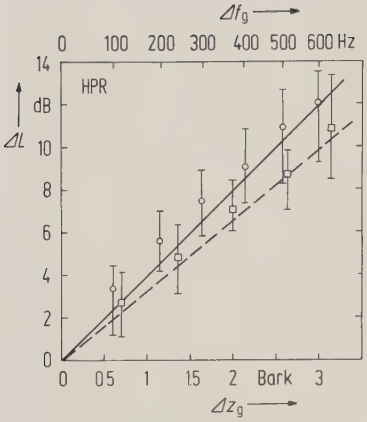

Abb. 5. Äquivalenter Pegelunterschied ΔL eines Paares von stationären Testschallen als Funktion des Grenzfrequenzunterschiedes Δf_g eines zweiten Testschallpaares, umgerechnet in eine Tonheitsdifferenz Δz_g. Testschalle waren Hochpaßrauschen mit dem Bezugspegel $L_0 = 60$ dB und mit der Grenzfrequenz $f_{g0} = 1$ kHz (Kreise, durchgezogene Gerade) bzw. $L_0 = 52$ dB und $f_{g0} = 700$ Hz (Quadrate, gestrichelte Gerade). Meßwerte für 6 Versuchspersonen. Die eingetragenen Äquivalenzgeraden wurden mit Hilfe des Funktionsschemas berechnet

5. Schlußbemerkungen

Es wurde ein Funktionsschema vorgeschlagen, das den Zusammenhang zwischen periodischen Änderungen des Schallspektrums und der dabei wahrnehmbaren subjektiven Schwankungsstärke quantitativ beschreibt. Mit Hilfe dieses Schemas konnten rechnerisch diejenigen Bedingungen ermittelt werden, unter denen Änderungen verschiedener Parameter eines Schalles zu der gleichen subjektiven Schwankungsstärke führen und deshalb subjektiv äquivalent erscheinen. Für eine Reihe von Beispielen wurde gezeigt, daß die rechnerischen Ergebnisse sehr gut mit den vorliegenden Versuchsergebnissen übereinstimmen. Die dem Funktionsschema zugrundeliegenden Annahmen erwiesen sich insoweit als zweckmäßig.

Die beim Vergleich zwischen Messung und Berechnung angeführten Beispiele bezogen sich ausschließlich auf Versuche mit Rauschspektren. Der Grund dafür besteht darin, daß der Zusammenhang zwischen Schallspektrum und Erregungspegel-Tonheitsmuster z. B. für Linienspektren oder Sinustöne nur unzureichend bekannt ist (Schöne, 1977). Unter grob vereinfachenden Annahmen ist jedoch auch bei Sinustönen eine Übereinstimmung zwischen Rechnung und Versuchsergebnis erzielbar (Suchowerskyj, 1976).

Das Funktionsschema ist nicht nur bei periodischen Schalländerungen anwendbar, vielmehr konnte gezeigt werden, daß es auch für die Beschreibung äquivalenter Unterschiede zwischen aufeinanderfolgenden, stationären Schallen geeignet ist. Das vorgeschlagene Schema ist offenbar von allgemeiner Bedeutung und beschreibt im Ansatz die Verarbeitung von beliebigen Änderungen des Schallspektrums.

Ich danke Herrn Prof. Dr.-Ing. E. Zwicker für zahlreiche Ratschläge bei der Durchführung der Experimente. Herrn Dr.-Ing. E. Terhardt danke ich für wertvolle Hinweise bei der Durchsicht des Manuskripts. Diese Arbeit wurde von der Deutschen Forschungsgemeinschaft im Rahmen des Sonderforschungsbereiches „Kybernetik" (München) gefördert.

Literatur

Carvellas, T., Schneider, B.: Direct estimation of multidimensional tonal dissimilarity. J. Acoust. Soc. Amer. **51**, 1839–1848 (1972)

Fastl, H.: Temporal masking effects. I. Broad band noise masker. Acustica **35**, 287–302 (1976)

Maiwald, D.: Beziehungen zwischen Schallspektrum, Mithörschwelle und der Erregung des Gehörs. Acustica **18**, 69–80 (1967)

Schöne, P.: Nichtlinearitäten im Mithörschwellen-Tonheitsmuster von Sinustönen. Acustica **37**, 37—44 (1977)

Scholl, H.: Über die Bildung von Hörschwellen und Mithörschwellen von Dauerschallen. Frequenz **15**, 58–64 (1961)

Suchowerskyj, W.: Zur subjektiven Bewertung zeitlich variabler Schallparameter. In: Fortschritte der Akustik, S. 315–318. Weinheim: Physik 1975

Suchowerskyj, W.: Untersuchungen über die subjektive Bewertung von Unterschieden zwischen akustischen Signalen. Diss. TU München (1976)

Suchowerskyj, W.: Beurteilung von Unterschieden zwischen aufeinanderfolgenden Schallen. Acustica (im Druck, 1977a)

Suchowerskyj, W.: Beurteilung kontinuierlicher Schalländerungen. Acustica (im Druck, 1977b)

Terhardt, E.: Über ein Äquivalenzgesetz für Intervalle akustischer Empfindungsgrößen. Kybernetik **5**, 127–133 (1968a)

Terhardt, E.: Über die durch amplitudenmodulierte Sinustöne hervorgerufene Hörempfindung. Acustica **20**, 210–214 (1968b)

Terhardt, E.: Über akustische Rauhigkeit und Schwankungsstärke. Acustica **20**, 215–224 (1968c)

Vogel, A.: Ein gemeinsames Funktionsschema zur Beschreibung der Lautheit und der Rauhigkeit. Biol. Cybernetics **18**, 31–40 (1975)

Zwicker, E.: Über psychologische und methodische Grundlagen der Lautheit. Acustica **8**, 237–258 (1958)

Zwicker, E.: Direct comparisons between the sensations produced by frequency modulation and amplitude modulation. J. Acoust. Soc. Amer. **34**, 1425–1430 (1962)

Zwicker, E.: Mithörschwellen-Periodenmuster amplitudenmodulierter Töne. Acustica **36**, 113–120 (1976)

Zwicker, E., Feldtkeller, R.: Das Ohr als Nachrichtenempfänger. Stuttgart: Hirzel 1967

Eingegangen am 28. November 1976

Dr. W. Suchowerskyj
Inst. f. Elektroakustik der T.U.
Arcisstr. 21
D-8000 München 2
Bundesrepublik Deutschland

Biol. Cybernetics 26, 175—185 (1977)

Biological Cybernetics

Neural Theory of Association and Concept-Formation

S.-I. Amari*
University of Tokyo, Tokyo, Japan; Center for Systems Neuroscience, University of Massachusetts, Amherst, MA, USA

Abstract. The present paper looks for possible neural mechanism underlying such high-level brain functioning as association and concept-formation. Primitive neural models of association and concept-formation are presented, which will elucidate the distributed and multiply superposed manner of retaining knowledge in the brain. The models are subject to two rules of self-organization of synaptic weights, orthogonal and covariance learning. The convergence of self-organization is proved, and the characteristics of these learning rules are shown. The performances, especially the noise immunity, of the association net and concept-formation net are analyzed.

I. Introduction

A typical "neural theory" builds a model of a specific portion of the brain in the beginning, and predicts the functioning of that portion by computer-simulated experiments. We, however, do not intend to build a model of a specific portion at the present stage. We rather intend to figure out possible neural mechanisms of learning, storing and using knowledge which might be found widely in the brain in various versions. We search for such mechanisms of distributed and multiply-superposed information processing as might underlie neural association and concept-formation. These mechanisms will help us in building more realistic models at the next stage.

The present work is a development of the model, consisting of mutually connected bistable neuron pools, proposed by Amari (1971) and partly analyzed in Amari (1972a). In order to make mathematical analysis tractable, the model is kept as simple as possible as long as the essential features are not missed. This is a common attitude of the author's neural researches (Amari, 1971; 1972a, b; 1974a, b; 1975; 1977a, b).

We consider the following association net. The net, learning from k pairs of stimulus patterns $(\boldsymbol{x}_1, \boldsymbol{z}_1), \ldots, (\boldsymbol{x}_k, \boldsymbol{z}_k)$, self-organizes in such a manner that, when the net receives a key pattern $\boldsymbol{x}_\alpha (\alpha = 1, \ldots, k)$, it correctly outputs the associated partner $\boldsymbol{z}_\alpha$. The self-organization is carried into effect through modification of the synaptic weights of the net. This type of neural association has been investigated by many authors (e.g., Nakano, 1972; Kohonen, 1972; Anderson, 1972; Amari, 1972a; Uesaka and Ozeki, 1972; Wigström, 1973), where the so-called "correlation" of pattern components is memorized in the synaptic weights. The correlational association works well when the patterns $\boldsymbol{x}_1, \ldots, \boldsymbol{x}_k$ are mutually orthogonal, but otherwise it does not work well by virtue of the mutual interference of superposed patterns. The present paper considers two methods of neural self-organization, orthogonal and covariance learning, which eliminate the above interference. Orthogonal learning is closely related to Kohonen's generalized inverse approach (Kohonen, 1974; Kohonen and Oja, 1976).

The concept-formation net, on the other hand, is a sequential net having recurrent connections. The net, receiving many stimulus patterns which are distributed in k clusters, self-organizes in such a manner that the net forms an equilibrium state corresponding to each cluster. The equilibrium states correspond to the concept patterns which the net retains. After the learning is completed, the net, receiving a pattern belonging to a cluster, falls into the equilibrium state corresponding to the cluster. The net keeps and reproduces any concept pattern in this manner (short-term memory), while forming many equilibrium states by changing synaptic weights yields the long-term memory. Orthogonal learning and covariance learning again play an important role.

* This research was supported in part by a grant by the Sloan Foundation to the Center for Systems Neuroscience, University of Massachusetts

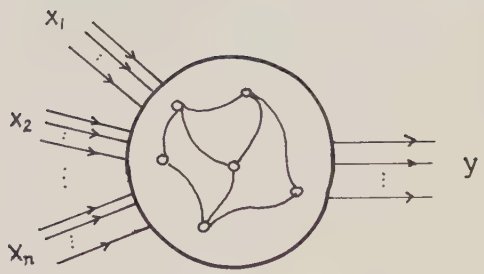

Fig. 1. Neuron pool

The main results of the present paper are: i) a mathematical analysis of the performance, especially noise immunity, of association and concept-formation nets, ii) the formulation of orthogonal and covariance learning, and iii) proof of convergence of neural self-organization including covariance and orthogonal learning.

II. Neural Models of Association and Concept-formation

2.1. Neuron Pool

We first consider the behavior of a neuron pool, which is composed of mutually connected neurons. Neuron pools play the role of building blocks of the models in the present paper. A neuron pool has a bundle of output axons. The output signal y of the neuron pool is represented by the average pulse rate over this bundle of axons. Let $x_1, x_2, \ldots, x_n$ be n signals entering into the neuron pool. A signal x_i is also carried by a bundle of axons (Fig. 1), representing the average pulse rate of the corresponding bundle.

The behavior of a neuron pool in which many neurons are connected in a random manner has been studied in detail (e.g., Amari, 1971, 1972b, 1974; Amari et al., 1977). Let us consider a bistable neuron pool. It has two states, an excited state which emits a high pulse rate output and a resting state which emits a low pulse rate output. It can be in either state. It enters the excited state when a weighted sum

$$u=\sum_{i=1}^{n} w_i x_i$$

of the input signals exceeds a threshold value h_1, and stays in that state. It enters the resting state, when the weighted sum u becomes lower than another threshold value h_2 ($h_2<h_1$).

We represent the high pulse rate output by $y=1$, and the low pulse rate by $y=0$. The behavior of a bistable neuron pool, then, can approximately be described by the following equation

$$y=\varphi[\textstyle\sum w_i x_i+(h_1-h_2)y-h_1]\,, \tag{2.1}$$

where φ is the step-function defined by

$$\varphi(u)=\begin{cases}1, & u>0\\ 0, & u\leqq 0\,.\end{cases}$$

When $h_1=h_2$ holds, the equation is simplified to yield the input-output relation

$$y=\varphi(\textstyle\sum w_i x_i-h)\,. \tag{2.2}$$

This is the behavior of the so-called McCulloch-Pitts formal neuron. If we attach a feedback connection to a McCulloch-Pitts neuron with weight h_1-h_2, (2.2) coincides with (2.1).

We hereafter use McCulloch-Pitts formal neurons as the constituent elements of our neuron nets, where an element may be a bistable neuron pool. A bundle of input or output axons of a neuron pool will also be treated as a single input or output line. We call w_i the connection weight of input x_i, and the weighted sum u the potential.

2.2. Model Net for Association

Let us consider a net of non-recurrent connections consisting of m elements (m neuron pools). The net receivers n input signals $x_1, \ldots, x_n$ and transforms them into m output signals $y_1, \ldots, y_m$, where y_i is the output from the i-th element (Fig. 2). Every input x_j is connected with all the elements. Let w_{ij} be the connection weight of x_j entering into the i-th element. Let h_i be the threshold of the i-th element.

The output y_i is determined by

$$y_i=\varphi\left(\sum_{j=1}^{n} w_{ij}x_j-h_i\right), \quad i=1,\ldots,m\,. \tag{2.3}$$

This determines the transformation from $x_1, \ldots, x_n$ to $y_1, \ldots, y_m$. It is convenient to use vector-matrix notation. We represent the input and output signals by column vectors, e.g.,

$$\boldsymbol{x}=(x_1, x_2, \ldots, x_n)^T$$

is the input vector, where the superscript T denotes transposition. The connection weights are also represented by a matrix

$$W=(w_{ij})\,,$$

which we call the connection matrix. The transformation (2.3) can then be rewritten in the form

$$\boldsymbol{y}=\varphi(W\boldsymbol{x}-\boldsymbol{h})\,, \tag{2.4}$$

where function φ operates component-wise. We symbolically write

$$\boldsymbol{y}=T\boldsymbol{x} \tag{2.5}$$

to show that $\boldsymbol{x}$ is transformed into $\boldsymbol{y}$.

An input vector $\boldsymbol{x}$ is called an input pattern. It represents a set of n features $x_1, x_2, \ldots, x_n$ of a signal pattern which the net processes. An output vector $\boldsymbol{y}$ is also called an output pattern.

The net has another set of inputs $z_1, \ldots, z_m$(Fig. 2). Signal z_i arrives directly at the i-th element, and plays the role of a "teacher" of this element. Since the teacher signal

$$\boldsymbol{z}=(z_1, z_2, \ldots, z_m)^T$$

is strong, the output signal $\boldsymbol{y}$ is always set equal to $\boldsymbol{z}$, when $\boldsymbol{z}$ arrives. The teacher signal $\boldsymbol{z}$ arrives at the net in the learning phase only. The net usually works without the teacher input.

Let us consider k pattern signals $\boldsymbol{x}_1, \ldots, \boldsymbol{x}_k$. When pattern $\boldsymbol{z}_\alpha$ is associated to pattern $\boldsymbol{x}_\alpha$, we have k pairs of patterns $(\boldsymbol{x}_\alpha, \boldsymbol{z}_\alpha)$'s. When the net, receiving input $\boldsymbol{x}_\alpha$, outputs the associated pattern $\boldsymbol{z}_\alpha$, i.e., when $\boldsymbol{z}_\alpha = T\boldsymbol{x}_\alpha$ holds, we say that the net associates $\boldsymbol{z}_\alpha$ with $\boldsymbol{x}_\alpha$. The net self-organizes such that $\boldsymbol{z}_\alpha$ is associated with $\boldsymbol{x}_\alpha$ by receiving k given pattern pairs $(\boldsymbol{x}_\alpha, \boldsymbol{z}_\alpha)$'s repeatedly, $\boldsymbol{x}_\alpha$ from the ordinary input and $\boldsymbol{z}_\alpha$ from the second input. This requires that $\boldsymbol{z}_\alpha = T\boldsymbol{x}_\alpha$ eventually holds when the second input is finally allowed to revert to zero.

This is a primitive model of a neural association mechanism. We can construct more complicated and plausible models of association based on the mechanism of this simple model. The mechanism can be incorporated with lateral-inhibition networks such as those of Spinelli (1970) and Malsburg (1973).

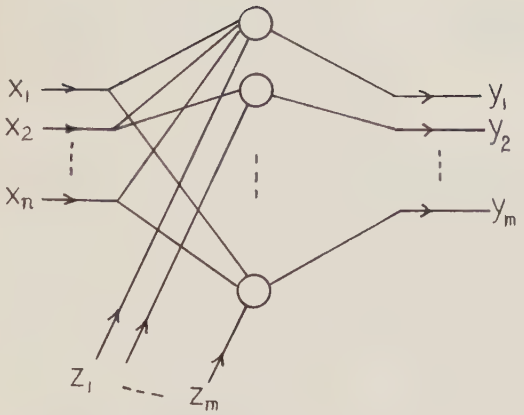

Fig. 2. Net for association

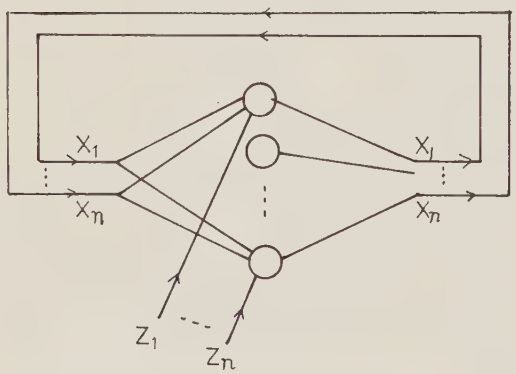

Fig. 3. Net for concept formation

2.3. Model Net for Concept Formation

A recurrent net can be obtained by connecting the outputs of a net to its inputs. We consider the net shown in Figure 3, where the net consists of n elements. Let $x_1(t), \ldots, x_n(t)$ be the outputs of the net at time t. We denote the outputs by

$$\boldsymbol{x}(t)=[x_1(t), \ldots, x_n(t)]^T$$

and call it the state of the net at time t. The output $\boldsymbol{x}(t+1)$ at time $t+1$ is determined by

$$\boldsymbol{x}(t+1)=\varphi[W\boldsymbol{x}(t)-\boldsymbol{h}] \tag{2.6}$$

which we write symbolically as

$$\boldsymbol{x}(t+1)=T\boldsymbol{x}(t)\,, \tag{2.7}$$

and call T the state-transition operator. The second input $\boldsymbol{z}$ plays the role of setting the net in the initial state specified from the outside. When signal $\boldsymbol{z}$ arrives at the second input, the net is set in the state $\boldsymbol{z}$. The net, then, begins its state transition, if no further signals come from the second input.

A state $\boldsymbol{x}$ which satisfies $T\boldsymbol{x}=\boldsymbol{x}$ is called an equilibrium state of the net. The net can have many equilibrium states. Equilibrium states represent information patterns which the net can retain persistently (the short term memory). We regard an equilibrium state as a concept pattern which the net has formed. The net can thus retain many concept patterns.

Many patterns will arrive at the net in the learning phase from the outside. When the patterns consists of a number of clusters, we consider that there is a concept corresponding to each cluster of patterns. We show in Figure 4 an example of a pattern distribution, where patterns are distributed around $\boldsymbol{x}_1$, $\boldsymbol{x}_2$, and $\boldsymbol{x}_3$, forming three clusters. The abscisa really is an n-dimensional pattern space and the ordinate represents the relative frequency of patterns.

Receiving a distribution of patterns one by one repeatedly, the net must self-organize by modifying the connection weights such that it automatically finds the clusters and forms equilibrium states. Moreover, when a pattern $\boldsymbol{x}'$ belonging to the cluster of $\boldsymbol{x}_\alpha$ is input later, the net, first entering state $\boldsymbol{x}'$, must tend to the equilibrium state $\boldsymbol{x}_\alpha$ thus formed. The net may be regarded as a pattern generator in which patterns $\boldsymbol{x}_1, \ldots, \boldsymbol{x}_k$ are coded in the form of equilibria.

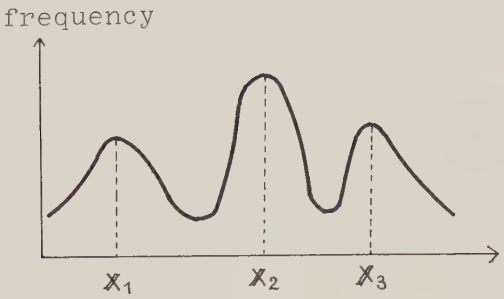

Fig. 4. Distribution of input patterns

III. Self-organization of Nerve Elements

3.1. Convergence of Learning

It is widely believed that a nerve net self-organizes by modifying its synaptic weights. Hebb (1949) proposed the rule that simultaneous firing of presynaptic and postsynaptic neurons brings an increase in that synaptic weight. This hypothesis has widely been accepted in various versions (e.g., Caianiello, 1961; Rosenblatt, 1961; Grossberg, 1969). We also adopt similar but somewhat extended rules of modification of connection weights.

A connection weight w_i of an element increases in proportion to a reinforcement signal r_i in the learning phase. It decays slowly at the same time. The rule of modification of a weight is, hence, formulated as

$$w_i(t+1)=(1-c)w_i(t)+dr_i(t)\,, \tag{3.1}$$

where c and d are constants, and $w_i(t)$ and $r_i(t)$ are respectively the connection weight and reinforcement signal at time t.

The reinforcement signal $r_i(t)$ is determined generally depending on the input signal $\boldsymbol{x}(t)$, the connection weight $\boldsymbol{w}(t)$, the output signal $y(t)$ and the teacher signal $z(t)$ (when it exists). Nerve nets can realize various possibilities of information processing if provided with appropriate reinforcement signals.

When $r_i(t)$ is given by $r_i(t)=x_i(t)y(t)$, it realizes the Hebbian rule. When a teacher signal $z(t)$ arrives at the element, we can consider the rule $r_i(t)=x_i(t)z(t)$. This may be called forced learning, because the teacher signal comes from outside. When the reinforcement signal is given by $r_i(t)=x_i(t)u(t)$, where $u(t)$ is the potential evoked by the input $\boldsymbol{x}(t)$

$$u(t)=\sum w_j(t)x_j(t)\,,$$

we obtain a learning rule based on the potential of the neuron. This plays an important role in orthogonal learning defined later.

We again use the vector notation, $\boldsymbol{w}=(w_1, \ldots, w_n)$, $\boldsymbol{r}(r_1, \ldots, r_n)$, where $\boldsymbol{w}$ and $\boldsymbol{r}$ are row vectors, so that $\boldsymbol{wx}$ gives the inner product of $\boldsymbol{w}$ and $\boldsymbol{x}$. The reinforcement signal $\boldsymbol{r}$ is a function of input $\boldsymbol{x}$, $\boldsymbol{w}$, and z. We represent it by

$$\boldsymbol{r}=\boldsymbol{r}(\boldsymbol{w}, \boldsymbol{x}, z)\,. \tag{3.2}$$

Let $\Delta\boldsymbol{w}(t)$ be the increment of the connection weight at time t

$$\Delta\boldsymbol{w}(t)=\boldsymbol{w}(t+1)-\boldsymbol{w}(t)\,.$$

Then, the rule of weight modification can be written as

$$\Delta\boldsymbol{w}(t)=-c\boldsymbol{w}(t)+d\boldsymbol{r}[\boldsymbol{w}(t), \boldsymbol{x}(t), z(t)] \tag{3.3}$$

for suitable positive constants c and d. This shows the direction of modification of $\boldsymbol{w}$.

We consider the case when there exists a function $R(\boldsymbol{w}, \boldsymbol{x}, z)$ for which

$$\frac{\partial R}{\partial \boldsymbol{w}}=\boldsymbol{w}-\frac{d}{c}\boldsymbol{r}(\boldsymbol{w}, \boldsymbol{x}, z) \tag{3.4}$$

holds[1], where $\partial R/\partial \boldsymbol{w}=(\partial R/\partial w_1, \ldots, \partial R/\partial w_n)$ is the gradient vector. Then

$$\Delta\boldsymbol{w}=-c\frac{\partial R}{\partial \boldsymbol{w}}\,. \tag{3.5}$$

This means that $\boldsymbol{w}$ is modified in the negative direction of the gradient of R with respect to $\boldsymbol{w}$.

The connection weight is modified depending on the $\boldsymbol{x}(t)$ and $z(t)$, $t=1, 2, 3, \ldots$. (We do not have any teacher signals in the case of concept formation.) We consider the situation where $[\boldsymbol{x}(t), z(t)]$'s are independent samples from a fixed distribution. A typical case is that there are k input signals $\boldsymbol{x}_1, \ldots, \boldsymbol{x}_k$, $\boldsymbol{x}_\alpha$ coming with probability or relative frequency p_α. The teacher signal z_α is paired with input signal $\boldsymbol{x}_\alpha$, in the case of association. We show the convergence of the connection weights.

Let $L(\boldsymbol{w})$ be the expected value of R for possible inputs $(\boldsymbol{x}, z)$,

$$L(\boldsymbol{w})=\langle R(\boldsymbol{w}, \boldsymbol{x}, z)\rangle\,, \tag{3.6}$$

where $\langle\ \rangle$ denotes the expectation with respect to $\boldsymbol{x}$ and z. In the above case,

$$L(\boldsymbol{w})=\sum_{\alpha=1}^{k} p_\alpha R(\boldsymbol{w}, \boldsymbol{x}_\alpha, z_\alpha)\,.$$

By taking the expectation of (3.5), we have

$$\langle\Delta\boldsymbol{w}\rangle=-c\partial L(\boldsymbol{w})/\partial\boldsymbol{w}\,.$$

This shows that $\boldsymbol{w}$ is modified on the average in the direction of the steepest descent of $L(\boldsymbol{w})$. Hence, it is expected that $\boldsymbol{w}$ eventually converges to the value which minimizes $L(\boldsymbol{w})$ to within small fluctuations.

[1] The necessary and sufficient condition for the existence of R is given by $\partial r_i/\partial w_j=\partial r_j/\partial w_i$. As will be shown later, the condition is satisfied for most interesting cases

Assume that $L(\boldsymbol{w})$ is a function which has a unique minimum and satisfies some regularity conditions. Then, we can apply the theory of stochastic approximation (e.g., Wasan, 1969). When c is small, we can show that the expected value $\langle \boldsymbol{w}(t) \rangle$ of the connection weights converges to the minimum of $L(\boldsymbol{w})$. Moreover, the deviation of $\boldsymbol{w}(t)$ from the expected value can be made as small as desired, by letting c be sufficiently small.

We assume in the following that the decay constant c is sufficiently small so that the connection weights converge to the minimum of $L(\boldsymbol{w})$. The minimum is attained at $\boldsymbol{w}$ satisfying

$$c\boldsymbol{w} = d\langle \boldsymbol{r}(\boldsymbol{w}, \boldsymbol{x}, z) \rangle \,. \tag{3.7}$$

3.2. Examples of Simple Learning

A) Hebbian Learning. In the case of Hebbian learning, r_i is given by $r_i = yx_i$, where $y = \varphi(\boldsymbol{w}\boldsymbol{x} - h)$. Let $\Phi(u)$ be the integral of φ

$$\Phi(u) = \int_0^u \varphi(x)dx \,.$$

The function

$$R(\boldsymbol{w}, \boldsymbol{x}) = \tfrac{1}{2}\boldsymbol{w}\boldsymbol{w}^T - \frac{d}{c}\Phi(\boldsymbol{w}\boldsymbol{x} - h)$$

satisfies (3.4). Therefore, by Hebbian learning, the connection weight converges to $\boldsymbol{w}$ satisfying

$$\boldsymbol{w} = \frac{d}{c}\langle \varphi(\boldsymbol{w}\boldsymbol{x} - h)\boldsymbol{x}^T \rangle \,. \tag{3.8}$$

B) Forced Learning. The reinforcement signal is given by $r_i = zx_i$ with teacher signal z. It is easy to see that

$$R(\boldsymbol{w}, \boldsymbol{x}, z) = \tfrac{1}{2}\boldsymbol{w}\boldsymbol{w}^T - \frac{d}{c}z\boldsymbol{w}\boldsymbol{x}$$

gives the forced rule (3.4). From

$$2L(\boldsymbol{w}) = \left(\left| \boldsymbol{w} - \frac{d}{c}\langle z\boldsymbol{x}^T \rangle \right| \right)^2 - \left(\frac{d}{c} |\langle z\boldsymbol{x}^T \rangle| \right)^2 ,$$

the minimum is attained at

$$\boldsymbol{w} = \frac{d}{c}\langle z\boldsymbol{x}^T \rangle \,.$$

This is sometimes called the "correlation" of z and $\boldsymbol{x}$.

C) Learning Based on Potential. The learning rule based on potential is given by

$$R(\boldsymbol{w}, \boldsymbol{x}) = \tfrac{1}{2}\left[\boldsymbol{w}\boldsymbol{w}^T - \frac{d}{c}(\boldsymbol{w}\boldsymbol{x})^2 \right],$$

where the reinforcement signal is $\boldsymbol{r} = (\boldsymbol{w}\boldsymbol{x})\boldsymbol{x}$. We have

$$L(\boldsymbol{w}) = \tfrac{1}{2}\left(\boldsymbol{w}\boldsymbol{w}^T - \frac{d}{c}\boldsymbol{w}\langle \boldsymbol{x}\boldsymbol{x}^T \rangle \boldsymbol{w}^T \right),$$

where $\langle \boldsymbol{x}\boldsymbol{x}^T \rangle$ is the matrix whose (i, j) entry is given by $\langle x_i x_j \rangle$. (It should be remembered that $\boldsymbol{x}$ is a column vector while $\boldsymbol{w}$ is a row vector.)

The function $L(\boldsymbol{w})$, however, has no minimum in this case. Therefore, the connection weight $\boldsymbol{w}(t)$ does not converge under the above rule of learning. If the connection weight is subject to the subsidiary condition $\boldsymbol{w}\boldsymbol{w}^T = \text{const}$, so that $\boldsymbol{w}(t)$ is normalized after each step of learning, we can prove that $\boldsymbol{w}(t)$ converges to the minimum of $L(\boldsymbol{w})$ under the subsidiary condition. It is the direction of the eigenvector of the matrix $\langle \boldsymbol{x}\boldsymbol{x}^T \rangle$ corresponding to the maximum eigenvalue.

3.3. Orthogonal Learning

An element may have both excitatory and inhibitory channels from the inputs. An input signal, therefore, not only excites it but also inhibits it at the same time through inhibitory interneurons. The connection weight w_i can be decomposed into $w_i = w_i^+ - w_i^-$, where w_i^+ and w_i^- represent, respectively, the excitatory and inhibitory efficiency.

Excitatory and inhibitory neurons may have different self-organization rules. We consider the case where the excitatory w_i^+ is modified subject to forced learning with teacher signal, while the inhibitory weight w_i^- is modified subject to learning based on potential;

$$\Delta \boldsymbol{w}^+ = -c\boldsymbol{w}^+ + dz\boldsymbol{x}^T \,,$$

$$\Delta \boldsymbol{w}^- = -c'\boldsymbol{w}^- + d'(\boldsymbol{w}\boldsymbol{x})\boldsymbol{x}^T \,.$$

The excitatory weight converges to

$$\boldsymbol{w}^+ = \frac{d}{c}\langle z\boldsymbol{x}^T \rangle \,. \tag{3.9}$$

Define

$$R(\boldsymbol{w}^-, \boldsymbol{w}^+, \boldsymbol{x}) = \tfrac{1}{2}\left[|\boldsymbol{w}^-|^2 + \frac{d'}{c'}|(\boldsymbol{w}^+ - \boldsymbol{w}^-)\boldsymbol{x}|^2 \right]. \tag{3.10}$$

We then have $\Delta \boldsymbol{w}^- = -c'\partial R/\partial \boldsymbol{w}^-$. The function

$$L(\boldsymbol{w}^-, \boldsymbol{w}^+) = \langle R \rangle = \tfrac{1}{2}\left[|\boldsymbol{w}^-|^2 + \frac{d'}{c'}(\boldsymbol{w}^+ - \boldsymbol{w}^-)\langle \boldsymbol{x}\boldsymbol{x}^T \rangle (\boldsymbol{w}^+ - \boldsymbol{w}^-) \right]$$

is quadratic in $\boldsymbol{w}^-$ and its coefficient matrix is positive definite. Hence, it has a unique minimum, and $\boldsymbol{w}^-$ converges to the minimum. Since $\boldsymbol{w}^+$ converges to

(3.9) independently of $\boldsymbol{w}^-$, the minimum $\boldsymbol{w}^-$ is given by the equation

$$\boldsymbol{w}^- = \frac{d'}{c'}[(\boldsymbol{w}^+ - \boldsymbol{w}^-)\langle \boldsymbol{x}\boldsymbol{x}^T\rangle] .$$

The total synaptic weight $\boldsymbol{w} = \boldsymbol{w}^+ - \boldsymbol{w}^-$, therefore, converges to one satisfying

$$\boldsymbol{w} = \frac{d}{c}\langle \boldsymbol{z}\boldsymbol{x}^T\rangle - \frac{d'}{c'}\boldsymbol{w}\langle \boldsymbol{x}\boldsymbol{x}^T\rangle . \tag{3.11}$$

or

$$\boldsymbol{w} = e\langle \boldsymbol{z}\boldsymbol{x}^T\rangle(\varepsilon E + \langle \boldsymbol{x}\boldsymbol{x}^T\rangle)^{-1} , \tag{3.12}$$

where E is the unit matrix and $e = c'd/cd'$, $\varepsilon = c'/d'$.

Let us consider the case where k signals $\boldsymbol{x}_1, \ldots, \boldsymbol{x}_k$ come to the input ($k < n$) with paired teacher signals z_α. We then have

$$\langle \boldsymbol{z}\boldsymbol{x}\rangle = \sum_\alpha p_\alpha z_\alpha \boldsymbol{x}_\alpha , \qquad \langle \boldsymbol{x}\boldsymbol{x}^T\rangle = \sum_\alpha p_\alpha \boldsymbol{x}_\alpha \boldsymbol{x}_\alpha^T .$$

We assume that k vectors $\boldsymbol{x}_1, \ldots, \boldsymbol{x}_k$ are linearly independent.

Let us introduce the set of dual orthogonal vectors $\boldsymbol{x}_1^*, \boldsymbol{x}_2^*, \ldots, \boldsymbol{x}_k^*$ associated with $\boldsymbol{x}_1, \ldots, \boldsymbol{x}_k$. The $\boldsymbol{x}_\alpha^*$ is a row vector satisfying the two conditions:

1) $\boldsymbol{x}_\alpha^*$ is a linear combination of $\boldsymbol{x}_1^T, \ldots, \boldsymbol{x}_k^T$,

2) $\boldsymbol{x}_\alpha^* \boldsymbol{x}_\beta = \begin{cases} 1, & \alpha = \beta \\ 0, & \alpha \neq \beta . \end{cases}$

In other words, $\boldsymbol{x}_\alpha^*$ belongs to the subspace spanned by $\boldsymbol{x}_1^T, \ldots, \boldsymbol{x}_k^T$ and is orthogonal to all the $\boldsymbol{x}_\beta$'s except $\boldsymbol{x}_\alpha$. The dual orthogonal vector is uniquely determined by

$$\boldsymbol{x}_\alpha^* = \frac{1}{n}\sum_{\beta=1}^{k} G_{\alpha\beta}^{-1}\boldsymbol{x}_\beta^T , \tag{3.13}$$

where $(G_{\alpha\beta}^{-1})$ is the inverse matrix of $(G_{\alpha\beta}) = (\boldsymbol{x}_\alpha^T \boldsymbol{x}_\beta)/n$.

Since $\langle \boldsymbol{x}\boldsymbol{x}^T\rangle$ is a singular matrix, it is impossible to expand (3.12) in a power series in ε, even when ε is small. By the method given in Appendix I,

$$\boldsymbol{w} = e\sum z_\alpha \boldsymbol{x}_\alpha^* - \frac{e\varepsilon}{n}\sum_{\alpha,\beta}\frac{1}{p_\beta} z_\alpha G_{\alpha\beta}^{-1}\boldsymbol{x}_\beta^* + O(\varepsilon^2) , \tag{3.14}$$

where $O(\varepsilon^2)$ represents the second-order term in ε.

3.4. Covariance Learning

We propose another possible neural rule of self-organization. The excitatory weight $\boldsymbol{w}^+$ is modified subject to forced learning as before, while the reinforcement signal r_i for the inhibitory synapse is given, in this case, by

$$r_i = e(b x_i + a z - ab) ,$$

where a and b are constants. We then have

$$\boldsymbol{w} = e'\langle (\boldsymbol{x} - \boldsymbol{a})(z - b)\rangle , \tag{3.15}$$

where $e' = d/c = (d'/c')e$ and $\boldsymbol{a} = (a, a, \ldots, a)^T$.

When a and b are, respectively, the expected values of x_i and z, $\langle (x_i - a)(z - b)\rangle$ is called the covariance of x_i and z. We call this rule of self-organization covariance learning.

When k input signals $\boldsymbol{x}_\alpha$'s come with z_α's we have

$$\boldsymbol{w} = e'\sum_\alpha p_\alpha (z_\alpha - b)(\boldsymbol{x}_\alpha - \boldsymbol{a})^T . \tag{3.16}$$

When a and b are put equal to zero, this learning reduces to simple forced learning or correlation learning.

IV. Self-organization under Noisy Situations

4.1. Self-organization of Neural Nets

A non-recurrent net model for association receives k pairs of patterns $(\boldsymbol{x}_\alpha, \boldsymbol{z}_\alpha)$ repeatedly, and the connection weight $\boldsymbol{w}_i$ of the i-th element converges to

$$\boldsymbol{w}_i = e\langle z_i \boldsymbol{x}^T\rangle(\varepsilon E + \langle \boldsymbol{x}\boldsymbol{x}^T\rangle)^{-1}$$

under orthogonal learning, where z_i is the teacher signal entering the i-th element. Hence, the connection matrix $W = (w_{ij})$ of the net converges to

$$W = e\langle \boldsymbol{z}\boldsymbol{x}^T\rangle(\varepsilon E + \langle \boldsymbol{x}\boldsymbol{x}^T\rangle)^{-1} . \tag{4.1}$$

This can be evaluated as

$$W = e\sum_\alpha \boldsymbol{z}_\alpha \boldsymbol{x}_\alpha^* - \frac{e\varepsilon}{n}\sum_{\alpha,\beta}\frac{1}{p_\beta}\boldsymbol{z}_\alpha G_{\alpha\beta}^{-1}\boldsymbol{x}_\beta^* + O(\varepsilon^2) . \tag{4.2}$$

When ε is sufficiently small, we have

$$W\boldsymbol{x}_\beta \doteqdot e\boldsymbol{z}_\beta , \qquad \beta = 1, \ldots, k .$$

Therefore, ε represents the inaccuracy of the orthogonalization effect which suppresses the interference among many patterns.

Under covariance learning, the connection matrix converges to

$$W = e'\sum_\alpha p_\alpha (\boldsymbol{z}_\alpha - \boldsymbol{b})(\boldsymbol{x}_\alpha - \boldsymbol{a})^T , \tag{4.3}$$

where $\boldsymbol{a}$ and $\boldsymbol{b}$ are constant vectors.

A recurrent net, on the other hand, is forced to be in state $\boldsymbol{x}$, when it receives an input $\boldsymbol{x}$ from the second or the initial-state setting terminals. The net immediately outputs the $\boldsymbol{x}$, which is fed back to the ordinary input terminals of the net. Learning takes place under this situation, so that $\boldsymbol{x}$ plays the roles of the input signal and the teacher signal at the same time.

The connection matrix of the net converges to

$$W = e\langle \boldsymbol{x}\boldsymbol{x}^T\rangle(\varepsilon E + \langle \boldsymbol{x}\boldsymbol{x}^T\rangle)^{-1} \tag{4.5}$$

by orthogonal learning. It converges to

$$W \doteqdot e'\langle (\boldsymbol{x} - \boldsymbol{a})(\boldsymbol{x} - \boldsymbol{a})^T\rangle , \tag{4.5}$$

by covariance learning.

4.2. Learning under Noisy Situation

We have so far considered noiseless learning, where patterns $\boldsymbol{x}_\alpha$ and $\boldsymbol{z}_\alpha$ arrive without noise disturbances. In reality, the net receives noisy versions of $\boldsymbol{x}_\alpha$'s and $\boldsymbol{z}_\alpha$'s. Let $\tilde{\boldsymbol{x}}_\alpha$ be a noisy version of $\boldsymbol{x}_\alpha$

$$\tilde{\boldsymbol{x}}_\alpha = \boldsymbol{x}_\alpha + \boldsymbol{n}\,,$$

where $\boldsymbol{n}$ is a noise vector. When the noise disturbs the i-th component of $\boldsymbol{x}_\alpha$, the i-th component n_i of $\boldsymbol{n}$ is equal to 1 or -1, according as $x_i=0$ or 1. The n_i is otherwise equal to 0. We consider a random noise, which independently disturbs every component of a pattern with probability δ. We call δ the noise rate of noisy pattern $\tilde{\boldsymbol{x}}_\alpha$. The noisy $\tilde{\boldsymbol{x}}_\alpha$ differs from $\boldsymbol{x}_\alpha$ in $n\delta$ components on the average.

We consider the case where the net receives noisy pattern pairs $(\tilde{\boldsymbol{x}}_\alpha, \tilde{\boldsymbol{z}}_\alpha)$. The noise independently disturbs the pattern pair $(\boldsymbol{x}_\alpha, \boldsymbol{z}_\alpha)$ each time. Let $\bar{\boldsymbol{x}}_\alpha$ be the average of noisy versions of $\boldsymbol{x}_\alpha$, i.e., the expectation of $\tilde{\boldsymbol{x}}_\alpha$ over all the possible noise. We easily have

$$\bar{\boldsymbol{x}}_\alpha = (1-2\delta)\boldsymbol{x}_\alpha + \mathbf{1}, \tag{4.6}$$

where $\mathbf{1}$ is the column vector defined by $\mathbf{1}=(1, 1, \ldots, 1)^T$.

Similarly, by taking the expectation over all possible patterns and noises,

$$\langle \boldsymbol{z}\boldsymbol{x}^T \rangle = \sum_\alpha p_\alpha \bar{\boldsymbol{z}}_\alpha \bar{\boldsymbol{x}}_\alpha^T\,,$$

$$\langle \boldsymbol{x}\boldsymbol{x}^T \rangle = \sum p_\alpha \bar{\boldsymbol{x}}_\alpha \bar{\boldsymbol{x}}_\alpha^T + \sigma E\,,$$

where $\sigma=\delta(1-\delta)$. Therefore, we see from (4.1) that the connection weight converges, under noisy orthogonal learning, to

$$W = e\sum \bar{\boldsymbol{z}}_\alpha \bar{\boldsymbol{x}}_\alpha^* + \frac{e\varepsilon'}{n}\sum \bar{\boldsymbol{z}}_\alpha G_{\alpha\beta}^{-1}\frac{1}{p_\beta}\bar{\boldsymbol{x}}_\beta^* + O(\varepsilon'^2)\,, \tag{4.7}$$

where $\varepsilon'=\varepsilon+\sigma$ and the $\bar{\boldsymbol{x}}_\alpha^*$'s are the dual orthogonal vectors of the $\bar{\boldsymbol{x}}_\alpha$'s.

Noisy learning results in changing $\boldsymbol{x}_\alpha$ and $\boldsymbol{z}_\alpha$ to $\bar{\boldsymbol{x}}_\alpha$ and $\bar{\boldsymbol{z}}_\alpha$, respectively. This is not so important, because they are similar. The important effect of the noise is that it apparently increases ε to $\varepsilon'=\varepsilon+\sigma$, thus increasing the inaccuracy of orthogonalization.

A cluster of patterns can be considered as being composed of noisy versions $\tilde{\boldsymbol{x}}_\alpha$'s of the representative patterns $\boldsymbol{x}_\alpha$ of that cluster. Let δ_α be the noise rate of $\tilde{\boldsymbol{x}}_\alpha$. A typical pattern $\tilde{\boldsymbol{x}}_\alpha$ in the cluster is different from $\boldsymbol{x}_\alpha$ in $n\delta_\alpha$ components on the average, so that δ_α represents the disperion of the cluster. Given a distribution of patterns consisting of k clusters, we have

$$\langle \boldsymbol{x} \rangle = \sum p_\alpha \bar{\boldsymbol{x}}_\alpha\,,$$

$$\langle \bar{\boldsymbol{x}}\bar{\boldsymbol{x}}^T \rangle = \sum p_\alpha \bar{\boldsymbol{x}}\bar{\boldsymbol{x}}_\alpha^T + \sigma E\,,$$

where $\sigma = \sum p_\alpha \delta_\alpha (1-\delta_\alpha)$.

The connection weight matrix of a recurrent net converges, under orthogonal learning of the above distribution, to

$$W = e(\sum p_\alpha \bar{\boldsymbol{x}}_\alpha \bar{\boldsymbol{x}}_\alpha^T + \sigma E)[(\sigma+\varepsilon)E + \sum p_\alpha \bar{\boldsymbol{x}}_\alpha \bar{\boldsymbol{x}}_\alpha^T]^{-1}\,. \tag{4.8}$$

When both ε and σ are small, we can expand it into

$$W = e\left(\frac{\sigma}{\sigma+\varepsilon}E + \frac{\varepsilon}{\sigma+\varepsilon}\sum \bar{\boldsymbol{x}}_\alpha \bar{\boldsymbol{x}}_\alpha^*\right) + O(\varepsilon) \tag{4.9}$$

(see Appendix II). When $\sigma \ll \varepsilon$, i.e., the dispersion of clusters is small compared to ε, we have

$$W \doteqdot e\sum \bar{\boldsymbol{x}}_\alpha \bar{\boldsymbol{x}}_\alpha^*\,.$$

However, when $\sigma \gg \varepsilon$, we have $W \doteqdot eE$ which carries no information about the distribution of patterns. Therefore, orthogonal learning works well only when the dispersion σ of patterns is smaller than ε. Hence, ε represents the degree of noise immunity for orthogonalization.

Covariance learning is not so sensitive to noise disturbances. The connection weight converges to

$$W = e'\sum p_\alpha (\bar{\boldsymbol{z}}_\alpha - \boldsymbol{b})(\bar{\boldsymbol{x}}_\alpha - \boldsymbol{a})^T \tag{4.10}$$

for a non-recurrent net, and to

$$W = e'[\sum p_\alpha (\bar{\boldsymbol{x}}_\alpha - \boldsymbol{a})(\bar{\boldsymbol{x}}_\alpha - \boldsymbol{a})^T + \sigma E] \tag{4.11}$$

for a recurrent net.

V. Behavior of Association and Concept-formation Net

5.1. Simple Illustration of Association Mechanism

The matrix

$$W = e'\sum p_\alpha \bar{\boldsymbol{z}}_\alpha \bar{\boldsymbol{x}}_\alpha^T \tag{5.1}$$

is sometimes called the correlation matrix of k pattern pairs, and many researchers have studied associative memory models by the use of this matrix (e.g., Nakano, 1972; Amari, 1972a; Kohonen, 1972; Anderson, 1972). Consider the very special case where k patterns $\boldsymbol{x}_1, \ldots, \boldsymbol{x}_k$ are mutually orthogonal,

$$\boldsymbol{x}_\alpha^T \boldsymbol{x}_\beta = 0 \quad (\alpha \neq \beta)\,. \tag{5.2}$$

In this case, for given input $\boldsymbol{x}_\beta$, the net produces the potential vector

$$\boldsymbol{u} = W\boldsymbol{x}_\beta = (e' p_\beta |\boldsymbol{x}_\beta|^2)\boldsymbol{z}_\beta$$

which is proportional to the associated pattern $\boldsymbol{z}_\beta$. Hence, if the threshold $\boldsymbol{h}$ is adequately chosen, the net outputs the associated pattern $\boldsymbol{z}_\beta$ from input $\boldsymbol{x}_\beta$ $(\beta=1, \ldots, k)$. The orthogonality condition (5.2) makes it possible to extract the necessary pattern from W in which many pattern pairs are superposed. Most studies of the so-called correlation memory have used

mutually orthogonal or nearly orthogonal patterns to take advantage of this fact.

When the orthogonality condition does not exactly hold, and when a noisy version $\boldsymbol{x}_\beta + \boldsymbol{n}$ is input as a key pattern, the induced potential vector is written as

$$W(\boldsymbol{x}_\beta + \boldsymbol{n}) = (e' p_\beta |\boldsymbol{x}_\beta|^2)\boldsymbol{z}_\beta + \boldsymbol{N} ,$$

where

$$\boldsymbol{N} = e' \sum_{\alpha \neq \beta} p_\alpha (\boldsymbol{x}_\alpha^T \boldsymbol{x}_\alpha)\boldsymbol{z}_\alpha + W\boldsymbol{n}$$

represents the term due to the interference from the other superposed patterns and the noise. When $\boldsymbol{N}$ is small enough, the interference is completely eliminated by operating the non-linear threshold function φ. The neural association is realized by the two mechanisms: 1) elimination of interference of patterns by orthogonalization; and 2) noise elimination by operating the non-linear function φ. Amari (1972a) has studied the condition of noise elemination by the use of the stability concept of threshold-element nets. Uesaka and Ozeki (1972) have shown the probability of noise elimination by using randomly generated patterns $\boldsymbol{x}_\alpha$'s, where each component takes on 1 and -1 with equal probability. In this case, two vectors are orthogonal on the average. Kohonen (1972) has studied the linear aspects of the correlation matrix memory. He also proposed the generalized-inverse approach, which uses the matrix W minimizing

$$L(W) = \sum_{\alpha=1}^{k} |W\boldsymbol{x}_\alpha - \boldsymbol{z}_\alpha|^2 .$$

An iterative method of obtaining W was also shown (Kohonen, 1974). Orthogonal learning of the present paper has a close relation with the generalized inverse approach.

It should be noted that holography-like memory such as the holophone (Willshaw and Longuet-Higgins, 1969; Pfaffelhuber, 1975) also uses correlation memory. However, the dimensionality of the memory is as small as that of the patterns, so that it is difficult to superpose many patterns in the holography-like case.

5.2. Noise Immunity of Association Net

Let $\boldsymbol{n}$ be a noise disturbing a pattern $\boldsymbol{x}_\alpha$ into $\boldsymbol{x}'_\alpha = \boldsymbol{x}_\alpha + \boldsymbol{n}$. We call

$$\delta = \frac{1}{n} \sum_{i=1}^{n} |x'_{\alpha,i} - x_{\alpha,i}| = \frac{1}{n} \sum |n_i| \tag{5.3}$$

the noise rate of $\boldsymbol{x}'_\alpha$. The noise rate of an output pattern $\boldsymbol{z}'_\alpha$ is defined similarly. An association net is said to have a high noise immunity, if the net, receiving a noisy input $\boldsymbol{x}'_\alpha$, outputs the correct or less noisy pattern $\boldsymbol{z}'_\alpha$. The behavior of an association net is evaluated by the noise immunity shown by the relation between the noise rates of the input and output.

This relation, of course, depends on the whole set of pattern pairs $(\boldsymbol{x}_\alpha, \boldsymbol{z}_\alpha)$ in a very complicated manner, so that it is almost impossible to obtain the relation. We, therefore, use the stochastic technique to evaluate the noise immunity. To this end, we assume that k pattern pairs $(\boldsymbol{x}_\alpha, \boldsymbol{z}_\alpha)$ are randomly generated. Let a be the probability that every component $x_{\alpha,i}$ of every $\boldsymbol{x}_\alpha$ is set equal to 1. Let b be the probability of $z_{\beta,j}$ being set equal to 1. All these components are independently determined.

We treat the case where n, m, and k are sufficiently large. Then, the law of large numbers holds and we can get an asymptotic evaluation of the noise immunity. The net must memorize k patterns $\boldsymbol{z}_\alpha$ which altogether include mk components. The net has nm modifiable connection weights w_{ij}. Therefore,

$$s = mk/nm = k/n \tag{5.4}$$

represents the ratio of the number of memorized components to that of the modifiable synapses.

We first consider a net subject to covariance learning of k pattern pairs, with $p_\alpha = 1/k$. By evaluating the probability distribution of the interference term $\boldsymbol{N}$ (where we use the central limit theorem, the law of large numbers and assume that h_i's are adequately chosen), we have the following relation between the input noise ratio δ and the output noise ratio δ':

$$\delta' = F\left[\frac{\sqrt{a(1-a)(1-2\delta)}}{2\sqrt{sb(1-b)(a+\delta-2a\delta)}}\right] \tag{5.5}$$

where

$$F(s) = \frac{1}{\sqrt{2\pi}} \int_s^\infty \exp(-u^2/2)du .$$

The relation is shown in Figure 5, where $a = b = 0.2$. When $s = 0.1$, i.e., when the number of superposed pattern pairs is 10% of the dimensionality of input patterns, the net has an ability of eliminating an input noise of $\delta = 0.1$ almost completely, outputting the precise associated pattern. When $s = 0.3$, noise reduction also takes place, but the output pattern includes a noise of rate 2%, even when the input pattern is noiseless. When $s = 0.4$, there is no noise reduction. The output noise rate is similar to that of the input. Therefore, the association net with covariance learning works well for $s < 0.3$ or $k < 0.3\,n$. It should be noted that the net works better for smaller a and b. Mere correlation learning (5.1) does not work well, even if the thresholds are adequately tuned.

Association by covariance learning, however, has the following shortcomings: 1) Even if $\delta = 0$, i.e., the correct cue pattern is input, the net outputs a noisy

pattern, $\delta' \neq 0$. 2) When the set of pattern pairs cannot be regarded as a typical sample from randomly generated patterns, it does not work well.

Association by orthogonal learning does not share these shortcomings. It works well for an arbitrary (non-random) set of pattern pairs, as long as the $\boldsymbol{x}_\alpha$'s are linearly independent. When $\delta = 0$, the output patterns are noiseless $\delta' = 0$. However, the above performances are guaranteed only when ε is neglisibly small. When the netself-organizes under the influence of noise, ε increases to $\varepsilon' = \varepsilon + \sigma$. Therefore, it is not realistic to ignore the term of order ε.

Since $\boldsymbol{x}_\alpha^*$'s depend on all the $\boldsymbol{x}_\alpha$'s in a very complicated manner, it is difficult to evaluate the noise immunity in the general situation. We again consider the case where the $(\boldsymbol{x}_\alpha, z_\alpha)$'s are randomly generated, though the net works well for non-randomly generated pattern sets. We treat the case where ε and δ are so small that their higher order terms can be neglected. We then have the following noise relation

$$\delta' \leqq F\left[\frac{a(1-a)-\varepsilon' s+\delta}{2\sqrt{abs\delta(1-a+s+sa)}}\right], \qquad (5.6)^2$$

which is shown in Figure 6, where $a=b=0.2$, $\varepsilon'=0.1$. For small δ, the performance is very good, even when $s=0.5$. In the case of $s=0.1$, even the fifteen percent noise is completely reduced. However, this evaluation holds only when $\varepsilon' = \varepsilon + \sigma$ is not so large.

5.3. *Dynamics of a Concept Formation Net*

When each cluster of patterns is so sharply distributed that $\sigma \fallingdotseq 0$, $\bar{\boldsymbol{x}}_\alpha \fallingdotseq \boldsymbol{x}_\alpha$ hold, the connection matrix (4.9) reduces to

$$W = e \sum \boldsymbol{x}_\alpha \boldsymbol{x}_\alpha^* + O(\varepsilon)\,.$$

Therefore, for small ε, $T\boldsymbol{x}_\alpha = \boldsymbol{x}_\alpha$ $(\alpha = 1, \ldots, k)$ holds. This shows that each pattern $\boldsymbol{x}_\alpha$ becomes an equilibrium state of the net. By receiving an input pattern $\boldsymbol{x}$, the net will tend to the state $\boldsymbol{x}_\alpha$ which is closest to it. The net can store k patterns $\boldsymbol{x}_\alpha$ in this manner. It can reproduce any of them correctly from a noisy input. The net may be regarded as a pattern generator, in which k patterns are coded.

In the case where the dispersion σ of the clusters is not neglisibly small, the net works only when $\sigma < \varepsilon$. Otherwise, the term $[\sigma/(\sigma+\varepsilon)]E$ dominates in W, which then gives no information about the necessary patterns. We may say in this sense that ε gives the degree of resolution of patterns: Only a pattern cluster whose dispersion σ is smaller than ε is treated as comprising versions of only one pattern. It is difficult for the net to recognize a cluster of patterns whose dispersion is larger than ε. The parameter ε, on the other hand, must be small, because otherwise we cannot neglect the harmful interference term $O(\varepsilon)$. Therefore, orthogonal learning works well for a trainable pattern generator in which the patterns to be generated are precisely taught. The cerebellum might have this mechanism in which the patterns are taught by the cerebrum.

When the net treats clusters of largely dispersed patterns, covariance learning works better. We hence analyze the behavior of the net with covariance learning. We consider again the case where k patterns $\boldsymbol{x}_\alpha$ are randomly generated. We moreover assume for the sake of simplicity in calculation that the connection weight w_{ii} has a fixed self-inhibition term of amount $-e'/4$.

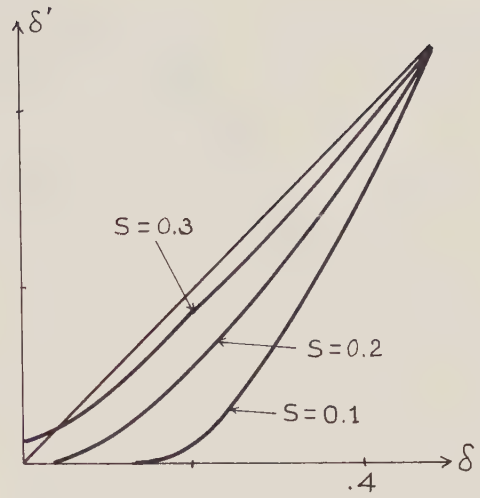

Fig. 5. Noise reduction rate of an association net with covariance learning

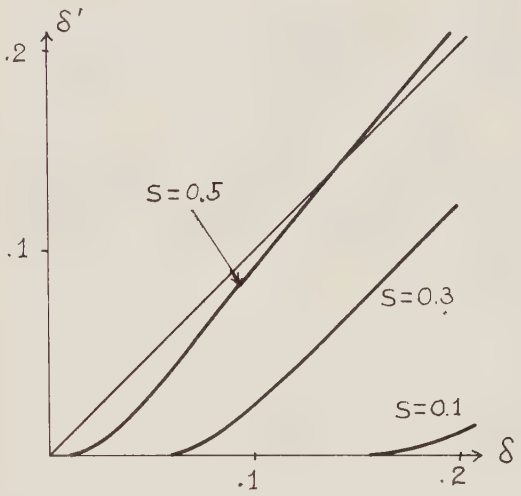

Fig. 6. Noise reduction rate of an association net with orthogonal learning

[2] The derivation is complicated and involves some stochastic assumptions

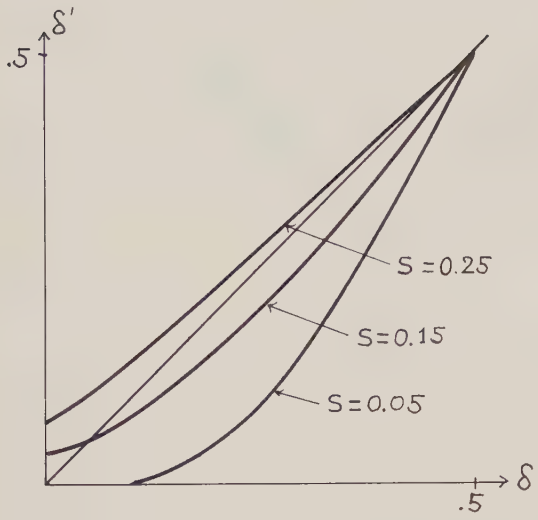

Fig. 7. Noise reduction rate of a concept-formation net with covariance learning

Assume that, in the neighborhood of a pattern $\boldsymbol{x}_\alpha$, the relation

$$\delta' = g(\delta), \tag{5.7}$$

holds, where δ and δ' are, respectively, the noise rates of states before and after state transition. Then, the noise rate δ_t at time t obeys the dynamical equation

$$\delta_{t+1} = g(\delta_t), \tag{5.8}$$

because the state $\boldsymbol{x}(t+1)$ of the net is determined from $\boldsymbol{x}(t)$. We can analyze the dynamical behavior of the net through the change in the noise rate. When δ_t of (5.8) converges to an equilibrium δ_0, the net tends to and remains in states close to $\boldsymbol{x}_\alpha$ whose noise rate is δ_0. We can say in this case that the net can retain pattern $\boldsymbol{x}_\alpha$ persistently within an error of noise rate δ_0. Unfortunately, there does not exist an exact relation like (5.7). We obtain instead the relation

$$\delta' \leqq g(\delta),$$

where

$$g(\delta) = F\left[\frac{k p_\alpha (0.5-\delta)(0.5-\delta_\alpha)^2}{\sqrt{s\gamma(0.5+\delta)}}\right] \tag{5.9}$$

for patterns around $\boldsymbol{x}_\alpha$, where we put $a=0.5$,

$$\gamma = k \sum_\beta p_\beta^2 (0.5-\delta_\beta)^4$$

and δ_α represents the dispersion of patterns around $\boldsymbol{x}_\alpha$.

We show the function $g(\delta)$ in Figure 7, where $p_\alpha = 1/k$, $\delta_\alpha = 0.2$ for all α. Since we have put $a=b=0.5$, the result is not so good compared to covariance association learning. For $s=0.1$, dynamical Equation (5.8) has a stable equilibrium at $\delta=0.01$. Therefore, the net forms the corresponding concept within a 1% noise rate. For $s=0.15$, the equation has a stable equilibrium at $\delta=0.06$, so that the concept pattern is formed in the net within a 6% noise rate. However, for $s=0.2$, there are no equilibria except for $\delta=0.5$. This means that the net fails to form concept patterns in the case when $s>0.2$, or $k>0.2n$. The situation seems better for for small a and b.

Appendix I. Derivation of (3.14)

Let X be a $k \times n$ matrix consisting of k column vectors $\boldsymbol{x}$

$$X = [\boldsymbol{x}_1, \boldsymbol{x}_2, \ldots, \boldsymbol{x}_k].$$

Let P be a $k \times k$ diagonal matrix, whose diagonal entries are p_α. We denote by $\sqrt{P}$ the diagonal matrix whose diagonal entries are $\sqrt{p_\alpha}$. Let $\boldsymbol{z}$ be the row vector

$$\boldsymbol{z} = (z_1, z_2, \ldots, z_k).$$

We easily have

$$\langle \boldsymbol{x}\boldsymbol{x}^T \rangle = XPX^T = (X\sqrt{P})(X\sqrt{P})^T,$$
$$\langle \boldsymbol{z}\boldsymbol{x}^T \rangle = \boldsymbol{z}PX^T = \boldsymbol{z}\sqrt{P}(X\sqrt{P})^T,$$
$$G = X^T X/n.$$

Equation (3.12) is rewritten as

$$\boldsymbol{w} = e\boldsymbol{z}PX^T(\varepsilon E + XPX^T)^{-1}.$$

We can use the identity

$$(X\sqrt{P})^T(\varepsilon E + XPX^T)^{-1} = (\varepsilon E_k + \sqrt{P}X^T X\sqrt{P})^{-1}\sqrt{P}X^T,$$

where E_k is the $k \times k$ identity matrix, and the expansion formula

$$(\varepsilon E_k + A)^{-1} = A^{-1} - \varepsilon A^{-2} + O(\varepsilon^2),$$

where A is a non-singular $k \times k$ matrix. (Since $k<n$, the $n \times n$ matrix XPX^T is singular, while the $k \times k$ matrix $\sqrt{P}X^T X\sqrt{P}$ is non-singular.) We obtain

$$\boldsymbol{w} = e\boldsymbol{z}(X^T X)^{-1}X^T - e\varepsilon \boldsymbol{z}(X^T X)^{-1}P^{-1}(X^T X)^{-1} + O(\varepsilon^2).$$

Taking account of $(X^T X)^{-1}X^T = G^{-1}X^T$, and rewriting the above $\boldsymbol{w}$ in the vector notation, we have (3.14). It should be noted that the $k \times n$ matrix $X^+ = G^{-1}X^T$, which is composed of k row vectors $\boldsymbol{x}_\alpha^*$'s, is the generalized inverse of X [Albert (1972), see also Kohonen (1972)].

Appendix II. Derivation of (4.9)

Let $\bar{X}$ be the matrix defined by $\bar{X} = [\bar{\boldsymbol{x}}_1, \ldots, \bar{\boldsymbol{x}}_k]$. We have

$$W = e(\sigma E + \bar{X}P\bar{X}^T)[(\sigma+\varepsilon)E + \bar{X}P\bar{X}^T]^{-1}.$$

Let $\lambda_1, \lambda_2, \ldots, \lambda_k$ be the non-zero eigenvalues of the matrix XPX^T, and let $\boldsymbol{e}_1, \ldots, \boldsymbol{e}_k$ be the corresponding eigenvectors. We add $n-k$ vectors $\boldsymbol{e}_{k+1}, \ldots, \boldsymbol{e}_n$ such that $\{\boldsymbol{e}_i\}$ $i=1, \ldots, n$ forms a set of orthonormal basis vectors. We then have

$$\bar{X}P\bar{X}^T = \sum_{i=1}^{k} \lambda_i \boldsymbol{e}_i \boldsymbol{e}_i^T,$$

$$E = \sum_{i=1}^{n} \boldsymbol{e}_i \boldsymbol{e}_i^T.$$

By the use of the relations

$$\left(\sum_{i=1}^{n} \mu_i \boldsymbol{e}_i \boldsymbol{e}_i^T\right)^{-1} = \sum_{i=1}^{n} \frac{1}{\mu_i} \boldsymbol{e}_i \boldsymbol{e}_i^T ,$$

$$(\sum \mu_i \boldsymbol{e}_i \boldsymbol{e}_i^T)(\sum \nu_i \boldsymbol{e}_i \boldsymbol{e}_i^T) = \sum \mu_i \nu_i \boldsymbol{e}_i \boldsymbol{e}_i^T ,$$

we obtain

$$W = e\left(\sum_{i=1}^{k} \frac{\sigma+\lambda_i}{\sigma+\varepsilon+\lambda_i} \boldsymbol{e}_i \boldsymbol{e}_i^T + \sum_{i=k+1}^{n} \frac{\sigma}{\sigma+\varepsilon} \boldsymbol{e}_i \boldsymbol{e}_i^T\right).$$

Expanding the above, where $\sigma+\varepsilon$ is assumed to be small, we obtain

$$W = \boldsymbol{e} \sum_{i=1}^{n} \frac{\sigma}{\sigma+\varepsilon} \boldsymbol{e}_i \boldsymbol{e}_i^T + e \sum_{i=1}^{k} \frac{\varepsilon}{\sigma+\varepsilon} \boldsymbol{e}_i \boldsymbol{e}_i^T - \varepsilon e \sum_{i=1}^{k} \frac{1}{\lambda_i} \boldsymbol{e}_i \boldsymbol{e}_i^T + O[\varepsilon(\varepsilon+\sigma)] .$$

Here, we put $\sigma=0$ and compare the result carefully with (4.2) or (4.7). We then have (4.9).

Conclusion

We have used two types of nets with recurrent connections and non-recurrent connections as models of association and concept-formation, respectively. We proposed two types of self-organization, one called orthogonal learning and the other covariance learning. We have analyzed the behavior of these nets and elucidated possible neural mechanism of information processing including association and concept-formation.

The present models are still too simple to be compared with the actual brain. However, the actual brain might have the mechanisms analyzed here commonly in its various portions. The present analysis will help in building more realistic models of the brain because it provides a possible neural logic.

Acknowledgement. This research was initiated at the University of Tokyo and completed during the author's visit to the Center for Systems Neuroscience of the University of Massachusetts on sabbatical leave from the University of Tokyo. The author would like to thank Professor M. A. Arbib for helpful comments on the manuscript.

References

Albert, A.: Regression and the Moore-Penrose pseudoinverse. New York: Academic Press 1972

Amari, S.: Characteristics of randomly connected threshold element networks and network systems. Proc. IEEE **59**, 35—47 (1971)

Amari, S.: Learning patterns and pattern sequences by self-organizing nets of threshold elements. IEEE Trans. Comp. C-**21**, 1197—1206 (1972a)

Amari, S.: Characteristics of random nets of analog neuron-like elements. IEEE Trans. on Systems, Man, and Cybernetics SMC-**2**, 643—657 (1972b)

Amari, S.: A method of statistical neurodynamics. Kybernetik **14**, 201—215 (1974a)

Amari, S.: A mathematical theory of nerve nets. In: Kotani, M. (Ed.): Advances in biophysics, Vol. 6, pp. 75—120. Tokyo: University Press 1974b

Amari, S.: Homogeneous nets of neuron-like elements. Biol. Cybernetics **17**, 211—220 (1975)

Amari, S.: Dynamics of pattern formation in lateral-inhibition type neural fields. To be published (1977a)

Amari, S.: A mathematical approach to neural systems. In: Arbib, M.A., Metzler, J. (Eds.): Systems neuroscience. I. New York: Academic Press 1977b

Amari, S., Yoshida, K., Kanatani, K.: Mathematical foundation of statistical neurodynamics. SIAM J. Appl. Math. **33** (1977)

Anderson, J.A.: A simple neural networks generating interactive memory. Math. Biosc. **14**, 197—220 (1972)

Caianiello, E.R.: Outline of a theory of thought processes and thinking machines. J. theor. Biol. **1**, 204—235 (1961)

Grossberg, S.: Onlearning, information lateral inhibition, and transmitters. Math. Biosc. **4**, 255—310 (1969)

Hebb, D.O.: The organization of behavior. New York: Wiley 1949

Kohonen, T.: Correlation matrix memories. IEEE Trans. Comp. C-**21**, 353—359 (1972)

Kohonen, T.: An adaptive associative memory principle. IEEE Trans. Comp. C-**23**, 444—445 (1974)

Kohonen, T., Oja, E.: Fast adaptive formation of orthogonalizing filters and associative memory in recurrent networks of neuron-like elements. Biol. Cybernetics **21**, 85—95 (1976)

Malsburg von der, C.: Self-organization of orientation sensitive cells in the striate cortex. Kybernetik **14**, 85—100 (1973)

Nakano, K.: Associatron—a model of associative memory. IEEE Trans. on Systems, Man, and Cybernetics SMC-**2**, 380—388 (1972)

Pfaffelhuber, E.: Correlation memory models—a first approximation in a general learning scheme. Biol. Cybernetics **18**, 217—223 (1975)

Rosenblatt, F.: Principles of Neurodynamics. Washington: Spartan 1961

Spinelli, N.: OCCAM: a computer model for a content-addressable memory in the central nervous systems. Biology of memory 293—306. New York: Academic Press 1970

Uesaka, Y., Ozeki, K.: Some properties of association-type memories. JIEECE of Japan (in Japanese), **55**-D, 323—330 (1972)

Wasan, M.T.: Stochastic approximation. Cambridge: University Press 1969

Wigström, H.: A neuron model with learning capability and its relation to mechanism of association. Kybernetik **12**, 204—215 (1973)

Willshaw, D.J., Longuet-Higgins, H.C.: The holophone—recent developments. In: Metzler, B., Michie, D. (Eds.): Machine intelligence, Vol. 4, pp. 349—357. Edinburgh: University Press 1969

Received: December 12, 1976

Dr. Shun-ichi Amari
Dept. of Mathematical Engineering
and Instrumentation Physics
University of Tokyo
Tokyo 113 Japan

Verantwortlich für den Textteil: Prof. Dr. W. Reichardt, Max-Planck-Institut für biologische Kybernetik, Spemannstr. 38, D-7400 Tübingen. Verantwortlich für den Anzeigenteil: L. Siegel, G. Sternberg, Springer-Verlag, Kurfürstendamm 237, D-1000 Berlin 15, Fernsprecher: (030) 882 1031, Telex: 01-85411. Springer-Verlag, Berlin · Heidelberg · New York.
Druck der Brühlschen Universitätsdruckerei, Lahn-Gießen. Printed in Germany.

Note to Authors

To simplify the printing of mathematical formulae, authors are asked to use the forms indicated in the following examples when preparing their manuscripts.

$7/8, (a+b)/c$	instead of	$\frac{7}{8}, \frac{a+b}{c}$
$\frac{(a/b)\,d}{(a/3)-(x/2)}$		$\frac{\frac{a}{b}d}{\frac{a}{3}-\frac{x}{2}}$
$\frac{\cos(1/x)}{(a+(b/x))^{1/2}}$ or $(a+(b/x))^{-\frac{1}{2}}\cos(1/x)$		$\frac{\cos\frac{1}{x}}{\sqrt{a+\frac{b}{x}}}$
$\exp(-(x^2+y^2)/a^2)$		$e^{-\frac{x^2+y^2}{a^2}}$

The use of such linearized forms can mean up to 50% saving of time to the compositor. Considering the danger of misinterpretation of formulae by a copyeditor or compositor, the publishers find it essential that this simplification in the use of such expressions should be adopted by the authors themselves who are in the best position to ensure that the meaning and intended emphasis within the formulae are preserved. Finally we ask authors to continue to follow the Instructions to Authors as usual.

We thank you for your cooperation.

Springer-Verlag

Biochemistry of Membrane Transport

FEBS-Symposium No. 42

Editors: G. Semenza, E. Carafoli

414 figures, 76 tables. Approx. 740 pages. 1977.
Cloth DM 97,–; US $ 42.70
(Proceedings in Life Sciences)
ISBN 3-540-08082-1
In preparation

Prices are subject to change without notice

This book contains 47 articles, dealing with various aspects of the topic "Biochemistry of Membrane Transport". The area covered spans the molecular architecture of biological membranes and the interaction of membrane lipids and proteins, the chemistry of ionophoric molecules and various theoretical aspects of transport processes, with a detailed discussion of the properties of several natural and reconstituted transport processes. Distinctive for the book is its interdisciplinary character, a quality frequently found in membrane transport research. A further characteristic is the balance between established knowledge, offered in some review-type articles and the numerous contributions presenting the most recent advances in the field.

Contents: Electron Microscopy of Membranes.–Lipid-Lipid and Lipid-Protein Interactions in Membranes.–Ionophores.–Kinetic Aspects of Membrane Transport.–Transport in Epithelia and in Some Other Mammalian Cells.–Transport in Erythrocyte Membranes.–Transport ATPhases.–Transport of CA^{2+} in Excitable and Other Cells.–Regulation of Transport Processes.–Ion Transport in Mitochondria.–Bacterial Transport Systems.

Springer-Verlag
Berlin
Heidelberg
New York

5120/4/2h

Communication and Cybernetics
Editors:
K.S. Fu, W.D. Keidel, W.J.M. Levelt, H. Wolter

Volume 17

T. Kohonen

Associative Memory

A System–Theoretical Approach

54 figures, 7 tables. IX, 176 pages. 1977
Cloth DM 48,–; US $ 21.20
ISBN 3-540-08017-1
Prices are subject to change without notice

This monograph is an introduction to the mathematical theory of associative memory. As it is addressed to researchers and students working in many different fields, for instance, cybernetics, computer science, biomathematics, and mathematical psychology. A considerable amount of tutorial material has been included: mathematical operations in linear vector spaces, matrix equations, principles of associative data structures, logic description of search operations, physical implementation of associative memories, and a review of the biological foundations of memory. The primary objective, however, is to familiarize the reader with various processes and transforms by which associations between patterned items can be represented and stored. This approach makes it possible to relate many abstract concepts of information processing to the theories of learning, pattern recognition, estimation theory, etc., in a fresh way. The implications of these methods to the study of biological associative memory are also considered.

Contents: Introduction.–Associative Search Methods. – Adaptive Formation of Optimal Associative Mappings. – On Biological Associative Memory.

Springer-Verlag
Berlin
Heidelberg
New York

5142/4/2h/a

Encyclopedia of Plant Physiology

New Series

Editors: A. Pirson, M.H. Zimmermann

Volume 1:
Transport in Plants I

Phloem Transport

Editors: M.H. Zimmermann, J.A. Milburn
With contributions by numerous experts

93 figures. XIX, 535 pages. 1975
Cloth DM 158,–; US $ 69.60
ISBN 3-540-07314-0
Distribution rights for India:
UBS Publishers' Distributors Pvt., Ltd., New Delhi

Contents:
Structural Considerations in Phloem Transport.–Nature of Substances in Phloem.–Phloem Transport: Assessment of Evidence.–Possible Mechanisms of Phloem Transport.–Phloem Loading: Storage and Circulation.–Author Index.–Subject Index.

Volume 2 (in 2 parts):
Transport in Plants II

Part A: Cells

Editors: U. Lüttge, M.G. Pitman
With a Foreword by R.N. Robertson
With contributions by numerous experts

97 figures, 64 tables.
XVI, 419 pages. 1976
Cloth DM 128,–; US $ 56.40
ISBN 3-540-07452-X
Distribution rights for India:
UBS Publishers' Distributors Pvt., Ltd., New Delhi

Contents:
Theoretical and Biophysical Approaches.–Particular Cell Systems.–Regulation, Metabolism and Transport.

Part B: Tissues and Organs

Editors: U. Lüttge, M.G. Pitman
With contributions by numerous experts

129 figures, 45 tables.
XII, 475 pages. 1976
Cloth DM 138,–; US $ 60.80
ISBN 3-540-07453-8
Distributions rights for India:
UBS Publishers' Distributors Pvt., Ltd., New Delhi

Contents:
Pathways of Transport in Tissues.–Particular Tissue Systems.–Control and Regulation of Transport in Tissues and Integration in Whole Plants.

Volume 3:
Transport in Plants III

Intracellular Interactions and Transport Processes

Editors: C.R. Stocking, U. Heber
With contributions by numerous experts

123 figures. XXII, 517 pages. 1976
Cloth DM 145,–; US $ 63.80
ISBN 3-540-07818-5
Distribution rights for India:
UBS Publishers' Distributors Pvt., Ltd., New Delhi

Contents:
Membrane Structure.–Intracellular Interactions.–Intracellular Transport in Relation to Energy Conservation.–Theory of Membrane Transport.

Volume 4:

Physiological Plant Pathology

Editors: R. Heitefuss, P.H. Williams
With contributions by numerous experts

92 figures. XX, 890 pages. 1976
Cloth DM 194,–; US $ 85.40
ISBN 3-540-07557-7
Distribution rights for India:
UBS Publishers' Distributors Pvt., Ltd., New Delhi

Contents:
General.–Spore Germination and Its Regulation.–Cytology and Physiology of Penetration and Establishment.–Forces by Which the Pathogen Attacks the Host Plant.–Physiology of Host Response to Infection.–Modification of the Host Response–Predisposition.–Biothrophic Parasites in Culture.–Genetics of Host-Parasite Interactions.–Author Index.–Index of Microorganisms and Nematodes.–Subject Index.–List of Symbols and Abbreviations.

Volume 5:
Photosynthesis I

Photosynthetic Electron Transport and Photophosphorylation

Editors: A. Trebst, M. Avron
With contributions by numerous experts

135 figures.
Approx. 820 pages. 1977
Cloth DM 194,–; US $ 85.40
ISBN 3-540-07962-9
In preparation
Distribution rights for India:
UBS Publishers' Distributors Pvt., Ltd., New Delhi

Contents:
Introduction.–History.–Electron Transport.–Energy Conservation.–Structure and Function.–Algal and Bacterial Photosynthesis.

Prices are subject to change without notice

Springer-Verlag
Berlin
Heidelberg
New York

5139/4/1